

**Advanced Technology Development Program  
For Lithium-Ion Batteries**

**Battery Technology Life Verification  
Test Manual**

February 2005



Idaho National Laboratory  
Idaho Falls, ID 83415  
Operated by Battelle Energy Alliance, LLC



***FreedomCAR & Vehicle  
Technologies Program***



## **Disclaimer**

This report was prepared as an account of work sponsored by an agency of the United States Government. Neither the United States Government nor any agency thereof, nor any of their employees, makes any warranty, express or implied, or assumes any legal liability or responsibility for the accuracy, completeness, or usefulness of any information, apparatus, product, or process disclosed, or represents that its use would not infringe privately owned rights. References herein to any specific commercial product, process, or service by trade name, trademark, manufacturer, or otherwise does not necessarily constitute or imply its endorsement, recommendation, or favoring by the United States Government or any agency thereof. The views and opinions of authors expressed herein do not necessarily state or reflect those of the United States Government or any agency thereof.

**Advanced Technology Development Program  
for Lithium-Ion Batteries**

**Battery Technology Life Verification Test Manual**

**Harold Haskins (USABC)  
Vince Battaglia (LBNL)  
Jon Christophersen (INEEL)  
Ira Bloom (ANL)  
Gary Hunt (INEEL)  
Ed Thomas (SNL)**

**February 2005**

**Idaho National Laboratory  
Transportation Technology Department  
Idaho Falls, Idaho 83415**

**Prepared for the  
U.S. Department of Energy  
Assistant Secretary for Energy Efficiency  
and Renewable Energy  
Under DOE Idaho Operations Office  
Contract DE-AC07-99ID13727**



# CONTENTS

GLOSSARY OF LIFE TESTING TERMS .....	vii
ACRONYMS .....	ix
1. INTRODUCTION .....	1
1.1 FreedomCAR Battery Life Goals .....	1
1.2 Battery Technology Life Verification Objectives .....	1
1.3 Battery Life Test Matrix Design Approach .....	2
1.4 Reference Performance Testing Approach .....	3
1.5 Life Test Data Analysis Approach .....	3
1.6 Organization of the Manual .....	3
2. LIFE TEST EXPERIMENT DESIGN REQUIREMENTS .....	5
2.1 Technology Characterization Requirements .....	5
2.2 Core Life Test Matrix Design Requirements .....	9
2.3 Core Life Test Matrix Design and Verification .....	12
2.3.1 Preliminary Design Stage .....	13
2.3.2 Final Design Stage .....	17
2.3.3 Final Verification Stage .....	18
2.4 Supplemental Life Test Matrix Design Requirements .....	19
2.4.1 Experimental Plan to Assess Path Independence .....	20
2.4.2 Experimental Plan to Assess Cold-Start Operation .....	20
2.4.3 Experimental Plan to Assess Low-Temperature Operation .....	21
3. LIFE TEST PROCEDURES .....	22
3.1 Initial Characterization Tests .....	22
3.1.1 General Test Conditions and Scaling .....	23
3.1.2 Minimum Characterization for All Cells .....	24
3.1.3 Additional Characterization of Selected Cells .....	24
3.1.4 BOL Reference Testing .....	26
3.2 Core Life Test Matrix .....	26
3.2.1 Stand Life (Calendar Life) Testing .....	26
3.2.2 Cycle Life (Operating) Testing .....	27
3.2.3 Reference Performance Tests and End-of-Test Criteria .....	28
3.3 Supplemental Life Tests .....	29
3.3.1 Combined Calendar and Cycle Life Tests .....	29

3.3.2	Cold-cranking Power Verification Tests.....	30
3.3.3	Low-temperature Operation Tests.....	30
4.	DATA ANALYSIS AND REPORTING .....	32
4.1	Initial Performance Characterization Test Results .....	32
4.1.1	Determination of Open Circuit Voltage versus State of Charge .....	33
4.1.2	Capacity Verification .....	33
4.1.3	Determine Temperature Coefficient of ASI (Selected Cells).....	33
4.1.4	Pulse Power Verification (MPPC) .....	34
4.1.5	Pulse Power Verification (HPPC).....	34
4.1.6	Rank Ordering of Cells .....	35
4.1.7	Self-Discharge Rate Characterization .....	36
4.1.8	Cold-Cranking Power Verification .....	36
4.1.9	AC EIS Characterization.....	36
4.1.10	ASI Noise Characterization.....	36
4.2	Core Matrix Life Test Results .....	39
4.2.1	Life on Test Estimates.....	39
4.2.2	Calendar Life Estimate.....	41
4.2.3	Effects of Cycling Stresses.....	43
4.2.4	Life in Service Estimate .....	44
4.3	Supplemental Life Test Results.....	45
4.3.1	Hypothesis Testing.....	45
4.3.2	Combined Calendar/Cycle Life tests.....	45
4.3.3	Cold-start Verification Tests .....	47
4.3.4	Low-temperature Operation Tests.....	48
5.	REFERENCES .....	49

Appendix A—Life Test Simulation Program .....	A-1
Appendix B—Methods for Modeling Life Test Data .....	B-1
Appendix C—Study of Life-Limiting Mechanisms in High-Power Li-Ion Cells .....	C-1
Appendix D—Use of the Monte Carlo Simulation Tool .....	D-1
Appendix E—Test Measurement Requirements.....	E-1

## FIGURES

Figure 2.1-1. Example of ASI "truth" functions. ....	8
Figure 2.3-1. Results for life test matrix example (estimated ( $\pm 1$ std dev) versus true life on test). ....	18
Figure 4.2-1. Comparison of bootstrap results with normal distribution for life on test at Calendar Life 1 test condition. ....	41
Figure 4.3-1. Expected ASI histories for combined cycle/calendar and calendar/cycle test conditions....	46

## TABLES

2.1-1. Test conditions for the minimum life test experiment example. ....	6
2.1-2. Hypothetical results from short-term tests of new and aged cells. ....	7
2.1-3. Estimated acceleration factors for the Minimum Life Test Experiment Example. ....	8
2.2-1. Basic stress factors and suggested stress levels for accelerated battery life testing. ....	10
2.2-2. Recommended calendar life matrix design.....	10
2.2-3. Cycle life matrix design (Design 1).....	11
2.2-4. Cycle life matrix design (Design 2).....	11
2.3-1. Expected lives on test for the Minimum Life Test Experiment example. ....	14
2.3-2. Preliminary allocation of cells for the Minimum Life Test Experiment example. ....	16
2.3-3. Simulation results for the Minimum Life Test Experiment example. ....	17
3.2-1. Reference performance test intervals for life testing. ....	29
4.2-1. Simulated experimental results: estimates compared with truth.....	40
4.2-2. Data and results for calendar life estimation for example matrix. ....	43
4.2-3. Data and results for estimation of cycle life acceleration factors for example matrix.....	44



## GLOSSARY OF LIFE TESTING TERMS

*Acceleration Factor* – Ratio of calendar life to life on test.

*Area-Specific Impedance (ASI)* – The impedance of a device relative to the electrode area of the device, defined as the change in cell voltage (V) as a result of a change in cell current divided by the change in cell current (A), all multiplied by the active superficial cell area (cm<sup>2</sup>), ohm-cm<sup>2</sup>.

*Available Capacity* – The capacity (in Ah) of a device between two state of charge conditions designated as SOC<sub>MAX</sub> and SOC<sub>MIN</sub>, as measured using a C<sub>1</sub>/1 constant current discharge rate after the performance of a HPPC pulse profile at SOC<sub>MAX</sub>,

*Beginning of Life (BOL)* – The point in time at which life testing begins. A distinction is made in this manual between the performance of a battery at this point and its initial performance, because some degradation may take place during early testing before the start of life testing. Analysis of the effects of life testing is based on changes from the BOL performance.

*C-rate* – A current (for discharge or charge) expressed as a multiple of the rated device capacity (in ampere-hours) for a reference (static capacity) discharge. For example, for a device having a capacity of 1 ampere-hour under this reference condition, a 5-A rate would be 5A/(1 Ah) or 5C, hr<sup>-1</sup>.

*C<sub>1</sub>/1 Rate* – The rate corresponding to completely discharging a fully charged device in exactly one hour. Otherwise, a rate corresponding to the manufacturer's rated capacity (in ampere-hours) for a one-hour constant current discharge. For example, if the battery's rated one-hour capacity is 1 Ah, then the C<sub>1</sub>/1 constant current rate is 1 A. The C<sub>1</sub>/1 rate is the reference discharge rate for power-assist applications; other applications may have different reference rates, hr<sup>-1</sup>.

*Calendar Life (L<sub>CAL</sub>)* – The time required to reach end of life at the reference temperature of 30°C at open-circuit (corresponding to key-off/standby conditions in the vehicle).

*Depth of Discharge* – The percentage of a device's rated capacity removed by discharge relative to a fully charged condition, normally referenced to a constant current discharge at the C<sub>1</sub>/1 rate. The capacity to be used is established (fixed) at the beginning of testing, %.

*End of Life (EOL)* – A condition reached when the device under test is no longer capable of meeting the applicable FreedomCAR goals. This is normally determined from RPT results, and it may not coincide exactly with the ability to perform the life test profile (especially if cycling is done at elevated temperatures.) The number of test profiles executed at end of test is not necessarily equal to the cycle life per the FreedomCAR goals.

*End of Test (EOT)* – The point in time where life testing is halted, either because criteria specified in the test plan are reached, or because it is not possible to continue testing.

*Hybrid Pulse Power Characterization (HPPC)* – A test whose results are used to calculate pulse power and energy capability under FreedomCAR operating conditions.

*Life in service* – The time required to reach end of life at the nominal conditions of normal usage in the vehicle (30°C and specified cycling conditions).

*Life on test ( $L_{TEST}$ )* – The time required to reach end of life at the test conditions specified for accelerated life testing.

*Minimum Pulse Power Characterization (MPPC)* – A shortened version of the Hybrid Pulse Power Characterization test conducted periodically to measure performance deterioration over time.

*SOC<sub>MAX</sub> and SOC<sub>MIN</sub>* – Two state of charge conditions that are chosen as reference conditions for a given life test program. They could represent the entire anticipated operating range for a given application, although for reference test purposes they are typically limited to the range of SOC values used in the life test matrix. SOC<sub>MAX</sub> and SOC<sub>MIN</sub> are represented by (i.e., measured as) the corresponding open circuit voltages when the device is in a stable condition (see Stable SOC Condition and Stable Voltage Condition.) SOC<sub>MAX</sub> can be selected as any value less than or equal to the maximum allowable operating voltage for a device. SOC<sub>MIN</sub> can be any value less than SOC<sub>MAX</sub> and greater than or equal to the minimum allowable operating voltage, %.

*Stable SOC (state of charge) Condition* – For a device at thermal equilibrium, its state of charge under clamped voltage conditions is considered to have reached a stable value when the current declines to less than 1% of its original or limiting value, averaged over at least 5 minutes. (For example, if a device is discharged at a C<sub>1</sub>/1 rate and then clamped at a final voltage, the SOC would be considered stable when the current declines to 0.01 C<sub>1</sub>/1 or less.)

*Stable Voltage Condition* – For a device at thermal equilibrium, its open circuit voltage (OCV) is considered stable if it is changing at a rate of less than 1% per hour when measured over at least 30 minutes. (Note that a stable voltage condition can also be reached by setting an arbitrary OCV rest interval (e.g., 1 hour), which is long enough to ensure that voltage equilibrium is reached at any SOC and temperature condition of interest. This is much simpler to implement with most battery testers than a rate-of-change criterion. However, it would result in a longer test and in longer rest intervals, which could be undesirable if a device had high self-discharge at the temperature where the test was conducted.)

*State of Charge (SOC)* – The available capacity in a battery expressed as a percentage of actual capacity. This is normally referenced to a constant current discharge at the C<sub>1</sub>/1 rate. For this manual, it may also be determined by a voltage obtained from a correlation of capacity to voltage fixed at beginning of life.  $SOC = (100 - DOD)$  if the rated capacity is equal to the actual capacity, %.

*State-of-health (SOH)* – The present fraction of allowable performance deterioration remaining before EOL. (SOH = 100% at beginning of life and 0% at end of life.)

*Stress factors* – External conditions imposed on a battery that accelerates its rate of performance deterioration.

## ACRONYMS

AF	acceleration factor
ASI	area-specific impedance
ATD	Advanced Technology Development (Program)
BOL	beginning of life
BSF	battery size factor
CLT	calendar life test
DOD	depth of discharge
EIS	electrochemical impedance spectrum
EOL	end of life
EOT	end of test
HEV	hybrid electric vehicle
HPPC	Hybrid Pulse Power Characterization (test)
MCS	Monte Carlo simulation
MPPC	Minimum Pulse Power Characterization (test)
OCV	open circuit voltage
OEM	original equipment manufacturer
ROR	robust orthogonal regression
RPT	reference performance test
SOC	state of charge
TLVT	Technology Life Verification Test



# Battery Technology Life Verification Test Manual

## 1. INTRODUCTION

This manual has been prepared to guide battery developers in their effort to successfully commercialize advanced batteries for automotive applications. The manual includes criteria for design of a battery life test matrix, specific life test procedures, and requirements for test data analysis and reporting. Several appendices are provided to document the bases for the procedures specified in the manual. Previous battery life test procedures published in FreedomCAR battery test manuals (References 8 through 11) are superseded by this present Technology Life Verification Test (TLVT) manual.

This introduction presents the FreedomCAR battery life goals and life verification objectives, along with the general approaches for life test matrix design, reference performance testing, and life test data analysis. Organization of the manual is then summarized.

### 1.1 FreedomCAR Battery Life Goals

FreedomCAR battery life goals for two representative power-assist hybrid-electric vehicle (HEV) applications are presented in Table 1 of Reference 8. The calendar life goals are the same for all automotive applications—15 years in service. The cycle life goals depend on the power-assist ratings—240,000 cycles at 60% of rated power, plus 45,000 cycles at 80% of rated power, plus 15,000 cycles at 95% of rated power. A cycle consists of a power profile that includes the vehicle operations of engine-off, launch, cruise, and regenerative braking. This set of three operating conditions corresponds to the 90<sup>th</sup> percentile of automotive customer requirements. Similar requirements have been specified by FreedomCAR for 42-volt applications (Reference 9), fuel cell powered vehicles (Reference 10) and ultracapacitors (Reference 11).

### 1.2 Battery Technology Life Verification Objectives

Commercialization of advanced batteries for automotive applications requires verification of battery life capability in two distinct stages. The first stage, addressed in this manual, demonstrates the battery technology's readiness for transition to production. The primary objective is to verify that the battery is capable of at least a 15-year, 150,000-mile life at a 90% confidence level. An important secondary objective is to provide data for optimization of the battery product design and usage. These objectives need to be met with minimum cost and time expended for life testing. This implies careful use of accelerated life testing at elevated levels of key stress factors. For promising technologies, it is expected that the life verification costs will be shared by the developer and FreedomCAR. Test articles will be prototypical battery cells.

The second stage of life verification is an integral part of product design verification, conducted jointly by a production battery supplier and an automotive original equipment manufacturer (OEM). The objectives are to (1) demonstrate that the complete battery system meets the life target for its intended usage by the 90<sup>th</sup> percentile customer, and (2) confirm product warranty policy and projected warranty costs. Detailed requirements for this stage of life verification are subject to OEM/supplier negotiation, under timing and budget constraints for vehicle development. Testing of full battery systems from production-capable facilities is generally required.

Prerequisites for battery technology life verification testing are as follows:

1. The development status of a candidate technology must be such that its key materials and fabrication processes are stable and completely traceable.
2. A high percentage of cells produced must represent the “best” of the technology.
3. Life-limiting wearout mechanisms must be identified and characterized by physical diagnostic tools.
4. Battery life models should be available, calibrated by special short-term test results as appropriate.
5. Parallel evaluation of alternative cell designs, materials, and fabrication processes should be completed.
6. Detailed cell production planning should be in progress.

### **1.3 Battery Life Test Matrix Design Approach**

Battery technology life verification testing includes a range of stress factors appropriate to achieving high, but relevant, acceleration factors. The goal is to verify (with 90% confidence) that the battery life is at least 15 years by using only one to two years of accelerated life testing. Thus, an acceleration factor of at least 7.5 is desired at the highest level of combined stress factors. To be relevant, an elevated stress factor must induce a wearout failure mode that truly represents the failure modes that will occur in normal service. Selection of specific stress factors and levels must be based on a thorough understanding of the relevant wearout modes for the candidate technology. Stress factors that should be considered include (a) temperature, (b) state of charge (SOC), (c) rate of discharge energy throughput, and (d) discharge and regenerative pulse power levels. Each combination of stress factors must correspond to a known (or estimated) acceleration factor.

Design of the life test matrix should be based on established design-of-experiment principles (e.g., Reference 5). This will minimize life test program cost and maximize confidence in the resulting life projections. Although test efficiency is desired, the life test matrix must also reflect known or suspected interactions of the stress factors. Confounding of effects for critical stress factor interactions must be avoided.

A life test simulation tool has been developed to support optimization of the core life test matrix. This tool uses the Monte Carlo approach to simulation, in which a simulated sample of cells is subjected to the life test, wherein the *true* response of the simulated cells is corrupted with specified *noise* levels induced by test measurement errors and cell-to-cell manufacturing variability. Numerous trials are simulated, each corresponding to a replication of the life test at the specified acceleration factor. Each Monte Carlo trial results in simulated cell performance deterioration from which the life on test can be estimated. The variation in estimated life on test across the set of trials provides a basis for developing confidence limits for life on test. The goal is to meet the 15-year, 150,000-mile life at a 90% confidence level. Given that the simulations accurately reflect actual cell performance and testing, the actual life test should yield, with 90% probability, a projected life of 15 years. The life test simulation can be used to optimize such matrix design variables as the number of cell replicates at each stress level and the frequency of reference performance tests (RPTs), given the test measurement and manufacturing noise levels. To facilitate this optimization process, a spreadsheet analysis tool is also provided to give preliminary, approximate estimates of the number of cells required at each test condition for the core life tests.

Another important use of the simulation tool is to verify by statistical analysis of the data that the test measurement and manufacturing noise levels are no greater than those assumed in the original core test matrix optimization. If the measurement and manufacturing noise levels are greater than those assumed, then the test matrix may need to be modified, for example by increasing the number of replicate cells at some of the critical stress conditions.

In supplemental life tests, some cells will be tested under sequential combinations of stand life (nonoperating) and cycle life (pulse-mode operation) to demonstrate the path-independence of life. This will use the highest levels of stress conditions, applied in complementary sequences of calendar/cycle and cycle/calendar time blocks. Other supplemental life tests will demonstrate the capability of the technology for periodic cold-cranking and low-temperature operation within specified regenerative pulse current limits without impacting cell life.

## **1.4 Reference Performance Testing Approach**

At fixed time intervals during life testing, each cell will be subjected to a reference performance test (RPT) to measure its cumulative deterioration at its specified stress levels. In contrast to previous life test protocols, the specified RPT procedure minimizes the time spent off-test and possible reduction in life due to irrelevant stresses induced by the RPT. More extensive RPTs may be conducted on supplemental life test cells (outside the core life test matrix) to assess deterioration in such performance parameters as rated capacity and cold-cranking power. The minimum RPT primarily will measure power at a reference temperature (30°C) and specified minimum operating SOC. Power at the maximum operating SOC, as well as capacity from the maximum SOC to the minimum SOC, will also be measured. The RPT power measurements will be adjusted to account for measured cell temperatures that differ from the reference temperature.

## **1.5 Life Test Data Analysis Approach**

An empirical procedure for estimating battery life from RPT data has been developed. Assuming a general model of ASI versus time (see Appendix A), it uses a proven data analysis method [Reference 4] that minimizes the effect of test measurement noise on the life projections. The assumption is that power fade mechanisms are the dominant mode of battery wearout. Reliable projection of battery life requires estimating the power fade rate at each stress level in the life test matrix. These deterioration rate estimates are then extrapolated back to the lower stress levels expected in normal vehicle usage.

The effects on battery life of stress factors included in the scope of the supplemental life test matrix will be estimated by comparing those factors with the results from the core life test matrix, using standard statistical methods.

## **1.6 Organization of the Manual**

This manual is organized into three major sections, plus references and appendices, as follows. Section 2 contains requirements for design and verification of the life test experiment, including (a) characterization of battery failure modes, (b) selection of stress factors and stress levels, (c) design and verification of the core life test matrix, and (d) design of a supplemental life test matrix. Section 3 contains specific life test procedures for (a) initial characterization of all cells, plus supplemental characterization of selected cells, (b) stand (i.e., nonoperating) test and cycling test of cells in the core life test matrix, and (c) special tests for cells in the supplemental life test matrix. Section 4 contains requirements for test data analysis and reporting, including (a) initial characterization of test cells, (b) results from the core life test matrix,

including estimation of battery life in normal service, and (c) results from the supplemental life test matrix, including identification of any additional stress factors, beyond those included in the core matrix, that significantly effect battery life. Section 5 lists all documents referenced in the four sections of the Manual.

Five appendices supplement the main manual. Appendix A documents the methodology used in the life test simulation programs supplied with the Manual. Appendix B documents the use of the robust orthogonal regression (ROR) method for modeling life test data and illustrates its application to the ATD Gen 2 cells. Appendix C summarizes the diagnostic results from the Advanced Technology Development (ATD) Program, including wearout modes observed in life tests of Gen 2 cells. Appendix D provides user instructions for the Battery MCS program. Appendix E documents the requirements for measurement of electrical test data and temperatures, and for data recording intervals.

## **2. LIFE TEST EXPERIMENT DESIGN REQUIREMENTS**

This section presents the general requirements for planning and designing a battery life test experiment. The overall experiment design process begins with characterizing a candidate technology: its performance degradation mechanisms, principal life-limiting stresses, maximum allowable stress levels to avoid irrelevant degradation mechanisms, and the general time-dependence of the performance degradation. Given these prerequisites, an initial matrix of test conditions is selected for evaluation. An acceleration factor—the ratio of expected life in service to expected life on test—is estimated for each test condition, based on a calibrated life model for the technology. If such a model has not been established, then a series of short-term tests (3–6 months duration) must be conducted to estimate the acceleration factors directly.

Once the candidate technology has been characterized, several decisions are to be made in the final design of the life test experiment. The life test facilities, total duration of the life testing, and frequency of performance measurement are specified first. The total number of cells to be tested is then a key planning decision. It strongly depends on (a) the desired confidence in the test results for projected life in service, (b) the expected cell-to-cell performance variation, and (c) the performance measurement capabilities of the test facilities. The experiment design objective is to allocate replicate cells to each test condition, such that the total number of cells is minimized for any specified level of confidence.

A life test simulation tool, a spreadsheet provided with this manual (“Battery MCS.xls”), supports the experiment design process. The simulation is to be used to maximize confidence in the final projection of life in service from the test data obtained, within practical constraints on the scope of the test program. The simulation is based on the Monte Carlo method and incorporates the empirical data analysis method described in Appendix B. A second spreadsheet tool is also provided to support a preliminary allocation of cells for the experiment (“Cell Allocator.xls”). The full simulation is then used to iteratively adjust and verify the final allocation. Later, at the start of testing, the simulation will be used to reverify the experiment design using initial characterization data for the actual test cells.

The complete life test experiment includes a supplemental life test matrix to verify that special operating conditions such as periodic cold-cranking and low-temperature operation do not adversely affect battery life. This verification will be done by comparing the results between the core matrix of test conditions and the supplemental test conditions.

Requirements for design of the life test experiment, based on this general process, are provided in the following. A design example is used to illustrate the process, assuming a minimum of eight test conditions are needed for the core matrix. Section 2.1 presents the requirements for characterizing candidate technologies before detailed life verification test planning. Section 2.2 provides guidelines for selecting the core matrix of test conditions. Section 2.3 describes how the Monte Carlo simulation tool is used to finalize the preliminary cell allocations and to reverify the overall experiment design using initial cell characterization data. Section 2.4 specifies the requirements for the supplemental life test matrix.

### **2.1 Technology Characterization Requirements**

The first requirement for characterization of a candidate long-life battery technology is to identify the physical mechanisms responsible for loss of performance (e.g., power fade) that limit battery life. Experience has shown that a comprehensive suite of electrochemical and diagnostic

analyses is the best approach to achieving this goal. Several potentially useful diagnostic techniques have been developed and applied to a lithium-ion model chemistry as part of the Department of Energy’s Advanced Technology Development (ATD) Program. The techniques are documented in a handbook (Reference 3) and the results (Reference 1) are summarized in Appendix C of this manual.

Once identified, the physical mechanisms should be integrated into phenomenological models that can, with calibration, support quantitative investigations of how candidate stress factors affect rates of performance degradation. This allows the principal life-limiting stresses to be identified.

As stress levels are increased, the physical mechanisms may change from those applicable under normal usage to ones that are irrelevant. It is necessary to determine limiting values of the stress factors to be used in the life test, such that abnormally high rates of degradation are avoided. If not, the influence of a given stress factor may be overestimated at high values of the life test acceleration factor. This could result in overestimation of the projected life in service.

Ideally, a technology developer will have completed this phase of technology characterization and used a calibrated battery life model to project an acceptable life in service, in accordance with the FreedomCAR goals. The next step in planning the life verification experiment would then be to modify the Monte Carlo simulation provided herein, incorporating the technology-specific life model in place of the simulation’s default model. As noted in Appendix B, the default model is a fully empirical model that, although flexible in its range of application, is limited to estimating simple empirical parameters. Guidelines for modification of the simulation tool are provided in Appendix D.

In the absence of a calibrated battery life model, it will be necessary to conduct short-term (3–6 months) screening tests using a matrix of stress factors at appropriate levels to estimate the life test acceleration factors that can be achieved. The method for estimating the acceleration factors is illustrated in the following example for a minimum core matrix of eight test conditions. The example test conditions are summarized in Table 2.1-1, and are assumed to be those proposed for the actual life test experiment. The measure of performance will be the cell’s area-specific impedance (ASI), a key parameter in determining cell power capability. The response variable in these short-term tests will be the estimated rate of change in ASI.

Table 2.1-1. Test conditions for the minimum life test experiment example.

Test Condition	Temperature (°C)	Maximum Pulse Power/Rated Power
Calendar Life 1	45	Zero
Calendar Life 2	50	Zero
Calendar Life 3	55	Zero
Calendar Life 4	60	Zero
Cycle Life 1	45	80%
Cycle Life 2	45	100%
Cycle Life 3	55	80%
Cycle Life 4	55	100%

Groups of new cells are assumed to be tested at all eight conditions for sufficient duration to yield the average rates of ASI increase shown in Table 2.1-2. Also shown in the table are rates of change in ASI for samples of aged cells at selected test conditions, where the aged cells have ASI values corresponding to about 80% of the allowable increase in ASI at end of life (EOL). The purpose of testing such aged cells is to estimate the shape of the ASI versus time curve for the technology, as discussed below.

Table 2.1-2. Hypothetical results from short-term tests of new and aged cells.

Test Condition	Measured Rates of Increase in ASI ( $\Omega\text{-cm}^2/\text{year}$ )	
	New Cells	Aged Cells ( $\Delta\text{ASI} \approx 4/5$ of $\Delta\text{ASI}$ at EOL)
Calendar Life 1	3.965	(not tested)
Calendar Life 2	5.317	(not tested)
Calendar Life 3	7.059	2.118
Calendar Life 4	9.282	2.785
Cycle Life 1	5.434	(not tested)
Cycle Life 2	6.253	(not tested)
Cycle Life 3	9.880	2.964
Cycle Life 4	11.47	3.444

The following simple model was assumed for the purposes of this example:

$$\dot{ASI} = \left( \dot{ASI}_{0,REF} \right) (F_{CAL}) (F_{CYC}) \left[ 1 + \left( \dot{ASI}_{RATIO} - 1 \right) \frac{(ASI - ASI_{BOL})}{ASI_{EOL} - ASI_{BOL}} \right]$$

where  $\dot{ASI}$  is the ASI rate of change estimated from the measured values of ASI, and where the calendar life and cycle life acceleration factors  $F_{CAL}$  and  $F_{CYC}$  are assumed to be of the form

$$F_{CAL} = e^{T_{ACT} \left[ \frac{1}{T_{REF} + 273.15} - \frac{1}{T + 273.15} \right]}$$

and

$$F_{CYC} = 1 + (K_P) \left( \frac{P}{P_{RATED}} \right)^\omega \left[ 1 + (K_T)(T - T_{REF}) \right].$$

Note that  $F_{CAL}$  equals 1 when  $T = T_{REF}$  and that  $F_{CYC}$  equals 1 when  $P/P_{RATED} = 0$ .

The measured values of  $\dot{ASI}$  from Table 2.1-2 imply the following values for the model parameters, given the reference conditions of  $T_{REF} = 30^\circ\text{C}$ ,  $P/P_{RATED} = 0$ ,  $ASI_{BOL} = 30$ , and  $ASI_{EOL} = 40$ :

$$\begin{array}{lll} \dot{ASI}_{0,REF} = 1.561 & \dot{ASI}_{RATIO} = 0.125 & T_{ACT} = 6000 \text{ K} \\ K_P = 0.5 & \omega = 2 & K_T = 0.01/^\circ\text{C} \end{array}$$

The resulting acceleration factors for the eight test conditions are given in Table 2.1-3.

Table 2.1-3. Estimated acceleration factors for the Minimum Life Test Experiment Example.

Test Condition	Temperature (°C)	$P/P_{RATED}$	$F_{CAL}$	$F_{CYC}$	$AF = (F_{CAL})(F_{CYC})$
Calendar Life 1	45	Zero	2.542	1.000	2.542
Calendar Life 2	50	Zero	3.404	1.000	3.404
Calendar Life 3	55	Zero	4.517	1.000	4.517
Calendar Life 4	60	Zero	5.943	1.000	5.943
Cycle Life 1	45	80%	2.542	1.368	3.478
Cycle Life 2	45	100%	2.542	1.575	4.004
Cycle Life 3	55	80%	4.517	1.400	6.323
Cycle Life 4	55	100%	4.517	1.625	7.340

The parameter  $\dot{A}SI_{RATIO}$  is the ratio of ASI rate of change at EOL to ASI rate of change at BOL. This ratio determines the shape of the ASI versus time curve, as illustrated in Figure 2.1-1.

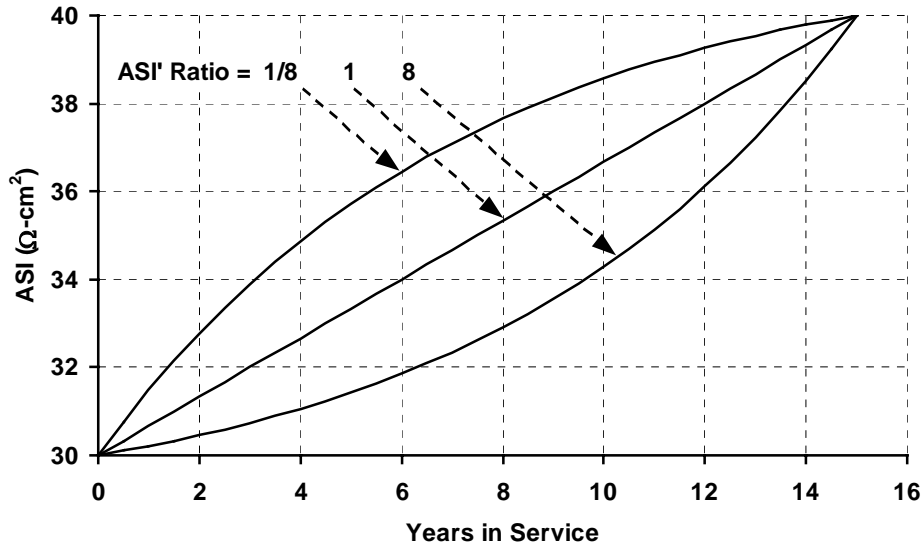


Figure 2.1-1. Example of ASI "truth" functions.

As seen from this figure, for  $\dot{A}SI_{RATIO} > 1$  the ASI increase is accelerating with time. Physically, this implies that the battery chemistry has an inherently destabilizing positive feedback effect. For  $\dot{A}SI_{RATIO} = 1$ , the ASI increase is perfectly linear, indicating a simple kinetically limited degradation mechanism. For  $\dot{A}SI_{RATIO} < 1$ , the ASI increase is decelerating with time. This implies an inherently stable self-limiting type of degradation mechanism, such as a diffusion-limited chemical reaction. It is quite likely that a successful, long-lived battery chemistry will exhibit the last of these three possible characteristics. The goal of battery research is always to find a stable, high-performance chemistry.

Finally, the cells tested in this short-term experiment should be examined using appropriate diagnostic techniques to verify that all cells exhibit the expected physical degradation mechanisms. If cells with the higher acceleration factors show abnormal mechanisms, the limits on the applied stress factors apparently were exceeded. The corresponding test conditions would have to be modified or deleted from the life test experiment.

## 2.2 Core Life Test Matrix Design Requirements

The minimum life test experiment example described in the previous section is not generally expected to provide adequate coverage of the stress factors of probable significance.<sup>1</sup> Additional factors such as operating state of charge (SOC), discharge energy throughput rate, and regenerative pulse power versus discharge pulse power may need to be included for a specific technology. A more extensive matrix of stress factors and levels is presented in Table 2.2-1. The rationale for selecting these factors and levels is summarized in the following.

Temperature (T) has been shown to be a major stress factor in most battery chemistries. It is expected that the dependence of the rate of performance degradation on temperature will be of the Arrhenius type. At least three values of temperature would be needed to assess curvature in the degradation rate with the inverse of absolute temperature. A fourth temperature should be added if the relevance limit for this factor is uncertain before life verification testing.

State of charge generally affects battery performance, and may have a strong effect on life, particularly at higher values. Battery system requirements for cold-cranking power may dictate that the minimum operating SOC be relatively high to minimize battery size. The required battery energy rating may then dictate a high maximum operating SOC. Two such levels of operating SOC are suggested to cover the range of possible vehicle application requirements.

The discharge energy throughput rate is expressed in average vehicle speed over the operating life of the battery—150,000 vehicle miles traveled. The two proposed speeds correspond to 6,000 and 7,500 hours of battery cycling at 25 and 20 mph, respectively. Thus, during the battery's life in service of 15 years, over 14 years will be spent in standby (key-off) mode at open-circuit conditions. This emphasizes the need for thorough calendar life testing within the core matrix.

Battery cycling normally will be very dynamic, with frequent high-power discharge and regenerative pulses. Having designed the battery system to meet end of life power ratings, the normal usage profiles will only stress the battery to some fraction of these ratings. The FreedomCAR cycle life goals allocate percentages of the total cycles to three levels of fractional rated power: 80% (240,000) of the 300,000 cycles at 60% of rated power, 15% (45,000) at 80% of rated power, and 5% (15,000) at 95% of rated power. The effects of pulse power levels on the battery's rate of performance loss may differ between discharge pulses and regenerative pulses. Therefore, independent variation of the power levels for the two types of pulses should be considered.

---

<sup>1</sup> The screening test approach described in Section 2.1 is not intended to be a substitute for a developer's detailed technology characterization. It is provided here primarily for use in illustrating how the previously determined life model and acceleration factors are used in the design of the core life test matrix.

Table 2.2-1. Basic stress factors and suggested stress levels for accelerated battery life testing.

Stress Factor	Number of Stress Levels	Suggested Stress Levels
Temperature (°C)	3	High (55–60°C) Medium (50–55°C) Low (45–50°C)
State of charge (%) (maximum operating)	2	High (80%) Medium (60%)
Discharge energy throughput rate (mph)	3	High (25 mph) Normal (20 mph) Standby (zero)
Fraction of pulse power Rating (%):		
Discharge pulses	2	High (100%), Medium (80%)
Regenerative pulses	2	High (100%), Medium (80%)

The core life test matrix will consist of two parts: a calendar-life matrix and a cycle life matrix. The recommended calendar-life matrix (see Table 2.2-2) is a 3 x 2 full factorial involving temperature and maximum operating SOC.

Table 2.2-2. Recommended calendar life matrix design.

Experiment Condition	Temperature	State of Charge (SOC)	Throughput Rate	Discharge Pulse (Fraction of Rating)	Charge Pulse (Fraction of Rating)
1	Low	Medium	Standby	n/a	n/a
2	Low	High	Standby	n/a	n/a
3	Medium	Medium	Standby	n/a	n/a
4	Medium	High	Standby	n/a	n/a
5	High	Medium	Standby	n/a	n/a
6	High	High	Standby	n/a	n/a

Two possible cycle life matrix designs are given in Tables 2.2–3 and 2.2–4. Each is a fractional factorial design in the five stress factors. The first (Table 2.2–3) is a resolution-III fractional factorial design involving 12 experimental conditions (Reference 14, page 200). If the intent was to assess the main effects and interactions among the stress factors, then we could separate the main effects from one another with this design. However, main effects would be confounded with two-factor interactions. This may not be a serious drawback, considering that the primary objective of the experiment is to verify the projected life-in-service using a variety of experimental conditions, and not necessarily to model life with the cycling stress factors. The relative importance of the calendar life testing should be considered in the overall experiment design.

Table 2.2-3. Cycle life matrix design (Design 1).

Experiment Condition	Temperature	State of Charge (SOC)	Throughput Rate	Discharge Pulse (Fraction of Rating)	Charge Pulse (Fraction of Rating)
1	Low	Medium	Normal	Medium	Medium
2	Low	High	Normal	High	Medium
3	Low	Medium	High	Medium	High
4	Low	High	High	High	High
5	Medium	High	High	Medium	Medium
6	Medium	Medium	High	High	Medium
7	Medium	Medium	Normal	Medium	High
8	Medium	High	Normal	High	High
9	High	High	High	Medium	Medium
10	High	Medium	Normal	High	Medium
11	High	High	Normal	Medium	High
12	High	Medium	High	High	High

The second cycle life test matrix (Table 2.2–4) is a resolution-IV fractional factorial design involving 24 experimental conditions. It is constructed as a  $2^{4-1}$  fractional factorial in 4 factors (SOC, throughput rate, discharge pulse, charge pulse) crossed with temperature at 3 levels. Temperature effects are not confounded with any of the other factors. Main effects of the other factors are not confounded with one another or any two-factor interactions.

This second cycle life test matrix (Design 2) provides a more comprehensive coverage of the cycling stress factor space than Design 1. In addition, Design 2 would provide information to augment a developer’s knowledge base that is deficient in the breadth of stress factors. Although Design 2 has twice the number of test conditions, it will not require as many cells per test condition. Therefore, the total number of cells in the core matrix may not be substantially greater for this design.

Table 2.2-4. Cycle-life matrix design (Design 2).

Experiment Condition	Temperature	State of Charge (SOC)	Throughput Rate	Discharge Pulse (Fraction of Rating)	Charge Pulse (Fraction of Rating)
1	Low	Medium	Normal	Medium	Medium
2	Low	Medium	Normal	High	High
3	Low	Medium	High	Medium	High
4	Low	Medium	High	High	Medium
5	Low	High	Normal	Medium	High
6	Low	High	Normal	High	Medium
7	Low	High	High	Medium	Medium
8	Low	High	High	High	High

Experiment Condition	Temperature	State of Charge (SOC)	Throughput Rate	Discharge Pulse (Fraction of Rating)	Charge Pulse (Fraction of Rating)
9	Medium	Medium	Normal	Medium	Medium
10	Medium	Medium	Normal	High	High
11	Medium	Medium	High	Medium	High
12	Medium	Medium	High	High	Medium
13	Medium	High	Normal	Medium	High
14	Medium	High	Normal	High	Medium
15	Medium	High	High	Medium	Medium
16	Medium	High	High	High	High
17	High	Medium	Normal	Medium	Medium
18	High	Medium	Normal	High	High
19	High	Medium	High	Medium	High
20	High	Medium	High	High	Medium
21	High	High	Normal	Medium	High
22	High	High	Normal	High	Medium
23	High	High	High	Medium	Medium
24	High	High	High	High	High

### 2.3 Core Life Test Matrix Design and Verification

Design and verification of the core life test matrix is conducted in three stages. In the first stage, a preliminary experiment design is developed by selecting the stress factors, stress levels, and number of test conditions in the matrix. The acceleration factor (AF) expected for each test condition is used to obtain values of expected life on test, which in turn are used to obtain expected uncertainties in life on test, based on expected uncertainties due to cell-to-cell manufacturing variations and ASI measurement errors. A target level is selected such that the projected life in service will be achieved with 90% confidence. An estimate is made of the total number of cells required in the core matrix to demonstrate the target projected life in service with 90% confidence. This estimate is made in conjunction with a preliminary allocation of the cells to each test condition (performed with the use of “Cell Allocator.xls”), such that the confidence is maximized for that total number of cells. This stage is described more fully in Section 2.3.1.

In the second stage, the Battery Monte Carlo Simulation tool (“Battery MCS.xls”) is used to adjust and verify the preliminary design from the first stage. This is done by simulating the life test—generating simulated ASI measurements with random variations in the cells’ performance and in the ASI measurements. These simulated data are analyzed as though they were from an actual test. The simulation is repeated for about 100 trials for each test condition to obtain estimates for the uncertainty in the estimated lives on test. The simulation results are used to show that the target confidence level selected can be achieved with the candidate matrix design. If the results are not as expected—primarily because the simulation-generated uncertainties in the estimated lives on test do not agree with the preliminary estimates—the number of cells and cell

allocations will have to be iterated until an acceptable design is obtained. This stage is described more fully in Section 2.3.2.

The third and final stage is reverification of the matrix design using test data from the initial characterization of the actual test cells. The primary objective is to verify that the test cells and test facilities have achieved the desired levels of repeatability and accuracy assumed in the original matrix design process. Simple analysis of the characterization data for ASI at the two SOC values can separate the effects of cell-to-cell variation from ASI measurement noise. Also, in-process data from the cell manufacturing operations can be used to estimate the variability in cell performance. If the noise estimates from these initial test data are significantly different from those assumed in the original experiment design, the design may need to be altered to achieve an acceptable level of confidence in the projection of minimum life in service. This stage is described more fully in Section 2.3.3.

### 2.3.1 Preliminary Design Stage

As discussed below, the preliminary design of the core life test matrix begins with the expected values of life on test, from whence estimated values of life on test and their associated uncertainties are developed.

#### 2.3.1.1 Expected Lives on test

Life verification testing of a mature technology will be based on a calibrated phenomenological model that predicts successful achievement of the FreedomCAR life goals. Such a model will be used to obtain expected AF values for the core matrix of test conditions and the corresponding expected lives on test:

$$L_{TEST} = L_{CAL} / AF$$

where  $AF = (F_{CAL}) (F_{CYC})$  and where the calendar life is related to the life in service by  $L_{SERV} = L_{CAL} / F_{CYC,NOM}$ .

For the default empirical model of Appendix A, calendar life is found by integrating the ASI rate of change and solving the result for the allowable power fade ( $PF$ ) with  $F_{CAL} = F_{CYC} = 1$ :

$$L_{CAL} = \frac{(PF)(ASI_{BOL}) \ln \left( \dot{ASI}_{RATIO} \right)}{(1-PF) \left( \dot{ASI}_{0,REF} \right) \left( \dot{ASI}_{RATIO} - 1 \right)}$$

Assuming that the phenomenological model is perfectly accurate, these expected lives on test would be the actual results of the life tests, in the absence of any cell-to-cell variation or ASI measurement error. For the default empirical model of Appendix A, the data analysis would yield the following “true” values of the three model parameters:

$$\beta_1 = \left( \dot{ASI}_{RATIO} \right)^{1/K_{EOL}}$$

$$\beta_0 = \frac{(\beta_1 - 1) (ASI_0) \left[ \frac{1}{1-PF} - \dot{ASI}_{RATIO} \right]}{\dot{ASI}_{RATIO} - 1}$$

$ASI_O = ASI_{BOL} = 30 \text{ } \Omega\text{-cm}^2$  for the present example

where  $K_{EOL} = L_{TEST} / \Delta t_{RPT}$ . ( $\Delta t_{RPT}$  is the RPT interval, 4/52 years for the example.)

The corresponding values of ASI would then be:

$$ASI_K = \frac{\beta_0 (\beta_1^K - 1)}{(\beta_1 - 1)} + ASI_0 \beta_1^K$$

where  $K = t / \Delta t_{RPT}$  is the test interval index running from  $K = 0$  to  $K = K_{EOT} = t_{EOT} / \Delta t_{RPT}$ .

For the simple model assumed for the design example in Section 2.1, the value for the cycle life acceleration factor under nominal conditions of normal usage is:

$$F_{CYC,NOM} = 1 + (K_P) \left[ (0.8)(0.6)^\omega + (0.15)(0.8)^\omega + (0.05)(0.95)^\omega \right] / 15$$

$\approx 1.014$  for the numerical values of  $K_P$  and  $\omega$  from Section 2.1.

Note that the allowable power fade is assumed to be 25% of the beginning of life pulse power capability for this example. Also, one equivalent year of battery operation has been assumed over its 15-year life in service. Also implied in this equation is that calendar and cycle life effects are path independent. This assumption is included in the recommended list of supplemental life tests. The implied calendar life is about 15.22 years.

Then, from Table 2.1-3, the values for AF at each test condition give the expected lives on test and “true” model parameters, as shown in Table 2.3-1.

Table 2.3-1. Expected lives on test for the Minimum Life Test Experiment example.

Test Condition	Temperature (°C)	$P/P_{RATED}$	$AF$	$L_{TEST}$ (y)	$\beta_0$ (ohm-cm <sup>2</sup> )	$\beta_1$
Calendar Life 1	45	Zero	2.542	5.99	1.092	0.9736
Calendar Life 2	50	Zero	3.404	4.47	1.456	0.9648
Calendar Life 3	55	Zero	4.517	3.37	1.920	0.9536
Calendar Life 4	60	Zero	5.943	2.56	2.509	0.9394
Cycle Life 1	45	80%	3.478	4.38	1.486	0.9641
Cycle Life 2	45	100%	4.004	3.80	1.708	0.9588
Cycle Life 3	55	80%	6.323	2.41	2.660	0.9358
Cycle Life 4	55	100%	7.340	2.07	3.081	0.9256

### 2.3.1.2 Estimated Lives on test

In the simulation, as in reality, the true performance of the test cells is corrupted by “noise” associated with cell-to-cell variations and ASI measurement errors. The data analysis model thus can provide only estimates of the three key fitting parameters:

$$\hat{\beta}_0 = \text{estimated value of } \beta_0$$

$\hat{\beta}_1$  = estimated value of  $\beta_1$

$A\hat{S}I_0$  = estimated value of  $ASI_0$ .

From these parameter estimates, the test data analysis yields an estimate of the life on test,  $\hat{L}_{TEST}$ :

$$\hat{L}_{TEST} = \frac{\Delta t_{RPT}}{\ln(\hat{\beta}_1)} \ln \left( \frac{\hat{\beta}_0 + (\hat{\beta}_1 - 1) \left[ A\hat{S}I_0 / (1 - PF) \right]}{\hat{\beta}_0 + (\hat{\beta}_1 - 1) (A\hat{S}I_0)} \right).$$

Differences between  $\hat{L}_{TEST}$  and  $L_{TEST}$  are due to the estimation errors inherent in  $\hat{\beta}_0$ ,  $\hat{\beta}_1$ , and  $A\hat{S}I_0$  that propagate into an uncertainty in the estimated life on test. The uncertainties in the model parameters can, in turn, be traced back to uncertainties in the measured ASI values. The assumed levels of the various ASI noise components are specified inputs to the simulation, which adds pseudo-random normally distributed noise to the idealized “true” ASI values. It is possible to approximate the standard deviation for the estimated life on test analytically via error-propagation methods, using the true values of the model parameters ( $\beta_0$ ,  $\beta_1$ , and  $ASI_0$ ) and the specified levels of uncertainties in the ASI values (see, e.g., Reference 20, pp. 136–137). It is important to recognize that such an estimate of the uncertainty will differ somewhat with the estimate generated by multiple trials of the simulation. This is due to the approximate nature of the error-propagation method, as well as to the random nature of the simulation.

The standard deviations for the lives on test obtained via an error propagation method are calculated using a spreadsheet routine, “Cell Allocator.xls.” (See Appendix A.) The specified ASI noise components ( $S_{MEASUREMENT}$ ,  $S_{OHMIC}$ , and  $S_{AREA}$ ) and truth parameters ( $\beta_0$ ,  $\beta_1$ , and  $ASI_0$ ) are used in these calculations, assuming first that only one cell is being tested at each test condition. These single-cell estimates are then used to estimate the standard deviation for the projected calendar life ( $S_{CAL}$ ). The calendar life estimate ( $\hat{L}_{CAL}$ ) is obtained using simple linear regression (equal weights for each test condition), with a forced-zero intercept, of the estimated lives on test ( $\hat{L}_{TEST}$ ) versus the reciprocal of the AFs. Since the calendar life corresponds to AF = 1, the estimate of calendar life is just the slope of the linear fit. The standard deviation of this extrapolation to AF = 1 is a function of the nonuniform standard deviations in the estimated lives on test ( $(S_i)_{L_{TEST}}$ ). These in turn depend on the number of cells tested at each test condition.

$$(S^2_i)_{L_{TEST}} = (S^2_{i,1})_{L_{TEST}} / n_i$$

where

$(S_i)_{L_{TEST}}$  = estimated standard deviation in life on test at the  $i^{\text{th}}$  test condition

$(S_{i,1})_{L_{TEST}}$  = estimated single-cell standard deviation in life on test at the  $i^{\text{th}}$  test condition

$n_i$  = number of cells allocated to the  $i^{\text{th}}$  test condition.

The result for the standard deviation in the estimated calendar life is:

$$S_{CAL} = \frac{\sqrt{\sum (1/AF_i)^2 (S_i^2)_{L_{TEST}}}}{\sum (1/AF_i)^2}$$

If weighted linear regression is used (weights inversely proportional to  $(S_i^2)_{L_{TEST}}$ ) to estimate  $\alpha$  in the model  $L = \alpha \cdot \left(\frac{1}{AF}\right)$ , then the standard error of  $\hat{\alpha}$  is

$$S.E.(\hat{\alpha}) = \sqrt{\frac{1}{\frac{n_1}{(S_1^2)_{L_{TEST}} \cdot AF_1^2} + \frac{n_2}{(S_2^2)_{L_{TEST}} \cdot AF_2^2} + \dots + \frac{n_m}{(S_m^2)_{L_{TEST}} \cdot AF_m^2}}}}$$

Suppose that for the example design (with an expected life in service of 15 years) we desire to show that the life in service is at least 13.5 years (10% less than expected) with 90% confidence. The corresponding calendar life must exceed 13.85 years with 90% probability. The expected calendar life of 15.22 years allows a standard deviation in calendar life of

$$S_{CAL} = (15.22 - 13.85)/1.415 = 0.97 \text{ years}$$

where 1.415 is the 90<sup>th</sup> percentile of the t-distribution with (8–1) degrees of freedom.

Using the “Cell Allocator.xls” tool gives the results shown in Table 2.3-2. The total number of cells chosen for this example design to obtain this value of  $S_{CAL}$  is 148. A minimum of 4 cells was specified for any one test condition. The assumed test duration was 2 years, with ASI measurements taken every 4 weeks. Also in this example, the assumed standard deviations for the three components of “noise” in the ASI data were as follows: (a) cell-to-cell fixed ohmic variation = 1%, (b) cell-to-cell electrode area variation = 0.5%, and (c) ASI measurement error = 1%.

Table 2.3-2. Preliminary allocation of cells for the Minimum Life Test Experiment example.

Test Condition	Temperature (°C)	$P/P_{RATED}$	$AF$	$L_{TEST}$	$(S_{i,1})_{L_{TEST}}$	$n_i$	$(S_i)_{L_{TEST}}$
Calendar Life 1	45	Zero	2.542	5.99	7.87	72	0.927
Calendar Life 2	50	Zero	3.404	4.47	3.01	24	0.614
Calendar Life 3	55	Zero	4.517	3.37	1.26	8	0.445
Calendar Life 4	60	Zero	5.943	2.56	0.71	4	0.354
Cycle Life 1	45	80%	3.478	4.38	2.80	24	0.572
Cycle Life 2	45	100%	4.004	3.80	1.79	8	0.633
Cycle Life 3	55	80%	6.323	2.41	0.65	4	0.326
Cycle Life 4	55	100%	7.340	2.07	0.56	4	0.278

It is possible to generalize the results displayed in Table 2.3–2 to provide additional guidance. First, the total number of cells required to meet a target level of uncertainty in the estimated calendar life and life in service is inversely proportional to the square of the target

standard deviation. Thus, the results of any one allocation can be easily scaled to obtain the total number of cells for an alternative target standard deviation. Second, allocation of replicate cells to the various test conditions should be weighted toward the lower AF values. The reason for this is that the “signal” of ASI growth is reduced as AF is decreased. The noise is approximately constant (within statistical fluctuations), and therefore the signal/noise ratio is decreasing. The noise must be correspondingly reduced to compensate for this by using more cells to estimate the life on test. Third, other calculations have shown that there is negligible advantage to more frequent ASI measurement. Finally, the number of cells may be reduced by extending the duration of testing. However, this adds to the cost of testing and delays the commercialization decision. Conversely, testing more cells could shorten the test duration, but not significantly, depending on the limitations of existing test facilities.

### 2.3.2 Final Design Stage

The battery Monte Carlo Simulation (MCS) tool is used at this stage to verify that the total number of cells and their preliminary allocation to the test conditions provide the desired 90% lower confidence limit in the projected life in service. Key inputs to the simulation are true calendar life,  $ASI$  ratio, test duration, RPT measurement interval, allowable power fade at end of life, and three components of noise in the ASI data. The noise components are specified as percentages of the initial ASI at beginning of life. They include variations in the cell electrode area and fixed ohmic resistance due to manufacturing process variations. The third noise source is ASI measurement error from test equipment limitations. The ASI at beginning of life is an arbitrary input that does not affect the predicted life but can be used to match the value of actual cells if desired.

The acceleration factor and number of cells are variable inputs to the simulation for each test condition. Finally, the number of trials for each test condition is specified. This will generally be the same for all test conditions and should be sufficient to obtain good estimates of the standard deviation of life on test. For example, consider normally distributed random variables with standard deviation,  $\sigma$ . About 90% of the time, the observed standard deviation based on a sample of size 100 from that distribution will be within about 10% of  $\sigma$ . The results of these calculations for the experiment design example are summarized in Table 2.3-3, where 100 trials were used for each test condition.

Table 2.3-3. Simulation results for the Minimum Life Test Experiment example.

Test Condition	Temperature	$P/P_{RATED}$	$n_i$	Life on test (y)		Standard Deviation (y)	
				True	MCS Estimate	$(S_i)_{LTEST}$	MCS Estimate
Calendar Life 1	45	Zero	72	5.99	5.98	0.927	0.721
Calendar Life 2	50	Zero	24	4.47	4.55	0.614	0.502
Calendar Life 3	55	Zero	8	3.37	3.46	0.446	0.374
Calendar Life 4	60	Zero	4	2.56	2.63	0.354	0.282
Cycle Life 1	45	80%	24	4.38	4.43	0.572	0.565
Cycle Life 2	45	100%	8	3.80	3.90	0.633	0.669
Cycle Life 3	55	80%	4	2.41	2.45	0.326	0.260
Cycle Life 4	55	100%	4	2.07	2.08	0.278	0.166

These results indicate that the expected standard deviations from the preliminary core matrix design given in Table 2.3-2 (based on the analytical approximation through propagation of errors) are slightly conservative, relative to the estimates generated by the full simulation, Table 2.3-3. As expected for the number of trials used, the estimated and expected lives on test are in close agreement. The linear regression of the estimated vs. true life on test is shown in Figure 2.3-1, along with the estimated standard deviations in the life on test estimates. (Note that the expected life on test values are, by definition, directly proportional to the inverse of the AF values.)

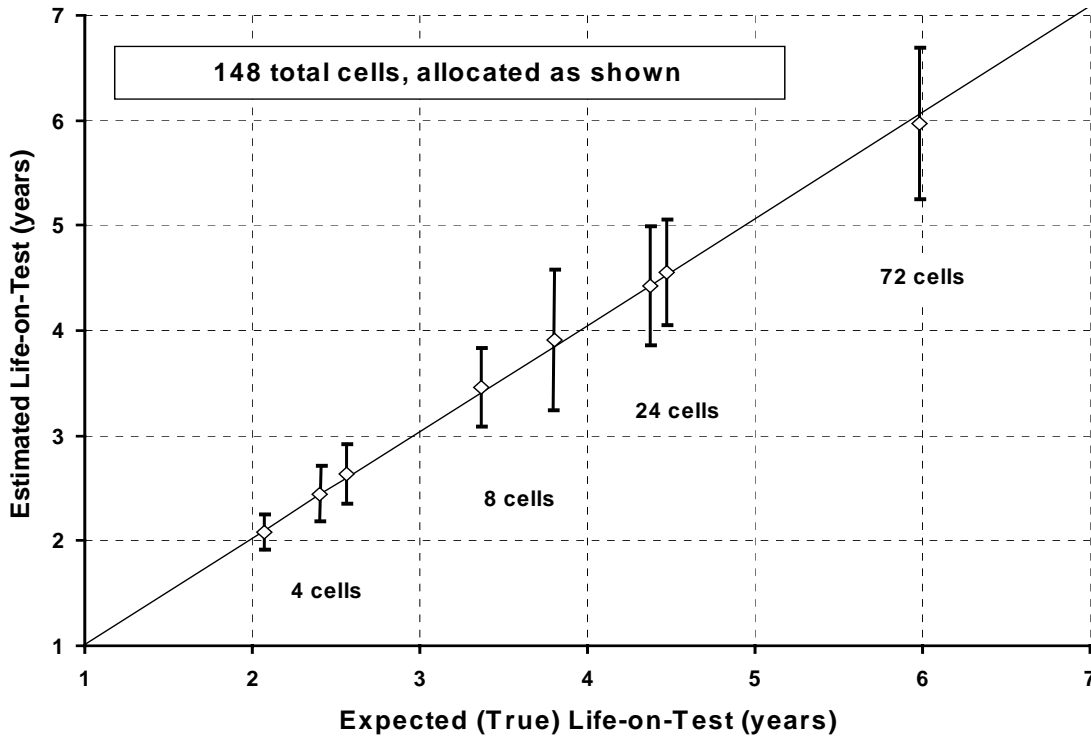


Figure 2.3-1. Results for life test matrix example (estimated ( $\pm 1$  std dev) versus true life on test).

The calendar life at the reference conditions ( $AF = 1$ ) is estimated to be 15.41 years, with a standard deviation of 0.79 year. The 90% lower confidence limits for calendar life and life in service are then 14.3 years and 14.1 years, respectively. This confirms the adequacy of the example core matrix design.

Note that the FreedomCAR goal of 15 years life in service cannot be assured with 90% probability unless the true life in service for the candidate technology exceeds that goal by a significant amount. This is due to the unavoidable presence of noise in the life verification testing.

### 2.3.3 Final Verification Stage

The third and final stage in the design of the life test experiment is to re-verify the design using actual cell manufacturing and initial characterization test data. (See Section 3.1.) The principal data of use from the manufacturing process would be the electrode area variation, which could be estimated from in-process electrode weight data. Alternatively, the variation in cell

capacity from the initial characterization tests could be used as an approximation to the electrode area variation.

The ASI measurements from the initial characterization tests are analyzed to verify that the cell-to-cell variations and ASI measurement errors are as expected. Each life test cell will have two ASI measurements to be used in this analysis—both at the 30°C reference temperature. The ASI measurements will be adjusted on the basis of the variation in the actual cell temperatures, relative to the nominal temperatures. The measured ASI temperature sensitivity for the cells will be used to make these adjustments (see Appendix B).

As presented in more detail in Section 4.1, the cells' ASI data are plotted such that the values at the maximum SOC are on the X-axis and the corresponding values at the minimum SOC are on the Y-axis. Ideally, these data will fall on a single straight line with no variation from cell to cell. In practice, there will be scatter about the line. The cell-to-cell variation can be distinguished from the measurement-to-measurement variation by variance components analysis. In the event that the magnitude of the estimated cell-to-cell variations and ASI measurement errors do not agree with the values assumed in the original design of the experiment, the series of 100-trial simulations should be rerun with the new estimates.

The results of this analysis may indicate that corrective actions are required to achieve the goals of the life test experiment. Such actions could include the following:

1. Upgrading the test facilities/test procedures to reduce ASI measurement error.
2. Adding cells to one or more of the test conditions.
3. Extending the test duration, especially for test conditions with the longest expected lives on test.
4. Culling of cells from the population to reduce the cell-to-cell variation, and manufacturing additional cells to populate the core and supplemental matrices.

## **2.4 Supplemental Life Test Matrix Design Requirements**

The primary objective of supplemental life testing (where used) is to confirm the validity of assumptions that are made in defining the core life test matrix, typically in order to reduce the core matrix to a manageable size. Each such assumption can be assessed experimentally by comparison with a result from the core life test matrix. The following assumptions are considered to be the most likely to need such confirmation:

1. The future state of health (SOH) of a cell depends only on the present SOH and future stresses, independent of the path taken to reach the present SOH.
2. Cold-start operation (i.e., cold cranking) does not have an adverse effect on cell life.
3. Low-temperature operation, within accepted performance constraints, does not have an adverse effect on cell life.

For each of these assumptions, a corresponding experimental plan is described in the following sections. In all cases, the assumptions are posed as null hypotheses to be assessed at an acceptable level of Type I error. The Type I error is the probability that the null hypothesis is rejected when it is in fact true. The appropriate analyses of the supplemental test results are described later in Section 4.

Additionally, a small group of selected cells (typically four) will be subjected to the same test conditions as one of the high AF groups of the core life test matrix, except that these cells will use the full HPPC test for their RPT regime. Data from these cells will be used to identify and isolate possible aging effects on the shape of the pulse power capability curve for aging cells. No formal hypothesis testing is involved, and a detailed experimental plan is not provided for this group of cells.

#### **2.4.1 Experimental Plan to Assess Path Independence**

The null hypothesis for this supplemental test is: the rate of change in ASI depends only on the present value of ASI and the applied stress factors, not on the history of use that resulted in the present value of ASI.

The experimental plan is to conduct combined calendar life and cycle life test regimes on two groups of cells in alternate sequences of exposure to the regimes. For example, the plan for this test corresponding to the minimum core life test matrix example of Section 2.3 would be to test alternately in the Calendar Life 3 test condition ( $T = 55^{\circ}\text{C}$ ) and in the Cycle Life 4 test condition ( $T = 55^{\circ}\text{C}$ ,  $P/P_{RATED} = 100\%$ ). One group would be tested in the cycle life regime until it had reached about half of its expected ASI increase for that regime, and then switched to the calendar life regime. The second group would be started on the calendar life regime and switched to the cycle life regime at the same ASI increase as the switchover for the first group. The switchover of the second group would occur at a later time than the switchover for the first group. The ASI data for the two groups, measured at the same frequency as for the core matrix life tests, would be compared to the ASI data for cells in the core life test matrix under the same conditions.

The criterion for rejecting the null hypothesis would be based on statistically significant differences in the ASI rates of change among the four groups. In the core matrix example design in Section 2.3, eight cells were allocated to the Calendar Life 3 condition and four cells to the Cycle Life 4 condition. Comparable numbers of cells would be used in the corresponding supplemental tests.

Selection of specific test conditions to use in making the comparison with the core matrix test results involves tradeoffs of relative ASI degradation “signal” versus the “noise” (standard deviation) in the estimated ASI degradation. High acceleration factors provide good signal to noise, but the differences between the core matrix and supplemental matrix values of life on test may be easier to detect for lower total ASI degradation. Such a tradeoff should be evaluated for any proposed supplemental test condition.

#### **2.4.2 Experimental Plan to Assess Cold-Start Operation**

The null hypothesis for this supplemental test is that periodic cold cranking does not adversely affect battery life.

It will not be practical to duplicate the significant number of cold starts that may be required of the vehicle in the most extreme climates in which it is to be marketed. Instead, two supplemental groups of cells will be tested in the cold cranking regime as part of their periodic reference performance test (RPT). Otherwise their RPT will be the same as for the corresponding groups in the core matrix. To maximize the possible interactive effects of cold-cranking on life, the test conditions for these two supplemental groups would be the same as for the core matrix cells in the Calendar Life 3 and Cycle Life 4.

In a two-year test duration, this would imply only 27 cold-cranking tests for these cells. However, the expected increases in ASI for these cells would be near the maximum, thus allowing an assessment of how the performance degradation correlates with degradation in cold-cranking capability. More frequent cold-cranking tests could be used for these groups, but it could make a direct comparison with the corresponding core matrix cells more difficult. Appropriate numbers of cells for these groups would be the same as for the core matrix cells with the same expected lives on test.

The criterion for rejecting the null hypothesis would be based on statistically significant differences in the ASI increases over the test duration among the four groups.

### **2.4.3 Experimental Plan to Assess Low-Temperature Operation**

The null hypothesis for this supplemental test is that battery operation at low temperatures does not adversely affect battery life.

This supplemental test is unique in that the test conditions cannot be matched to any of the core matrix test conditions. For that reason, the conditions for the test need to be reasonably extreme to detect any enhanced ASI increase. On the other hand, any failure mechanism associated with low-temperature operation should be well understood before life verification testing. If operating limits have been identified to avoid adverse effects on life, the test would be conducted at those limits (e.g., maximum operating SOC, but limited regenerative pulse power). One possible plan is to use two groups of cells, one control group operating well within the specified limits, and one operating exactly at the limits. The number of cells in each group would have to be determined on the basis of the acceptable error in rejecting the null hypothesis when it should be accepted. As with the other test conditions, the criterion for rejection would be based on a comparison of the ASI increases for the two groups. A further criterion could also be the absence of any physical diagnostic evidence showing that the two groups experienced different low-temperature failure mechanisms. If this is included in the hypothesis test, the number of cells could be minimized for this part of the supplemental matrix. No fewer than four cells per group would be recommended in any case.

### **3. LIFE TEST PROCEDURES**

Successful battery technology life verification will require careful implementation of the procedures specified in this section. The procedures described in the following sections are grouped into initial characterization (Section 3.1), core matrix life test (Section 3.2), and supplemental life test (Section 3.3). Several performance test procedures are incorporated by reference to existing FreedomCAR battery test manuals. Test facility measurement and data recording requirements are provided in Appendix E. It is assumed throughout that the test articles are individual battery cells sized to meet the performance ratings of at least one FreedomCAR battery system target application.

The initial cell characterization tests fall into two categories: basic tests applied to all cells and additional tests applied only to selected cells. Basic tests, all conducted at the nominal reference temperature of 30°C, include (a) capacity verification at a nominal C/1 discharge rate; and (b) pulse power verification using a minimum pulse power profile at only two states of charge. Additional characterization tests on selected cells, for all temperatures to be used in the life tests, include (a) open-circuit voltage measurement versus state of charge, (b) pulse power verification using the standard hybrid pulse power characterization (HPPC) procedure, (c) self-discharge, (d) cold-cranking power verification (low temperature only), and (e) AC electrochemical impedance spectral analysis. Cells receiving the additional characterization tests will not be used in the core life test matrix, and may be used only selectively in the supplemental life test matrix.

Core matrix life tests include both calendar/standby at open-circuit and cycling tests at various levels of pulse power relative to the cell rated power. All core matrix tests are conducted at elevated temperature, with periodic reference performance tests (RPTs) at the nominal reference temperature. The RPTs for the core matrix will be limited to application of the minimum pulse power characterization (MPPC) profile at two states of charge at the test temperature and the reference temperature. The states of charge will correspond to the maximum and minimum values intended for normal battery operation, as defined by the corresponding open-circuit voltages. The RPT will include measurement of the available capacity (at C/1 rate) between the two limiting states of charge.

Three types of supplemental life test are envisioned as part of the overall technology life verification program. They include (a) combined calendar and cycle life, (b) periodic verification of cold-cranking power, and (c) verification of low-temperature operation. Results from these supplemental tests will be compared with core matrix test results to assess the effects, if any, of the supplemental test conditions on the projected life in service for the candidate technology.

#### **3.1 Initial Characterization Tests**

The objectives of the initial cell characterization are to (1) establish the appropriate test parameters consistent with accepted technology limitations and requirements for the target application, (2) verify the initial capabilities of the life test cells, and (3) verify the readiness of the test facilities to meet the data acquisition requirements of the program. Although the two categories of characterization testing are presented first for all cells, followed by tests for only selected cells, they will be conducted in a logical sequence to provide the appropriate flow of information from one test to the next.

This manual primarily deals with life testing and the associated reference performance testing. The minimum regime of initial characterization tests is also described. Note that such

tests are generally application dependent. The test procedures specified in the following are based on the power assist application and should be modified appropriately for life testing directed at other applications (References 8-11).

### 3.1.1 General Test Conditions and Scaling

Certain standard checks should be made of all cells in their as-received condition to ensure that the cells have not been damaged in shipment to the test facility. These checks will minimally include (a) visual inspection for damage, (b) measurement of open-circuit voltage, and (c) a reference measurement of AC impedance at 1 kHz. All cells should also be weighed on receipt.

A life test regime must establish and maintain a consistent set of conditions under which tests are conducted. These include device environment (primarily temperature), test limitations imposed by either the application or the device under test, and the appropriate scaling of test loading for the target application.

Accurate temperature control and measurement is especially important during the reference performance tests because they are used to track performance changes over time, which are the basis for verification of life. The default temperature for the characterization and reference performance tests specified in this manual is the reference temperature of 30°C. All testing should be conducted using environmental chambers.

Operating limits for the test articles may vary between target applications, and may include technology-specific constraints. In this manual, such limits are assumed to be controlled as required to meet the objectives of the life verification testing, and implemented in modified test procedures as appropriate.

The allowable operating voltage range (and by implication the allowable state of charge range) for a device is established by the manufacturer. For purposes of this manual, an application-specific operating range (that may be a subset of this allowable range) is specified, typically in a test plan for the life test program. This range extends from  $SOC_{MAX}$  to  $SOC_{MIN}$ , and the standard MPPC reference testing for all cells is conducted over this range. In addition to manufacturer operating limits, the following guidelines should be considered for choosing these test limits: (a)  $SOC_{MAX}$  should generally be equal to the maximum test SOC used in the core life test matrix; (b)  $SOC_{MIN}$  can be equal to the minimum test SOC used in the core life test matrix, provided that the MPPC pulse profile at  $SOC_{MAX}$  will not bring the SOC below this value. (Otherwise  $SOC_{MIN}$  will need to be a lower value to avoid the need to recharge the cell before the second pulse profile can be performed.) During life testing, these SOC values are not measured directly; instead the corresponding open circuit voltages are used to represent them. (See the Glossary for more information on  $SOC_{MAX}$  and  $SOC_{MIN}$ .)

Scaling of test loads is necessarily done using the methods defined for the target application, so that performance can fairly be compared to the application goals. Test power levels for devices targeted to power assist applications are scaled using a “battery size factor” (BSF) which is defined as “the minimum number of cells or modules expected to be required to meet all the FreedomCAR performance and life goals.” The determination and use of the BSF is described in detail in Reference 8. The minimum characterization tests for all cells described in this manual do not depend on such application-based scaling, although cycle life test profiles are application-specific.

### 3.1.2 Minimum Characterization for All Cells

Two basic characterization tests will be conducted for all cells in the overall life verification program: (1) verification of rated capacity at the C/1 rate and (2) verification of pulse power capabilities at the minimum and maximum SOCs. Both tests will be conducted only at the reference temperature.

#### 3.1.2.1 Capacity Verification

The static capacity test will consist of (a) a recharge to 100% SOC, using the manufacturer's recommended procedure, (b) a one-hour rest at open-circuit, and (c) a constant-current discharge at C/1 rate to the manufacturer's recommended cutoff voltage. This sequence will be repeated a minimum of three times until three successive discharge capacities agree within a total spread of 2%.

#### 3.1.2.2 Pulse Power Verification (MPPC)

Initial verification of all cells' pulse power capabilities will be done using the following minimum pulse power characterization (MPPC) procedure. This test is an abbreviated version of the low current hybrid pulse power characterization (HPPC) test described in Reference 8. The current-based pulse profile used for the MPPC is identical to that for the HPPC. For power assist applications, pulse currents are 5C and 3.75C for the 10-second discharge and regenerative pulses, respectively, which are separated by a 40-second rest interval.

The MPPC sequence is as follows:

1. The cell is recharged at a maximum rate of C/1 to the maximum SOC ( $SOC_{MAX}$ ), based on the corresponding open-circuit voltage (OCV) determined from the OCV versus SOC characterization test described in Section 3.1.3.1 below. A taper current is used to complete the recharge to the specified OCV, within the limit of a specified minimum taper current. (See Section 3.1.1 and the Glossary for more information on  $SOC_{MAX}$  and  $SOC_{MIN}$ .)
2. The cell is allowed to rest at open-circuit for one hour.
3. The specified MPPC profile is applied, followed by discharge at the maximum rate of C<sub>1</sub>/1 to the minimum SOC ( $SOC_{MIN}$ ). A taper current is used to complete the discharge to the corresponding specified minimum OCV.
4. The cell is allowed to rest at open-circuit for one hour.
5. The specified MPPC profile is applied.

### 3.1.3 Additional Characterization of Selected Cells

Additional characterization tests will be conducted on a limited number of cells to meet the following objectives: (1) mapping of OCV versus SOC to determine the OCVs that correspond to the specified minimum and maximum SOCs, (2) verification of pulse power capabilities over the full range of cell SOC using the HPPC procedure, (3) verification of self-discharge rates, (4) verification of cold-cranking power capabilities, and (5) initial measurement of AC electrochemical impedance spectra (EIS) for comparison with end-of-test spectra. These additional tests will be conducted at all specified test temperatures to be used in the core life-test matrix, including the reference temperature. Recommendations for numbers of cells for each of these additional tests are provided in the following.

### **3.1.3.1 Open-circuit Voltage versus State of charge**

The procedure to measure OCV versus SOC is as follows:

1. Recharge the cell to 100% SOC using the manufacturer's recommended procedure.
2. Allow the cell to rest at open-circuit for a minimum of one hour, or until the voltage has reached a stable condition. (See the Glossary for information.)
3. Discharge the cell at a maximum rate of C/1 for a specified fraction (e.g., 5%) of the rated capacity.
4. Allow the cell to rest at open-circuit for a minimum of one hour, or until the voltage has reached a stable condition.
5. Repeat steps 3 and 4 above until the manufacturer's recommended minimum discharge voltage is reached.

This test should be conducted on a minimum of two cells at each temperature.

### **3.1.3.2 Pulse Power Verification**

The HPPC procedure of Reference 8 (for power assist applications) will be used to verify the cells' pulse power capabilities over the full range of SOC. In addition to the normally specified values of SOC used in this test, the HPPC profile should also be applied at the minimum and maximum specified SOCs. (This may require a separate test in some cases.) To enable comparison of these results with those obtained using the MPPC, a minimum of eight cells should be tested at each temperature to be used for life testing.

### **3.1.3.3 Self-discharge Rate Characterization**

The self-discharge test of Reference 8 will be used to estimate the rate of cell self-discharge from  $SOC_{MAX}$  as a function of test temperature. The normal test duration of one week may be reduced for any cells that reach  $SOC_{MIN}$  prior to the end of this test. A minimum of two cells is recommended for each test temperature. (This testing may be considered optional for cell designs whose self-discharge behavior is already well-characterized, since the general behavior is also observable during calendar life testing.)

### **3.1.3.4 Cold-cranking Power Verification**

Depending on the target application, the cold-cranking test procedure of the appropriate FreedomCAR manual (References 8-11) will be conducted on all cells selected for the supplemental test conditions of Section 2.4.2. The appropriate cold-cranking power profile will be applied at both the maximum and minimum SOCs. Note that the same test procedure will be used in the periodic RPTs applied to the cells of the cold-cranking portion of the supplemental life-test matrix (Section 3.3.2).

### **3.1.3.5 AC Electrochemical Impedance Spectrum (EIS) Testing**

An initial full-spectrum sweep of AC complex impedance (as defined in a cell-specific test plan) will be conducted only for the cells to be life tested in the supplemental life-test matrix. Results from this beginning of life characterization will be compared to results obtained for all cells (from both supplemental and core matrices) at the end of life testing. These comparisons will be used to help identify any anomalous cell characteristics for the several test conditions used in the overall experiment.

### 3.1.4 BOL Reference Testing

An initial MPPC reference test will be performed at the beginning of life testing on all cells. This test will be executed at the reference temperature (nominally 30 °C) just prior to initial heatup, and then again at the life test temperature for each cell immediately after heatup. Results of these BOL tests will form the baseline for comparison with later reference performance tests, which will be performed at the end of each life test interval.

## 3.2 Core Life Test Matrix

The objectives of the core matrix life tests are to expose the test cells to the specified conditions that are intended to accelerate the cells' performance degradation in a controlled, measurable manner. The key accelerating stress factor will be cell temperature. Calendar life tests will be conducted with cells at open-circuit to simulate actual standby (key-off) conditions in the vehicle. Cycle life tests will be conducted at various power profiles, none of which will require the cells to exceed their performance ratings. Test conditions for the core matrix will be invariant over the full duration of the life testing, except when performing periodic reference performance tests which require temperature cycling from the specified test temperatures down to the reference temperature and back to the test temperatures. General requirements for the Technology Life Verification Test facilities are provided in Appendix E.

The core life test matrix defined as in Section 2.3 is implemented by subjecting the various groups of cells to the matrix test conditions using one of two common test procedures. Cells that are to be tested at conditions not including load stresses follow the stand life (calendar life) test procedure. Cells whose stressors include some type of operating load cycle follow the cycle life (operating) test procedure.

### 3.2.1 Stand Life (Calendar Life) Testing

Test setup requirements and the specific calendar life procedure are presented in the following.

#### 3.2.1.1 Calendar Life Test Setup Requirements

Specific calendar life test setup and control requirements are as follows:

- All calendar life test cells will be kept in an open-circuit condition during exposure to the test temperature.
- Cell voltages will be monitored using standard high-impedance sensing circuits, with recording of voltage data every hour or less depending on the test temperature.
- As cells self-discharge to the voltage corresponding to  $SOC_{MIN}^2$ , they will be recharged at a specified rate (e.g.,  $C_1/1$ ) back to the calendar life SOC. Measure and record the total capacity required for this recharge operation, including final taper charge.
- Cells at any given test temperature should be contained in a single temperature-controlled chamber with adequate provisions for maintaining the cells at a uniform temperature with minimum fluctuations over time.
- All cells at any given test temperature must have their RPTs conducted at the same time at a fixed time interval between each RPT.

---

<sup>2</sup> A manufacturer-specified voltage limit less than this would be required if calendar-life testing were done at or below  $SOC_{MIN}$ .

- Whenever possible, the same test equipment should be used for all RPTs on a given cell throughout life testing.

### **3.2.1.2 Calendar Life Test Procedure**

Following an initial MPPC reference performance test, the following sequence of test operations is repeated for intervals as specified in Table 3.2-1 (or in a detailed test plan) until an end-of-test condition is reached for each designated calendar life test cell.

#### 1. Heatup:

- Charge the cell to a stable SOC condition at the SOC value specified by the test matrix.<sup>3</sup> (See the Glossary for more information on stable SOC condition.) Place the cell in an open-circuit condition.
- Increase cell temperature to the specified test temperature at the specified rate
- (For the first life test interval only, perform an MPPC test at the test temperature.)

#### 2. Stand at test temperature:

- During the open-circuit stand periods, monitor and record cell voltage and temperature as specified in Appendix E.
- If the cell self-discharges to the voltage corresponding to SOC<sub>MIN</sub>, recharge the cell back to the calendar life SOC.

#### 3. Reference testing at test temperature:

- When the specified RPT interval is reached, perform the MPPC test as described in Section 3.1.2.2.

#### 4. Reference Testing at Reference Temperature:

- Reduce cell temperature to the reference temperature (30°C) at the specified rate.
- Perform the MPPC test as described in Section 3.1.2.2.
- If testing is continuing, return to Step 1 above.

### **3.2.2 Cycle Life (Operating) Testing**

Test setup requirements and the specific cycle life procedure are presented in the following. The development of specific power profiles to be used in the cycle life tests will use the methods of Reference 13.

#### **3.2.2.1 Cycle Life Test Setup Requirements**

Specific cycle life test setup requirements are as follows:

- Cycle life tests will be conducted using power-based profiles, with provisions for maintaining charge neutrality over time at the specified state-of-charge.
- Power profiles will be based on the appropriate FreedomCAR target application requirements. (See References 8-11 for application-specific profiles.)

---

<sup>3</sup> Except as otherwise defined, *specified* means as specified in a test plan for the cell life test program. Parameters such as heatup and cooldown limits are necessarily technology- and device-dependent.

- Measure and record cell voltage, current and temperature during cycling and RPTs at specified intervals and conditions as described in Appendix E.
- Cells at any given test temperature and power profile should be contained in a single temperature-controlled chamber with adequate provisions for maintaining the cells at a uniform temperature with minimum fluctuations over time.
- All cells at any given test temperature and power profile must have their RPTs conducted at the same time at a fixed time interval between each RPT.
- Whenever possible, the same test equipment should be used for all RPTs on a given cell.

### **3.2.2.2 Cycle Life Test Procedure**

Following an initial MPPC reference performance test, the following sequence of test operations is repeated for intervals as specified in Table 3.2-1 (or in a detailed test plan) until an end-of-test condition is reached for each designated cycle life test cell.

#### **1. Heatup:**

- Charge the cell to a stable SOC condition at the SOC value specified by the test matrix. (See the Glossary for more information on stable SOC condition.)
- Place the cell in an open-circuit condition.
- Increase cell temperature to the specified test temperature at the specified rate.
- (For the first life test interval only, perform an MPPC test at the test temperature.)

#### **2. Cycling:**

- Conduct a sequence of 100 or more of the specified power profiles to verify that charge neutrality is being maintained.
- Continue application of the specified power profiles for the specified number of profiles.

#### **3. Reference Testing at Test Temperature:**

- When the specified RPT interval is reached, perform the MPPC test as described in Section 3.1.2.2.

#### **4. Reference Testing at Reference Temperature:**

- Reduce cell temperature to the reference temperature (30°C) at the specified rate.
- Perform the MPPC test as described in Section 3.1.2.2.
- If testing is continuing, return to Step 1.

### **3.2.3 Reference Performance Tests and End-of-Test Criteria**

Reference performance tests (RPTs) are performed (a) before the start of life testing, (b) at defined periodic intervals, and (c) at end of testing, for all devices undergoing either cycle life testing or stand life (calendar life) testing.

The minimum reference performance test regime during life testing consists of performing the minimum pulse power capability (MPPC) test at both the test temperature and the reference temperature (30°C).

Table 3.2-1. Reference performance test intervals for life testing.

Type of Life Testing	Interval Between RPTs	Reference Performance Tests
Cycle life testing	A number of cycle life profiles corresponding to (typically) 4 weeks (fixed intervals)	Minimum Pulse Power Characterization Test (plus cold-cranking test for selected cells, as described in Section 3.3.2)
Calendar life testing	Typically 4 weeks (fixed intervals)	
Combined calendar/ cycle life testing	Same interval as used for other cells undergoing Calendar or Cycle Life testing	

End-of-test conditions will be defined in a test plan for the life test program. Common end-of-test conditions include (a) RPT performance is less than the applicable FreedomCAR goals, or (b) sufficient data are acquired to project cell life with the required degree of confidence. Inability to perform the required test regime is automatically an end-of-test condition.

### 3.3 Supplemental Life Tests

The objective of the supplemental life tests is to assess the effects of potentially significant variations in operating and reference test conditions on battery life. Three such variations have been identified as candidates for inclusion in a technology life verification program. Other variations may be appropriate for some technologies. Because candidate technologies are expected to be insensitive to these variations, the supplemental life tests are designed to verify null hypotheses by comparison with similar tests from the core matrix. This reduces the number of test conditions required in the core matrix to just the essential calendar and cycling variations.

The three identified supplemental test variations are (1) alternate sequences of combined calendar and cycle life conditions to verify the path-independence of the cell performance degradation, (2) application of cold-cranking tests as part of the periodic RPT regime, and (3) cycling at low temperature. Test setup requirements and procedures for these supplemental life tests are provided in the following sections.

#### 3.3.1 Combined Calendar and Cycle Life Tests

Requirements and procedures for the combined calendar and cycle life supplemental tests are identical to those for the corresponding groups of cells in the core life test matrix. A minimum of two groups of cells will be tested using the following sequences.

##### 3.3.1.1 *Cycle Life/Calendar Life Sequence*

One group will be tested under the specified cycle life test conditions until the cells, on average, reach one-half of the expected ASI increase for the given test condition. The cells will then continue testing under the specified calendar life test conditions for the remainder of the overall test program.

##### 3.3.1.2 *Calendar Life/Cycle Life Sequence*

The second group will be tested under the specified calendar life test conditions until the cells, on average, reach the same value of ASI increase as the first group (Section 3.3.1.1) reached when they were switched from the cycle life to calendar life regime. These cells will

then continue testing under the specified cycle life test conditions for the remainder of the overall test program.

### 3.3.2 Cold-cranking Power Verification Tests

Two groups of cells will be used in this supplemental life test. One group will be calendar life tested at the same (elevated) test temperature as one of the core life test matrix conditions. The second group will be cycle life tested at the same (elevated) test temperature and pulse power profile as one of the core life test matrix conditions. Both groups will be subjected to a cold-cranking test at each specified RPT interval throughout the duration of the overall test program. The requirements and procedures for the calendar life, cycle life, and cold-cranking tests are as previously specified above. The cold-cranking test will be inserted into the two life test sequences (in Section 3.2.2.1 or 3.2.2.2 as appropriate) just after the completion of the normal MPPC test at the reference temperature, as follows:

After completion of the MPPC profile at  $SOC_{MIN}$ ,

- a. Recharge the cell to  $SOC_{MAX}$ , including taper charge to the specified cutoff taper current.
- b. Reduce the cell temperature to the specified temperature for the cold-cranking test at the specified rate.
- c. Perform the cold-cranking test profile in accordance with Section 3.1.3.4.
- d. Discharge the cell to  $SOC_{MIN}$  at a maximum  $C_1/1$  constant current rate, including taper discharge to the specified cutoff taper current.
- e. Perform the cold-cranking test profile.
- f. Increase the cell temperature to the specified reference temperature at the specified rate.

The life testing regime is then resumed by returning to Step 1 of the appropriate procedure.

### 3.3.3 Low-temperature Operation Tests

Two groups of cells will be used in this supplemental life test. Both groups will be cycle life tested at  $SOC_{MAX}$ , each at a different specified test temperature below the reference temperature. The power profile will be the same for both groups, with a limited regenerative pulse power to be specified by the cell manufacturer. This special power profile will be developed and agreed upon jointly by FreedomCAR and the manufacturer. It will be applied at both test temperatures, with the expectation that there will be no difference in the life-on-test between the two groups. *Note that the normal reference tests will not be performed at (low) test temperatures for these cells.*

Following an initial MPPC reference performance test, the cells designated for low-temperature cycle life testing are brought to the voltage corresponding to  $SOC_{MAX}$  at the reference temperature. The following sequence of test operations is then repeated for the duration of the overall test program for intervals specified in Table 3.2-1 (or in a detailed test plan).

#### 1. Cooldown:

- Maintain the cell at open-circuit condition.
- Reduce cell temperature to the specified test temperature at the specified rate.

2. Cycling at (Low) Test Temperature:

- Conduct a sequence of 100 or more of the specified power profiles to verify that charge neutrality is being maintained.
- Continue application of the specified power profiles for the specified number of profiles between successive RPTs.

3. Reference Testing at Reference Temperature:

- Increase cell temperature to the reference temperature (30°C) at the specified rate.
- Perform the MPPC test as described in Section 3.1.2.2.
- Taper recharge the cell to  $SOC_{MAX}$ .
- If testing is continuing, return to Step 1.

## 4. DATA ANALYSIS AND REPORTING

The objectives and methods for analysis and reporting of the overall program data and results are provided in this section. All analyses are directed at reaching a valid conclusion regarding the life capabilities of the candidate technology.

Section 4.1 addresses the analysis and reporting requirements for the initial characterization test results. The principal objectives are to establish the baseline performance of the test cell population, assess the variability of the population, and assign cells from the population to the core and supplemental life test matrices.

Section 4.2 addresses the data analysis for the core life test matrix cells, and the methods of interpreting these data to estimate the life in service for the technology. The two estimates of primary concern are the mean and 90% lower confidence limit for the life in service, based on the estimated means and standard deviations for the lives on test at the several test conditions.

Section 4.3 addresses the data analyses required to support the null hypothesis tests for the lives on test at the supplemental test conditions.

Additional details of the data analysis methods are provided in Appendix B, along with examples of their application to typical life test data from DOE's ATD program.

### 4.1 Initial Performance Characterization Test Results

The baseline performance of the test cell population will be established in the following sequence of analyses. Details for the steps of this sequence are provided in Sections 4.1.1 through 4.1.10 respectively.

1. Map cell open-circuit voltage (OCV) data versus state of charge (SOC), relative to the  $C_1/1$  capacity, to determine the OCVs corresponding to the maximum and minimum operating SOCs. (Selected cells only, data from Section 3.1.3.1)
2. Estimate the means and standard deviations for the  $C_1/1$  capacity, and for the available capacity between the maximum and minimum operating SOCs. (All cells, data from Section 3.1.2.1 and 3.1.2.2.)
3. Estimate the derivative  $dASI/dT$  and the adjusted ASI at the reference temperature from ASI data obtained using the both MPPC and HPPC procedures at the reference temperature and elevated temperatures. (Selected cells only, data from Sections 3.1.2.2 and 3.1.3.2)
4. Estimate the means and standard deviations for the adjusted ASIs at the two SOC limits at the reference temperature, as measured by the MPPC procedure. (All cells)
5. Estimate the means and standard deviations for the adjusted ASIs at the two SOC limits at the reference temperature, as measured by the HPPC procedure. Test the null hypothesis that the MPPC-based ASIs are equivalent to the HPPC-based ASIs. (Selected cells only)
6. Rank the data by  $C_1/1$  capacity, ASI at maximum SOC, and ASI at minimum SOC to assign cells to the core and supplemental life test matrices. (All cells)
7. Estimate the means and standard deviations of the measured self-discharge rates at all temperatures. (Selected cells only, data from Section 3.1.3.3)
8. Estimate the mean and standard deviation of the measured cold-cranking power. (Selected cells only, data from Section 3.1.3.4)

9. Examine the AC electrochemical impedance spectra (EIS) for anomalous characteristics. (Selected cells only, data from Section 3.1.3.5)
10. Assess the variability in the cell population to estimate the magnitudes of noise in the ASI data from cell-to-cell manufacturing variations, and from ASI measurement errors.

#### 4.1.1 Determination of Open Circuit Voltage versus State of Charge

For each temperature tested, plot the measured OCVs for all cells tested against the corresponding SOC<sub>s</sub> and develop curve fits of these data for the averaged values of OCV, excluding cells with any anomalous OCV values.<sup>4</sup> The SOC values will be based on the actual total capacity of each cell:

$$SOC(\%) = 100 \times \frac{(Actual\ Capacity - Capacity\ Removed)}{Actual\ Capacity}$$

From the curve fits, determine the OCVs corresponding to SOC<sub>MAX</sub> and SOC<sub>MIN</sub> at all temperatures.

#### 4.1.2 Capacity Verification

For all cells at the reference temperature, calculate the average total C<sub>1</sub>/1 capacity for the final two discharge cycles. Calculate the mean and standard deviation of these C<sub>1</sub>/1 actual capacities for the cell population. Verify that the distribution(s) appear to be unimodal and approximately normal. Identify any outlier cells with capacities that differ more than three standard deviations from the mean. If necessary, recalculate the mean and standard deviation in capacity after excluding all outlier cells.

Also, for all cells at the reference temperature, estimate the capacity available at the C<sub>1</sub>/1 discharge rate between the two OCVs corresponding to SOC<sub>MAX</sub> and SOC<sub>MIN</sub>. For this purpose, use the measured capacity data from the MPPC test. Calculate the mean and standard deviation of these available capacities, after identifying and excluding outlier cells as was done for the total C<sub>1</sub>/1 capacities.

#### 4.1.3 Determine Temperature Coefficient of ASI (Selected Cells)

The ASI adjustment procedure is intended to eliminate correlated temperature control errors, leaving only the random temperature measurement error.

ASI measurements at the reference temperature (30°C) and any elevated temperature, T<sub>ELEV</sub>, will be used to estimate the temperature sensitivity of ASI at the reference temperature. An Arrhenius function is assumed:

$$ASI = ASI_{REF} e^{T_{ASI} \left[ \frac{1}{T_{ELEV} + 273.15} - \frac{1}{T_{REF} + 273.15} \right]}$$

where

ASI<sub>REF</sub> = ASI at the reference temperature, and

---

<sup>4</sup> Polynomial fits can be used in well-behaved cases, but piecewise-linear interpolation gives more broadly usable results.

$$T_{ASI} = \frac{\ln(ASI_1/ASI_2)}{\frac{1}{T_1 + 273.15} - \frac{1}{T_2 + 273.15}}$$

for any two ASI measurements on the same device(s) at two temperatures  $T_1$  and  $T_2$ , with all other conditions (e.g., SOC) the same.

The value of  $ASI_{REF}$  is then found (based on the assumed Arrhenius function) as

$$ASI_{REF} = \frac{ASI_1}{e^{\left\{T_{ASI} \left[ \frac{1}{T_1 + 273.15} - \frac{1}{T_{REF} + 273.15} \right] \right\}}} = \frac{ASI_2}{e^{\left\{T_{ASI} \left[ \frac{1}{T_2 + 273.15} - \frac{1}{T_{REF} + 273.15} \right] \right\}}}.$$

Note that at least one of the temperatures  $T_1$  and  $T_2$  should be significantly different from  $T_{REF}$ .

This computed value of  $ASI_{REF}$  is used for comparisons between different iterations of the reference performance test, since it represents the best estimate of the device ASI at the (fixed) reference temperature.

A measured ASI value at any nominal test temperature  $T_{NOMINAL}$  can be similarly corrected by substituting  $T_{NOMINAL}$  for  $T_{REF}$  above.

These adjustments are to be made for each ASI measurement from the MPPC reference performance tests. The test temperature for the specific life test condition should be the datum for the second ASI measurement.

#### 4.1.4 Pulse Power Verification (MPPC)

For all cells at the reference temperature, determine the ASI values from the MPPC test, where the ASI is calculated using the measured cell resistance times the nominal electrode area. The cell resistance values will be calculated from the voltage and current measurements using the “Lumped Parameter Battery Model” defined in Appendix D of Reference 8. (The parameter values obtained for the cells should be recorded in the cell database for future reference.)

Adjust the measured ASI values using the measured cell temperatures in accordance with the procedure specified in Section 4.1.3. For the initial characterization tests only, where no elevated temperature data are available for most cells, use the average temperature sensitivity coefficient calculated for the selected cells in Section 4.1.5 to adjust the ASI values. Calculate the pulse power capabilities for all cells at the reference temperature at the two SOCs using the BSF for the target application specified for the life verification program.

Calculate the mean and standard deviation of these adjusted ASI values at the two SOCs for the cell population. Verify that the distribution(s) appear to be unimodal and approximately normal. Identify any outlier cells with ASI values that differ more than three standard deviations from the mean. If necessary, recalculate the mean and standard deviation in the ASIs after excluding all outlier cells.

#### 4.1.5 Pulse Power Verification (HPPC)

For the selected cells tested using both the MPPC and HPPC procedures, calculate the measured ASI values at all DODs/SOCs and temperatures. As previously noted, the measured

ASIs will be calculated using the cell resistances estimated using the “Lumped Parameter Battery Model” of Reference 8, Appendix D. As specified in Section 4.1.3, use measured cell temperatures to obtain adjusted ASI values at the reference temperature and at the nominal test temperatures.

Compare the adjusted ASI values at each temperature and the two SOC<sub>s</sub> obtained using the MPPC with the corresponding values obtained using the HPPC. Calculate the means and standard deviations for the sub-population of cells (minimum of 8 cells). Next, calculate the following statistic for each temperature and SOC:

$$t = (ASI_{HPPC} - ASI_{MPPC}) \sqrt{\frac{N_{HPPC}}{S_{HPPC}^2 + S_{MPPC}^2}}$$

where

- $ASI_{HPPC}$  = mean adjusted ASI from HPPC test
- $S_{HPPC}$  = standard deviation in adjusted ASI from HPPC test
- $ASI_{MPPC}$  = mean adjusted ASI from MPPC test
- $S_{MPPC}$  = standard deviation in adjusted ASI from MPPC test
- $N_{HPPC}$  = number of cells used in the HPPC/MPPC comparisons.

For a level of significance of 0.05, the null hypothesis that the two means are not significantly different must be rejected if  $|t| > t_{0.025}$  for  $(N_{HPPC} - 1)$  degrees of freedom<sup>5</sup>.

For example, if  $N_{HPPC} = 8$  cells, then a table of t-statistics will give the value  $t_{0.025} = 2.365$ . (Note that the 0.025 level needs to be adjusted if the t-test is performed for multiple temperature and SOC conditions. For example, if there are 4 conditions, then 0.025/4 should be used as the level for the individual conditions. Otherwise, the aggregate Type I error will be larger than expected.)

If any of these hypothesis tests results in failure (i.e., rejection of the null hypothesis) the cause must be investigated and resolved to assure the adequacy of the MPPC procedure for its use in the life verification program.

In addition to this analysis, the results of the HPPC test may be used to verify the BSF for the target application (or to determine it if necessary), using the procedure defined in Reference 8.

#### 4.1.6 Rank Ordering of Cells

Tabulate the  $C_1/1$  capacity and adjusted ASIs at the two SOC<sub>s</sub> for the complete cell population, excluding identified outliers. Rank the cells three ways, using capacity and the ASIs each as the sorting criterion. By default, allocation of cells into the core and supplemental life test conditions will be done at random from the center-most cells in the ranking of ASI at SOC<sub>MAX</sub>, excluding cells ranked overly high or low in the other two rankings. This selected subpopulation of cells for life testing will be further checked for acceptable noise characteristics (i.e., agreement with the test matrix design assumptions) using the analysis of Section 4.1.10.

---

<sup>5</sup> The t-statistic can be calculated using the TINV() function in Microsoft Excel, or it can be looked up in a statistical reference book.

#### 4.1.7 Self-Discharge Rate Characterization

Calculate the average self-discharge rate (in Ah per day) for the cells tested at each temperature, using periodic measurements of OCV over the one-week test duration. The end-of-test OCV is used to estimate the final SOC (using the results of Section 4.1.1) and average loss rate, which are also confirmed by the residual discharge at the end of the test. These data may be used to develop a correlation between self discharge and SOC (voltage) and to predict the frequency of recharge needed to maintain the calendar life test cells within the specified minimum and maximum SOCs. Plot the estimated self-discharge rates versus test temperature for all cells tested to determine the level of consistency in these data. If necessary to obtain reliable estimates, repeat the self-discharge tests at selected temperatures using additional cells.

#### 4.1.8 Cold-Cranking Power Verification

For each selected cell, calculate the pulse resistance and cold-cranking power capability at beginning of life for each of the three test pulses at the two SOCs using the method described in Reference 8, Section 4.5. Also compute the estimated mean and standard deviation of the resistance and cold-cranking power for each of the pulses. (Ignore any data where voltage limiting is encountered during a test pulse.) For each cell tested, plot the pulse resistance from the first pulse versus the ASI at the reference temperature for each of the two SOCs to determine whether outliers are present.

Recalculate the mean and standard deviation after excluding any outliers with first-pulse resistances that differ more than three standard deviations from the mean. If necessary, select additional cells from the population to conduct the cold-cranking test, such that the desired number of cells is obtained for this supplemental test condition.

Verify that the mean measured cold-cranking power capability meets or exceeds the requirement of the target application.

#### 4.1.9 AC EIS Characterization

Examine the AC impedance spectra for anomalous characteristics, primarily in the form of cells whose behavior differs greatly from the average of the test population. This can be done by determining the equivalent series resistance (ESR) and/or the ionic impedance of each cell and plotting these characteristics versus the ASI at the SOC value used for the EIS testing. (Some information on the interpretation of EIS results is found in Appendix C of Reference 11, and in Reference 17.)

#### 4.1.10 ASI Noise Characterization

The variation in ASI measurements for all cells from the initial characterization using the MPPC procedure will be analyzed using the following method. Each adjusted ASI measurement may be seen as the “true” ASI value for the technology, plus a random effect due to cell-to-cell manufacturing variation, plus an independent random error in the ASI measurement. That is:  $ASI_{meas} = ASI_{tech} + \delta_{cell} + \varepsilon_{meas}$ . Without the measurement error, the true (but unobservable) ASI value for a cell is given by  $ASI_{true} = ASI_{tech} + \delta_{cell}$ .

Three sources of variation are considered: cell-to-cell differences in electrode area, cell-to-cell differences in the (fixed) ohmic resistance, and measurement-to-measurement differences in the ASI measurement error. The last of these sources is primarily due to random errors in the cell temperature measurement used to adjust the ASI measurement, plus random errors in the

measured electrical parameters used to calculate ASI. The cell-to-cell effects are assumed to be perfectly reproducible, in the sense that they will be repeatable from measurement to measurement. The measurement variation is assumed to be perfectly uncorrelated, in the sense that it is purely random, with zero mean and constant standard deviation.

The standard deviation of the measurement error ( $\sigma_\varepsilon$ ) can be estimated by considering the relationship between the ASI measurements from the same cell at two different SOC's, denoted by  $SOC_{MAX}$  and  $SOC_{MIN}$ . The assumed underlying relationship between the true ASI values of the  $i^{th}$  cell at the two different SOC's is given by  $ASI_{true(MIN)}^i = \beta_0 + \beta_1 \cdot ASI_{true(MAX)}^i$ . The observed ASI measurements are given by  $Y_i = ASI_{meas}^i(SOC_{MIN}) = ASI_{true(MIN)}^i + \varepsilon_{meas(MIN)}^i$  and  $X_i = ASI_{meas}^i(SOC_{MAX}) = ASI_{true(MAX)}^i + \varepsilon_{meas(MAX)}^i$ . Two procedures for estimating the model parameters ( $\beta_0$  and  $\beta_1$ ) are given here.

The first procedure, simple orthogonal regression, is recommended when there are no anomalous observations with unusually large deviations from the assumed linear relationship. In this case, the estimated model parameters are

$$\hat{\beta}_1 = \frac{S_{YY} - S_{XX} + \sqrt{(S_{YY} - S_{XX})^2 + 4 \cdot S_{XY}^2}}{2 \cdot S_{XY}} \text{ and}$$

$$\hat{\beta}_0 = \bar{Y} - \hat{\beta}_1 \cdot \bar{X},$$

$$\text{where } S_{XX} = \frac{\sum_{i=1}^n (X_i - \bar{X})^2}{(n-1)}, S_{YY} = \frac{\sum_{i=1}^n (Y_i - \bar{Y})^2}{(n-1)}, S_{XY} = \frac{\sum_{i=1}^n (X_i - \bar{X}) \cdot (Y_i - \bar{Y})}{(n-1)},$$

$$\bar{X} = \frac{\sum_{i=1}^n X_i}{n}, \bar{Y} = \frac{\sum_{i=1}^n Y_i}{n},$$

and  $n$  is the number of cells.

The second procedure uses robust orthogonal regression to estimate  $\beta_0$  and  $\beta_1$  (see section 1.2 of Appendix B for details) with  $X_i$  and  $Y_i$  defined as above. This procedure is relatively insensitive to outliers and thus can be useful even when there are a few anomalous observations.

In either case of orthogonal regression (simple or robust), the orthogonal distance from the point  $(X_i, Y_i)$  to the fitted line is given by

$$D_i = \frac{|Y_i - \hat{\beta}_0 - \hat{\beta}_1 \cdot X_i|}{\sqrt{\hat{\beta}_1^2 + 1}}.$$

When simple orthogonal regression is used, an estimate of  $\sigma_\varepsilon$  is given by

$$S_{MEASUREMENT} = \sqrt{\frac{\sum_{i=1}^n D_i^2}{(n-1)}}.$$

When robust orthogonal regression is used, a useful estimate of  $\sigma_\varepsilon$  is given by  $S_{MEASUREMENT} = 1.48 \cdot \text{median}\{D_i\}$ . Estimates of the standard deviation of the variation in ASI measurements ( $ASI_{MAX}$  and  $ASI_{MIN}$ ) induced by manufacturing are given by

$$(S_{MFG})_{MAX} = \sqrt{S_{MAX}^2 - S_{MEASUREMENT}^2} \quad \text{and}$$

$$(S_{MFG})_{MIN} = \sqrt{S_{MIN}^2 - S_{MEASUREMENT}^2}, \quad \text{where}$$

- $S_{MEASUREMENT}$  = estimated standard deviation of the measurement error
- $(S_{MFG})_{MAX}$  = estimated standard deviation of the component of variation in the adjusted ASIs at  $SOC_{MAX}$  induced by manufacturing
- $(S_{MFG})_{MIN}$  = estimated standard deviation of the component of variation in the adjusted ASIs at  $SOC_{MIN}$  induced by manufacturing
- $S_{MAX}$  = standard deviation of the adjusted ASIs at  $SOC_{MAX}$
- $S_{MIN}$  = standard deviation of the adjusted ASIs at  $SOC_{MIN}$

The two estimates for the standard deviation in the manufacturing variations are expected to be nearly equal.

Then, the values of ASI at maximum OCV will be plotted versus the inverse of the  $C_1/1$  capacity to estimate the variations in ASI due to variation in electrode area. (Alternatively, in-process data from the cell manufacturing operations may be used to assess the variation in ASI due to variation in electrode area.) The balance of the variation is assumed to be due to cell-to-cell variation in the ohmic component of resistance. The result is as follows:

$$S_{OHMIC} = \sqrt{S_{MFG}^2 - S_{AREA}^2} = \text{estimated standard deviation in cell-to-cell ohmic ASI}$$

where

$$S_{MFG} = \sqrt{\frac{(S_{MFG})_{MAX}^2 + (S_{MFG})_{MIN}^2}{2}}$$

= rms estimated standard deviation in cell-to-cell manufacturing variation

$$S_{AREA} = (\text{Average ASI at BOL}) \frac{S_{C/1}}{\text{Average } C/1 \text{ capacity}}$$

= estimated standard deviation in cell-to-cell electrode area variation

where  $S_{C/1}$  = standard deviation in  $C_1/1$  capacity.

These estimated values of  $S_{MEASUREMENT}$ ,  $S_{OHMIC}$ , and  $S_{AREA}$  are to be compared to the values used in the original experiment design to verify that the design will meet the TLVT program objectives.

## 4.2 Core Matrix Life Test Results

ASI test data for the core matrix of calendar life and cycle life test conditions will be analyzed to estimate the mean and 90% lower confidence limit for the battery life in service at the specified reference temperature and mix of cycling power levels. The preferred analysis method would be based on the calibrated life models for each specific candidate technology. Otherwise, the empirical model presented in Appendix B will be used.

Regardless of which data analysis model is used, there are three main steps involved in projecting life in service from the test results. First, the ASI data are analyzed to estimate the life on test (with the associated uncertainty) at each test condition in the matrix, ( $\hat{L}_{TEST}$  and  $\hat{S}_{L_{TEST}}$ ). A method called the “bootstrap” is suggested for estimating the uncertainty of the estimated life-on-test. Second, the lives-on-test for the calendar life test conditions, ( $P/P_{RATED} = 0$ ) are analyzed to estimate the calendar life acceleration factor ( $\hat{F}_{CAL}$ ) using a weighted regression method. The results are estimates for the mean and standard deviation of calendar life at the specified reference temperature, ( $\hat{L}_{CAL}$  and  $\hat{S}_{CAL}$ ). Third, the lives on test for the cycle life test conditions are correlated with the cycling stress factors and levels to estimate the contributions of the  $\hat{F}_{CYC}$  function to the acceleration factors. Finally, the mean and 90% lower confidence limit for the battery technology’s life in service are estimated for the FreedomCAR-specified combination of cycle life requirements applied at the specified reference temperature, ( $\hat{L}_{SERV}$  and  $\hat{S}_{SERV}$ ).

The analysis methods used in this process are summarized in the following.

### 4.2.1 Life on Test Estimates

At each experimental condition, ASI data are analyzed to estimate the life on test (with associated uncertainty). To illustrate, consider the default empirical data analysis model (see Appendix A),  $ASI(t + \Delta t_{RPT}) = \beta_0 + \beta_1 \cdot ASI(t)$ , where there are three model parameters:  $ASI_0$ ,  $\beta_0$ , and  $\beta_1$ . It is assumed that there are  $m$  observed values of ASI,  $\{ASI_{i_0}, ASI_{i_1}, ASI_{i_2}, \dots, ASI_{i_m}\}$ , for the  $i^{th}$  of  $n$  cells on test. These values form the basis for the Robust Orthogonal Regression (ROR) estimation procedure for  $ASI_0$ ,  $\beta_0$  and  $\beta_1$  (see Appendix B) given by  $\hat{A}\hat{S}I_0$ ,  $\hat{\beta}_0$  and  $\hat{\beta}_1$ . Using these parameter estimates, we estimate life-on-test as:

$$\hat{L}_{TEST} = \frac{\Delta t_{RPT}}{\log(\hat{\beta}_1)} \cdot \left\{ \log \left[ \hat{\beta}_0 + (\hat{\beta}_1 - 1) \cdot \left( \frac{\hat{A}\hat{S}I_0}{(1 - PF)} \right) \right] - \log \left[ \hat{\beta}_0 + (\hat{\beta}_1 - 1) \cdot \hat{A}\hat{S}I_0 \right] \right\}$$

where  $PF$  is the maximum allowable fraction of degradation.

To illustrate this process (normally applied to real test data), a single simulation was conducted for each of the conditions described in Table 2.3-3 with the indicated number of cells used for each condition. The noise levels used are as described in Section 2.3.1: (a) cell-to-cell fixed ohmic variation = 1%, (b) cell-to-cell electrode area variation = 0.5%, and (c) ASI measurement error = 1%. The simulated ASI data were analyzed by ROR (see Appendix B) to obtain estimates of the model parameters. Using the parameter estimates,  $L_{TEST}$  was estimated as described above.

The uncertainty of the various estimated model parameters and life on test can be assessed by using the bootstrap, which is a procedure for estimating the uncertainty associated with complex estimation procedures. The bootstrap is a well-established, well-accepted procedure used by many statisticians (e.g., see Reference 7). The motivation for using the bootstrap here is the complex nature of the estimation procedure ROR for which it is difficult to analytically derive a useful estimate of the standard errors for the model parameters:  $ASI_0$ ,  $\beta_0$ , and  $\beta_1$ .

Table 4.2-1 summarizes the analysis of the simulated ASI data, including bootstrap standard errors based on 100 bootstrap samples. The bootstrap standard error provides a notion of the uncertainty of each estimated quantity given a single set of experimental data as would be the case in an actual experiment. Confidence intervals for  $L_{TEST}$  should be derived directly from percentiles of the empirical distributions of the bootstrap estimates of  $L_{TEST}$ .

Table 4.2-1. Simulated experimental results: estimates compared with truth. (Bootstrap standard errors of estimates are in parentheses.)

Test Condition	$ASI_0$	$\hat{A}SI_0$	$\beta_0$	$\hat{\beta}_0$	$\beta_1$	$\hat{\beta}_1$	$L_{TEST}$	$\hat{L}_{TEST}$
Calendar Life 1	30	29.98 (0.06)	1.092	1.04 (0.06)	0.974	0.975 (0.0019)	5.99	5.53 (0.46)
Calendar Life 2	30	29.93 (0.11)	1.456	1.43 (0.10)	0.965	0.966 (0.0028)	4.47	4.26 (0.77)
Calendar Life 3	30	29.90 (0.17)	1.921	2.19 (0.15)	0.954	0.946 (0.0044)	3.37	3.76 (0.93)
Calendar Life 4	30	30.04 (0.24)	2.509	2.22 (0.20)	0.939	0.947 (0.0057)	2.56	2.49 (0.24)
Cycle Life 1	30	30.01 (0.08)	1.486	1.47 (0.10)	0.964	0.965 (0.0031)	4.38	4.53 (0.63)
Cycle Life 2	30	30.18 (0.16)	1.708	1.52 (0.15)	0.959	0.965 (0.0045)	3.80	3.20 (0.32)
Cycle Life 3	30	29.65 (0.23)	2.660	2.97 (0.24)	0.936	0.927 (0.0069)	2.41	2.51 (0.82)
Cycle Life 4	30	29.89 (0.20)	3.081	3.38 (0.24)	0.926	0.918 (0.0067)	2.07	1.96 (0.19)

Figure 4.2-1 compares the cumulative distribution of the bootstrap results for the simulated ASI results in the Calendar Life 1 case in Table 4.2-1. It can be seen in Figure 4.2-1 that despite the skewed distribution of the bootstrap values of life on test in this particular example, the normal approximation of the distribution of bootstrap values (based on  $L_{TEST}$  and the bootstrap standard error) can still be used to obtain a useful lower 90% confidence limit for the life on test.<sup>6</sup>

<sup>6</sup> Because the distribution of  $\hat{L}_{TEST}$  is highly skewed, however, it may not be generally appropriate to derive confidence limits for  $L_{TEST}$  based on a normal approximation using the bootstrap standard error of  $\hat{L}_{TEST}$ .

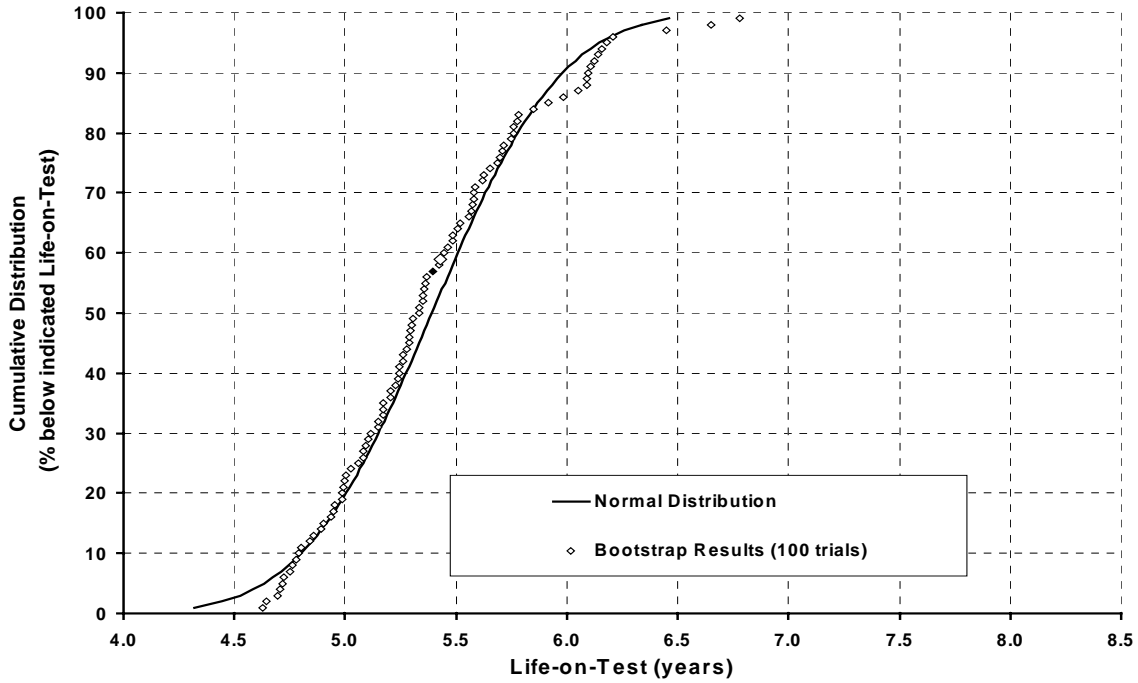


Figure 4.2-1. Comparison of bootstrap results with normal distribution for life on test at Calendar Life 1 test condition.

#### 4.2.2 Calendar Life Estimate

The above results of Table 4.2-1 are used to estimate the calendar life and calendar life acceleration factors using the general equation for the calendar life test conditions:

$$L_{TEST,I} = L_{CAL} / F_{CAL,I} \quad \text{for } I = 1..N_{CAL}$$

where  $F_{CAL,I} = F_{CAL,I}(T_I, SOC_I)$ .

For the example life test matrix,<sup>7</sup>

$$F_{CAL,I} = \exp \left\{ T_{ACT} \left[ \frac{1}{T_{REF} + 273.15} - \frac{1}{T_I + 273.15} \right] \right\}$$

where

$$SOC_I = SOC_{REF} \quad \text{for } I = 1..N_{CAL} \quad (\text{i.e. all calendar life testing is at the same SOC})$$

$$N_{CAL} = 4$$

$$T_I = 45, 50, 55, \text{ and } 60^\circ\text{C} \quad \text{for } I = 1..4.$$

In this case, the following weighted linear regression method can be used to estimate  $L_{CAL}$  and  $T_{ACT}$  :

<sup>7</sup> Note that the example life test matrix is based on the simple model of Section 2.1. Extension to additional stress factors (e.g. SOC, throughput,  $P_{DIS}$  and  $P_{RGN}$  etc. is not performed in this manual.)

$$Y_i = \ln(L_{TEST,I}) = \alpha + \beta X_i$$

$$\text{where } X_i = \frac{1}{T_{REF} + 273.15} - \frac{1}{T_i + 273.15}, \alpha = \ln(L_{CAL}) \text{ and } \beta = -T_{ACT}.$$

The weights used in the linear regression are  $W_i = \left( \frac{\hat{L}_{TEST,I}}{S_{L_{TEST,I}}} \right)^2$ . The slope and intercept of the linear regression model are then estimated by

$$B = \left( D^T \cdot \text{diag}(W) \cdot D \right)^{-1} \cdot D^T \cdot \text{diag}(W) \cdot Y,$$

where  $D$  is a  $4 \times 2$  matrix (first column is a vector of ones, second column contains the  $X_i$ 's),  $Y$  is a  $4 \times 1$  vector containing the  $Y_i$ 's, and  $W$  is a diagonal matrix with the  $W_i$ 's on the diagonal. The first element of  $B$  is  $\hat{\alpha}$ , which estimates the intercept. The second element of  $B$  is  $\hat{\beta}$ , which estimates the slope.

Using the values for  $\hat{L}_{TEST,I}$  and  $S_{L_{TEST,I}}^2$  from Table 4.2-1 in these equations gives the results summarized in Table 4.2-2, based on the following derived values of the slope and intercept, respectively:

$$\hat{\alpha} = 2.583$$

$$\hat{\beta} = -5575.$$

These give the following results for the calendar life (at  $T_{REF} = 30^\circ\text{C}$ ) and activation temperature:

$$\hat{L}_{CAL} = \exp\{\hat{\alpha}\} = 13.23 \text{ years}$$

versus the true value of  $L_{CAL} = 15.22$  years

and

$$\hat{T}_{ACT} = -\hat{\beta} = 5575 \text{ K}$$

versus the true value of  $T_{ACT} = 6000$  K.

In addition to these results, Reference 6 provides a method for estimating the uncertainty in  $\hat{\alpha}$ , which can be used to estimate the uncertainty in  $\hat{L}_{CAL}$ . For this example, the standard error of  $\hat{\alpha}$  is 0.085. By error propagation (see Reference 20), an approximate standard error of  $\hat{L}_{CAL}$  is 1.1 years. Although this uncertainty is significantly larger than expected, it is due to the relatively small number of test conditions (four) and the sensitivity of the life estimate to the parameter uncertainties for the example technology, with its low value of  $ASI_{RATIO}$  (0.125). In such cases it may be desirable to use an alternative response variable, as discussed further in Appendix A.

Table 4.2-2. Data and results for calendar life estimation for example matrix.

$I$	Temp (°C)	$X_I$	$\hat{L}_{TEST}$ (years)	$Y_I$	$S_{L_{TEST}}$	$W_I$	$\hat{Y}_I$	$\hat{F}_{CAL}$	Expected $F_{CAL}$
1	45	0.0001555	5.53	1.710	0.46	145	1.716	2.38	2.542
2	50	0.0002042	4.26	1.449	0.77	30.6	1.444	3.12	3.404
3	55	0.0002513	3.76	1.324	0.93	16.3	1.182	4.06	4.517
4	60	0.0002970	2.49	0.912	0.24	108	0.927	5.24	5.943

### 4.2.3 Effects of Cycling Stresses

The above results for the estimated calendar life and associated acceleration factors are then used to estimate the cycle life acceleration factors:

$$\hat{F}_{CYC,J} = \hat{L}_{CAL} / (\hat{F}_{CAL,J} \hat{L}_{TEST,J}) \text{ for } J = 1..N_{CYC}$$

where

$$\hat{F}_{CYC,J} = \hat{F}_{CYC,J} \{ T_J, SOC_J, (P/P_{RATED})_J, MPH, P_{DIS}, P_{RGN} \}$$

For the example life test matrix:

$$\hat{F}_{CYC,J} = 1 + \hat{K}_P (P/P_{RATED})_J^{\hat{\omega}} \left[ 1 + \hat{K}_T (T_J - T_{REF}) \right]$$

where

$$SOC_J = SOC_{REF} \text{ for } J = 1..N_{CYC} \text{ and } N_{CYC} = 4$$

$$T_J = 45, 45, 55, \text{ and } 55^\circ\text{C for } J = 1..4$$

$$(P/P_{RATED})_J = 80\%, 100\%, 80\%, \text{ and } 100\% \text{ for } J = 1..4$$

$$P_{DIS} = P_{RGN} = P_J \text{ for } J = 1..4.$$

$MPH$  (throughput rate) is assumed to be the nominal reference rate of 20 miles/hour. (For this example,  $SOC$ ,  $P_{DIS}$ ,  $P_{RGN}$  and  $MPH$  are the same for all cycle life test conditions.)

The four test conditions provide four equations in the three parameters to be estimated:

$\hat{K}_P$ ,  $\hat{\omega}$ , and  $\hat{K}_T$ . The values of  $\hat{K}_P$  and  $\hat{K}_T$  are estimated using the two results where  $P/P_{RATED}$  is 100%, which are independent of the estimate for  $\hat{\omega}$ . Then, the value of  $\hat{\omega}$  is estimated as the average of the two values obtained from the two results for  $P/P_{RATED} = 80\%$ . The following parameter values are thus obtained:

$$\hat{K}_P = 0.45 \text{ (versus the expected value of } K_P = 0.5)$$

$$\hat{K}_T = 0.04 \text{ (versus the expected value of } K_T = 0.01)$$

$$\hat{\omega} = 4 \text{ (versus the expected value of } \omega = 2).$$

Note that instead of an average value for  $\hat{\omega}$ , the fourth test condition could be used to estimate the temperature dependence of  $\omega$ . In general, there will be more test conditions than parameters

to be estimated from those conditions. The method of estimation to be used will depend on the exact nature of the assumed functional form of the cycle life acceleration factor.

The results for the values of  $\hat{F}_{CYC}$  are summarized in Table 4.2-3.

Table 4.2-3. Data and results for estimation of cycle life acceleration factors for example matrix.

J	Temp (°C)	(P/P <sub>RATED</sub> )	$\hat{L}_{TEST}$	$\hat{F}_{CAL}$	$\hat{F}_{CYC}$	$\hat{F}_{CYC}$	Expected $F_{CYC}$
1	45	80%	4.53	2.38	1.22	1.29	1.368
2	45	100%	3.20	2.38	1.73	1.72	1.575
3	55	80%	2.51	4.06	1.50	1.38	1.400
4	55	100%	1.96	4.06	1.92	1.90	1.625

#### 4.2.4 Life in Service Estimate

The estimated life in service is found using the following general expression:

$$\hat{L}_{SERV} = \hat{L}_{CAL} / \hat{F}_{CYC,NOM}$$

where

$$\begin{aligned} \hat{F}_{CYC,NOM} &= 1 + \hat{K}_P \frac{(0.8)(0.6)^{\hat{\omega}} + (0.15)(0.8)^{\hat{\omega}} + (0.05)(0.95)^{\hat{\omega}}}{15} \\ &= 1.006 \end{aligned}$$

versus  $F_{CYC,NOM} \approx 1.014$  for the numerical values of  $K_P$  and  $\omega$  from Section 2.1. The result is  $\hat{L}_{SERV} = 13.1$  years.

This estimate implies that there is a 50% chance that the actual life in service is greater than this value. Conversely, there is a 50% chance that the actual life in service is less than this value. An interesting question is then, "How much less could it be?" One way to answer this question is to estimate the 90% lower confidence limit for the life in service. There is a 90% chance that the actual life-in-service will be greater than this limit.

In the present example, the life in service is primarily determined by the calendar life, due to the value of  $\hat{F}_{CYC,NOM}$  being nearly unity. A reasonable approximation is then:

$$\hat{S}_{SERV} \approx \hat{S}_{CAL}$$

so that the estimate for the 90% lower confidence limit of life in service is approximately

$$\hat{L}_{SERV,90\%LCL} = \hat{L}_{SERV} - \left( \hat{S}_{CAL} \right) \left( t \{ p_{ST} = 0.1, \nu = N_{TC} - 1 = 7 \} \right) = 11.6 \text{ years}$$

where

$$\begin{aligned} t \{ p_{ST}, \nu \} &= \text{value of t-statistic for } \nu \text{ degrees of freedom and } p_{ST} \text{ single-tailed probability} \\ &= 1.415 \text{ for the example life test matrix.} \end{aligned}$$

## 4.3 Supplemental Life Test Results

In all cases except for the HPPC life test cells noted in Section 2.4, the supplemental life test data are used to test hypotheses based on differences in the measured ASI data between samples from different groups of cells. The general procedure for this statistical analysis is summarized below, followed by summaries of how this procedure would be applied in the three candidate supplemental life tests.

### 4.3.1 Hypothesis Testing

Hypothesis testing associated with the supplemental life test matrix may be done using the general t-statistic, based on small samples, for the difference between two means:

$$t = \frac{\bar{X}_1 - \bar{X}_2}{\sqrt{(n_1 - 1) \cdot S_1^2 + (n_2 - 1) \cdot S_2^2}} \cdot \sqrt{\frac{n_1 \cdot n_2 \cdot (n_1 + n_2 - 2)}{n_1 + n_2}}$$

where

- $\bar{X}_1, \bar{X}_2$  = estimated means for a parameter for each of two groups of cells (e.g. ASI)
- $S_1, S_2$  = standard deviations of the data for each of the two groups
- $n_1, n_2$  = number of cells for each of the two groups.

The hypothesis to be tested is that there is no underlying difference in mean performance between the two groups. That is  $\mu_1 = \mu_2$ , where  $\mu_1$  and  $\mu_2$  are the population averages associated with the two groups that are sampled.  $\bar{X}_1$  and  $\bar{X}_2$  are sample estimates of  $\mu_1$  and  $\mu_2$ .

There are three possible corresponding alternate hypotheses:

- (1)  $\mu_1 - \mu_2 < 0$
- (2)  $\mu_1 - \mu_2 > 0$
- (3)  $\mu_1 - \mu_2 \neq 0$

The first two are one-sided alternates; the last alternate is two-sided.

A level of significance,  $\alpha$ , must be specified before the test. For the purposes of this manual, a value of 0.05 is suggested for  $\alpha$ . Then, the corresponding criteria for rejection of the null hypothesis in favor of one of the alternate hypotheses are:

- (1)  $t < -T_\alpha$
- (2)  $t > T_\alpha$
- (3)  $|t| > T_{\alpha/2}$

Values of  $T_\alpha$  and  $T_{\alpha/2}$  are available from standard tables for the t-distribution with varying degrees of freedom,  $\nu$ . In general, for these tests  $\nu = n_1 + n_2 - 2$ .

### 4.3.2 Combined Calendar/Cycle Life tests

There are four groups of cells that must be analyzed to assess the path-independence of the ASI growth. Two groups are from the core matrix, both at the same test temperature, but with one group in the calendar life submatrix and the second group in the cycle life submatrix. The corresponding two groups in the supplemental life test matrix use the same test conditions as the core matrix groups, but with a switchover from one test condition to the other at a specified value of ASI.

An example of the expected ASI time histories for the two supplemental matrix groups is shown in Figure 4.3-1. These histories are based on the expected performance for the corresponding core matrix test conditions for the example minimum experiment design presented in Section 2. The dashed histories show the expected ASI growth for the core matrix conditions, while the solid histories show the expected ASI growth for the supplemental matrix conditions with the switchover from one condition to the other occurring at a prespecified ASI of 34.7  $\Omega\text{-cm}^2$ . It is apparent that the ASI rates of change for the two supplemental groups of cells are shifted at the switchover point. The two hypotheses to be considered are whether the shifted ASI rates of change are equal to the rates of change of the corresponding groups in the core matrix at the same ASI values.

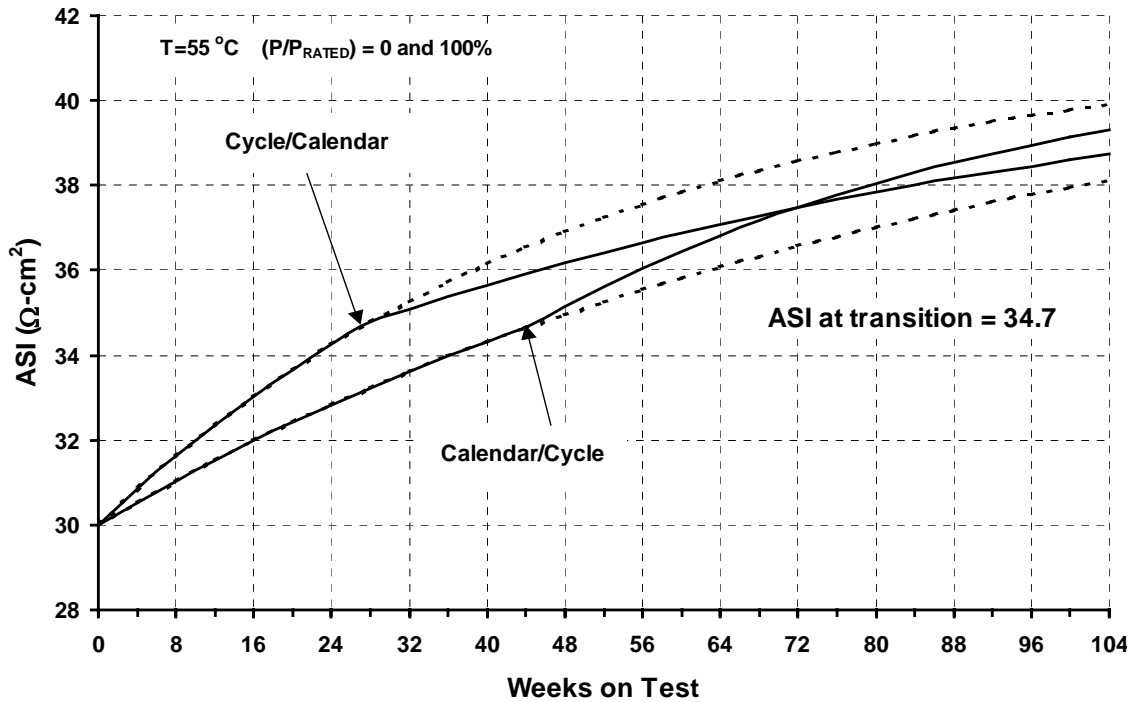


Figure 4.3-1. Expected ASI histories for combined cycle/calendar and calendar/cycle test conditions.

Define the four groups of cells as follows:

Core<sub>1</sub> = group of  $m_1$  calendar life cells in the core matrix at the specified temperature

Core<sub>2</sub> = group of  $m_2$  cycle life cells in the core matrix at the specified temperature

Combined<sub>1</sub> = group of  $n_1$  cycle/calendar life cells in the combined matrix at the specified temperature

Combined<sub>2</sub> = group of  $n_2$  calendar/cycle life cells in the combined matrix at the specified temperature

The four groups are analyzed to estimate the average ASI rates of change *from the switchover ASI value to the end of the test*. Due to noise in the ASI data, there will be uncertainty in the estimated rates of change. The test statistics to be used are:

$$t_i = \frac{\bar{Y}_i - \bar{X}_i}{\sqrt{(m_i - 1) \cdot R_i^2 + (n_i - 1) \cdot S_i^2}} \cdot \sqrt{\frac{m_i \cdot n_i \cdot (m_i + n_i - 2)}{m_i + n_i}}, \text{ for } i = 1, 2,$$

where

- $\bar{Y}_i$  = average ASI rate of change associated with the  $i^{\text{th}}$  Combined group of cells
- $S_i$  = standard deviation of ASI rate of change associated with the  $i^{\text{th}}$  Combined group of cells
- $\bar{X}_i$  = average ASI rate of change associated with the  $i^{\text{th}}$  Core group of cells
- $R_i$  = standard deviation of ASI rate of change associated with the  $i^{\text{th}}$  Core group of cells

In general, these statistics are used to assess whether or not the future ASI rate of change, beginning at a fixed/elevated ASI level, depends on how a cell has been previously been degraded to that fixed ASI level. The first t-statistic ( $t_1$ ) is used to assess whether or not the rate of calendar life degradation is affected unexpectedly by previous exposure to cycle life aging. The second t-statistic ( $t_2$ ) is used to assess whether or not the rate of cycle life degradation is affected unexpectedly by previous exposure to calendar life aging.

For example, if  $|t_1| > T_{0.025}$  with  $(m_1 + n_1 - 2)$  degrees of freedom, we conclude that future calendar life aging (measured by the ASI level) depends on not just the current ASI level and future calendar life stresses, but also the nature of the previous aging (calendar life versus cycle life). Alternately, if  $|t_1| < T_{0.025}$ , then one would not reject the hypothesis that future calendar life aging depends only on the current ASI level and future calendar life stresses. If both  $|t_1| < T_{0.025}$  and  $|t_2| < T_{0.025}$ , then one would not have evidence to reject the hypothesis that future cell aging depends only on the current ASI level and future stresses (i.e. path independence).

### 4.3.3 Cold-start Verification Tests

To verify that cold starts do not significantly affect battery life, the estimated lives on test for two of the core life test conditions will be compared with those for two supplemental groups of cells tested under the same conditions, but with the addition of a cold start test conducted as part of every periodic reference performance test. See Section 4.2.1 for details on estimating the life on test of cells under a specific condition. Here, the underlying hypothesis is that

$$(L_{TEST})_{COLD-START} = (L_{TEST})_{CORE}.$$

The alternate hypothesis is that:

$$(L_{TEST})_{COLD-START} < (L_{TEST})_{CORE}.$$

Rather than using a t-statistic, we use a standardized normal Z-statistic for each of the two comparisons. The Z-statistics will be based on the estimated mean lives on test ( $\bar{X}_{COLD-START}$  and  $\bar{X}_{CORE}$ ) and the corresponding bootstrap standard errors of the estimates ( $S_{COLD-START}$  and

$S_{CORE}$ ). That is:  $Z_{COLD-START} = \frac{\bar{X}_{COLD-START} - \bar{X}_{CORE}}{\sqrt{S_{COLD-START}^2 + S_{CORE}^2}}$ . The criterion for rejecting the null

hypothesis is then:  $Z_{COLD-START} < -1.65$

#### 4.3.4 Low-temperature Operation Tests

For the supplemental life tests involving low-temperature operation, it may be impossible to reliably estimate life on test due to limited cell degradation. Hence, it would be inappropriate to base a statistical test on such estimates. Instead, the average ASI rates of change over the full test duration will be used to evaluate the test statistic. Even then, the uncertainties in these rates will be relatively high, since there will be little ASI change if the tests are successful. Two groups of cells are considered. The first group ( $T=LIMIT$ ) represents very low temperature operation. In the second group ( $T>LIMIT$ ), the operating temperature is still low but close enough to standard test conditions so as to expect no significant ASI growth. If the first group of cells operating at the limits of the performance constraints ( $T=LIMIT$ ) exhibit any significant ASI growth, it should be possible to differentiate the performance of the two groups and hence identify a degrading low temperature effect. The statistical test described in Section 4.3.1 will be used to determine if low-temperature operation affects battery life, without necessarily quantifying the magnitude of the effect from these test results. Here, the underlying hypothesis is that the rate of ASI change over the two conditions is the same:  $\dot{ASI}_{T=LIMIT} = \dot{ASI}_{T>LIMIT}$ .

The alternate hypothesis is that  $\dot{ASI}_{T=LIMIT} > \dot{ASI}_{T>LIMIT}$ . The statistic to be used in this case is

$$t_{LOW-TEMP} = \frac{\bar{X}_{T>LIMIT} - \bar{X}_{T=LIMIT}}{\sqrt{(n_1 - 1) \cdot S_{T>LIMIT}^2 + (n_2 - 1) \cdot S_{T=LIMIT}^2}} \cdot \sqrt{\frac{n_1 \cdot n_2 \cdot (n_1 + n_2 - 2)}{n_1 + n_2}}, \text{ where}$$

$\bar{X}_{T>LIMIT}$  and  $\bar{X}_{T=LIMIT}$  denote the observed average ASI change for the two groups consisting of  $n_1$  and  $n_2$  cells, respectively.  $S_{T>LIMIT}$  and  $S_{T=LIMIT}$  denote the standard deviation of the ASI change for the two groups. In the case of 8 cells per group, the criterion for rejecting the null hypothesis is  $t_{LOW-TEMP} > t_{0.05}$  (14 degrees of freedom).

## 5. REFERENCES

1. *Advanced Technology Development Li-Ion Failure Modes Analysis* (report in preparation).
2. *Advanced Technology Development Program for Lithium-Ion Batteries: Gen 2 Performance Evaluation Interim Report*, INEEL/EXT-03-00095, February 2003.
3. *Advanced Technology Development Program for Lithium-Ion Batteries: Handbook of Diagnostic Techniques*, LBID-2464, April 2003.
4. Ammann, L. and Van Ness, J., "A Routine for Converting Regression Algorithms into Corresponding Orthogonal Regression Algorithms," *ACM Transactions on Mathematical Software*, 14, 1988, pp. 76–87.
5. Box, G.E.P., Hunter, W. G., and Hunter, S. J., *Statistics for Experimenters*, New York: John Wiley & Sons, 1978.
6. Draper, N. R. and Smith H., *Applied Regression Analysis*, 3rd edition, New York: John Wiley & Sons, 1998.
7. Efron, B., and Tibshirani, R. J., *An Introduction to the Bootstrap*, New York: Chapman and Hall, 1993.
8. *FreedomCAR Battery Test Manual for Power-Assist Hybrid Electric Vehicles*, DOE/ID-11069, 2003.
9. *FreedomCAR 42-volt Battery Test Manual*, DOE/ID-11070, 2003.
10. *FreedomCAR Battery Test Manual for Fuel Cell Powered Vehicles* (to be published).
11. *FreedomCAR Ultracapacitor Test Manual*, DOE/NE-ID-11173, September 2004.
12. Haskins, H. J., 2003, private communication, October 24, 2003.
13. Haskins, H. J., *Development of Power Profiles for Hybrid Electric Vehicle Battery Cycle life Testing* (report in preparation).
14. Hedayat, A. S., Sloane, N. J. A., and Stufken, J., *Orthogonal Arrays: Theory and Applications*, New York: Springer-Verlag, 1999.
15. Holland, P. and Welsch, R., "Robust Regression Using Iteratively Reweighted Least Squares," *Communications in Statistics, Part A – Theory and Methods*, 6, 1977, pp. 813–828.
16. Iglewicz, B., "Robust Scale Estimators and Confidence Intervals for Location," *Understanding Robust and Exploratory Data Analysis*, D. C. Hoaglin, F. Mosteller, and J. W. Tukey, eds., New York: Wiley, p. 417, 1983.
17. Linden, David and Reddy, T. B., eds., *Handbook of Batteries*, third edition, New York: McGraw-Hill, 2002.
18. Meeker, W. Q. and Escobar, L. A., *Statistical Methods for Reliability Data*, Chapter 21, "Accelerated Degradation Tests," 1998, John Wiley and Sons, Inc.
19. *PNGV Battery Test Manual*, DOE/ID-10597, 2001.
20. Sveshnikov, A. A., *Problems in Probability Theory, Mathematical Statistics and Theory of Random Functions*, W. B. Saunders, 1968.
21. Thomas, E. V., Case, H. L., Doughty, D. H., Jungst, R. G., Nagasubramanian, G. and Roth, E. P., "Accelerated Power Degradation of Li-Ion Cells", *Journal of Power Sources*, 124, 2003, pp. 254-260.

22. *Uncertainty Study of INEEL EST Laboratory Battery Testing Systems*, INEEL/EXT-01-00505, Vol. 1, December 2001, and Vol. 2, March 2003.

**Appendix A**  
**Life Test Simulation Programs**



# Appendix A

## Life Test Simulation Programs

### A-1. INTRODUCTION

Two Excel spreadsheet programs have been developed to support planning of battery technology life verification testing. The primary objectives of these programs are to (1) optimize allocation of cells to each test condition in the core life test matrix; and (2) estimate the 90% lower confidence limit for life in service as a function of the total number of cells tested for candidate matrix designs. Evaluations of such matrix design variables as the number and level of stress factors, the test duration, and reference performance test intervals are facilitated for specified levels of manufacturing and test measurement variation. A secondary objective of the two programs is final verification of the matrix design, given real test data from initial characterization of the actual test cell population.

The first program is an Excel spreadsheet routine called *Cell Allocator*. It is used in the preliminary stage of the overall life test experiment design to provide initial allocation of cells to the test conditions of the core life test matrix. It uses analytical approximations for the propagation of “noise” in the area-specific impedance (ASI) measurements to determine uncertainties in the expected values of life on test at each matrix condition. The approximations are based on the expected, i.e., “true,” life capabilities of the candidate technology.

The second program, *Battery MCS*, is a Visual Basic Application spreadsheet for Monte Carlo simulation (MCS) and analysis of test data from one given test condition at a time. This routine also runs in the Excel environment and can automatically replicate the simulation of the test results for any given number of cells and any specified number of MCS trials. It is used to confirm the results of the preliminary experiment design generated using *Cell Allocator*. It also may be used to analyze either simulated or real test data for estimating the life on test for a given test condition, as well as estimating the uncertainty in that estimate.

The general approach used in the Battery MCS program assumes the particular methods of Appendix B for analysis of life test data. As noted in that appendix, the baseline, or default, analysis method is empirical, with flexibility to accommodate a wide range of performance degradation behaviors. However, substitution of a physics-based model appropriate to the specific candidate technology is strongly encouraged and is supported by the simulation program. The general simulation approach documented herein will then serve as a guide for customization of the programs by each developer.

The Monte Carlo method of simulation, as used in these programs, starts with a “truth” function for ASI, the parameter used to characterize battery performance degradation. Growth in ASI over time results in reduction in battery pulse power capability. Battery design guidelines established by FreedomCAR allow an initial margin of only 30% in pulse power capability, relative to the specified end of life performance goals. Thus, a power fade of 23% relative to power at beginning of life defines the battery’s end of life.<sup>a</sup> The acceleration factor (AF) at each test condition is input to the simulation, defining the expected life on test at that condition.

The ASI truth function is corrupted by three sources of “noise” applied as additive or multiplicative random variables to simulate actual ASI measurements over time. The simulation program applies the

---

<sup>a</sup> Note that both programs default to an arbitrary value of 25% power fade for EOL. The user should change this to the appropriate program-specific value.

same data analysis model that was used for the ASI truth function to these simulated test data. The data analysis results are estimates of the model parameters for the particular simulated data set. These estimated model parameters will differ from the true model parameters due to the noise added to the ASI truth function. In general, the level of uncertainty of the model parameters will reflect the magnitudes of the specified noise levels. The estimated model parameters are used to estimate life on test for the particular test condition. Uncertainty in the estimated life on test is also estimated as part of the data analysis procedure. As described in Appendix B, this is based on a standard statistical procedure called the “bootstrap” method.

Results for the complete core matrix of test conditions can be combined to obtain an estimate of the mean life in service at the conditions of normal usage. Further, the estimated uncertainties in the lives on test can be used to provide a 90% lower confidence limit for the mean life in service. This final step has not been built into the simulation tool, due to the wide variety of possible stress factors and levels for any specific technology.

This appendix is organized into the following major sections. Section A-2 documents the equations used in the *Battery MCS* program, although the details of the test data analysis method are documented in Appendix B. Section A-3 documents the equations used in the *Cell Allocator* program. Section A-4 describes an example life test experiment design.

## A-2. SIMULATION EQUATIONS

The equations used in the Cell Allocator and Battery MCS programs are documented in the following. First, the ASI truth function is described. Second, generating simulated ASI data using three specified noise parameters is described. Third, the baseline empirical data analysis model is briefly summarized. Finally, an alternative approach for estimating life on test is provided for use with technologies that may have self-limiting degradation mechanisms.

### A-2.1 ASI Truth Function

The ASI truth model is based on the following empirical model of test data, originally developed to analyze the results of cell life testing conducted on Gen 2 cells in the DOE Advanced Technology Development program. (See Appendix B for details.) The empirical model equation is:

$$ASI\{t + \Delta t_{RPT}\} = \hat{\beta}_0 + \hat{\beta}_1 ASI\{t\}$$

where

- $ASI\{t\}$  = measured area-specific impedance ( $\Omega\text{-cm}^2$ ) at time  $t$  (weeks)
- $\Delta t_{RPT}$  = interval (weeks) between reference performance test (RPT) measurements of ASI
- $\hat{\beta}_0$  and  $\hat{\beta}_1$  = estimates of the intercept and slope, respectively, of the linear relationship between  $ASI\{t + \Delta t_{RPT}\}$  and  $ASI\{t\}$ .

Given  $\hat{\beta}_0$  and  $\hat{\beta}_1$  from the data analysis, the following general expression can be derived:

$$ASI\{t\} = \frac{[\hat{\beta}_0 + (\hat{\beta}_1 - 1) A\hat{S}I_0] e^{\ln(\hat{\beta}_1) t / \Delta t_{RPT}} - \hat{\beta}_0}{\hat{\beta}_1 - 1}$$

where  $A\hat{S}I_0$  = estimated ASI at  $t = 0$  (beginning of life, BOL).

This expression can be simplified by using a test interval index,  $K$ , instead of the time,  $t$ :

$$t = K \Delta t_{RPT}$$

which results in:

$$A\hat{S}I_K = \hat{\beta}_0 (\hat{\beta}_1^K - 1) / (\hat{\beta}_1 - 1) + A\hat{S}I_0 \hat{\beta}_1^K .$$

The corresponding estimated rate of change in ASI with time is:

$$A\hat{S}I = d(ASI_K) / dt = [ \hat{\beta}_0 / (\hat{\beta}_1 - 1) + A\hat{S}I_0 ] \hat{\beta}_1^K \ln(\hat{\beta}_1) / \Delta t_{RPT}$$

which can be transformed into the following:

$$A\hat{S}I_K = A\hat{S}I_0 \hat{\beta}_1^K .$$

Whereas data analysis yields estimates of  $\beta_0$  and  $\beta_1$  from the ASI measurements, specification of the “true” ASI function for the simulation requires that true values of  $\hat{\beta}_0$  and  $\hat{\beta}_1$  be determined from the (presumably) known shape of the ASI-versus-time curve. This is done by specifying (a) the allowable power fade over the specified cell life, which determines the ratio of  $ASI_{EOL}$  to  $ASI_{BOL}$ , and (b) the ratio of  $A\dot{S}I_{EOL}$  to  $A\dot{S}I_{BOL}$ . The result is:

$$\beta_1 = \exp[( \Delta t_{RPT} / L_{TEST} ) \ln(A\dot{S}I_{RATIO} )]$$

$$\beta_0 = (\beta_1 - 1) ASI_{BOL} [(ASI_{EOL} / ASI_{BOL}) - A\dot{S}I_{RATIO}] / (A\dot{S}I_{RATIO} - 1)$$

where

$$(ASI_{EOL} / ASI_{BOL}) = 1 / (1 - PF)$$

$$A\dot{S}I_{RATIO} = A\dot{S}I_{EOL} / A\dot{S}I_{BOL}$$

and where

$$L_{TEST} = \text{true cell life on test (weeks)}$$

$$PF = \text{allowable power fade at end of life, as a fraction of the power at beginning of life.}$$

The true life on test is given by the target cell life in service of 15 years, divided by a calendar life de-rating factor, and then divided by an acceleration factor ( $AF$ ) associated with the specific actual test conditions:

$$L_{TEST} = L_{CAL} / AF$$

where

$$L_{CAL} = \text{true cell calendar life} = L_{SERVICE} / (L_{CAL} \text{ de-rating factor})$$

where  $L_{SERVICE} = \text{true life-in-service}$ , including cycling effects at the nominal conditions of usage.

The conditions are that (a) ambient temperature is equal to reference temperature and (b) no battery cycling corresponds to  $AF = 1$ . The calendar life de-rating factor accounts for the effect on battery life of cycling at the nominal conditions of usage specified by FreedomCAR.

The shape of the ASI versus time curve is related to  $\dot{ASI}_{RATIO}$  as follows:

$$\text{Increasing ASI rate of change} \Rightarrow \dot{ASI}_{RATIO} > 1 \Rightarrow \beta_1 > 1$$

$$\text{Decreasing ASI rate of change} \Rightarrow \dot{ASI}_{RATIO} < 1 \Rightarrow \beta_0 > 0 \text{ and } \beta_1 < 1 .$$

The special case for constant ASI rate over life implies  $\dot{ASI}_{RATIO} = 1$ , which then implies:

$$\beta_1 = 1$$

$$\beta_0 = ASI_{BOL} [(ASI_{EOL} / ASI_{BOL}) - 1] (\Delta t_{RPT} / L_{TEST}) > 0$$

$$\begin{aligned} ASI\{t\} &= ASI_0 + \beta_0 t / \Delta t_{RPT} \\ &= ASI_0 + ASI_{BOL} [(ASI_{EOL} / ASI_{BOL}) - 1] t / L_{TEST} . \end{aligned}$$

Thus, a wide range of ASI shapes can be selected as the “true” ASI function in the simulation. Representative examples of such functions are illustrated in Figure 2.1-1 in the manual.

Note that the true ASI rate of change is given by:

$$\begin{aligned} \dot{ASI} &= [\beta_0 / (\beta_1 - 1) + ASI_0] (\beta_1)^K \ln(\beta_1) / \Delta t_{RPT} \\ &= \beta_0 / \Delta t_{RPT} \text{ for the special case of } \dot{ASI}_{RATIO} = 1. \end{aligned}$$

## A-2.2 ASI Simulated Test Data Generation

In the simulation, the true ASI is “corrupted” by random cell-to-cell variations in ASI due to manufacturing and by random errors in each ASI measurement over time. The simulated ASI measurements are combinations of truth and three random variables:

$$\text{Measured ASI} = (F_{AREA}) (ASI_{TRUE}) + \Delta ASI_{FIXED} + \Delta ASI_{MEASUREMENT}$$

where

$$\begin{aligned}
 ASI_{TRUE} &= \{ [\beta_0 + (\beta_1 - 1) ASI_0 ] \exp[\ln(\beta_1) t / \Delta t_{RPT}] - \beta_0 \} / (\beta_1 - 1) \\
 &= \beta_0 [(\beta_1)^K - 1] / (\beta_1 - 1) + ASI_0 (\beta_1)^K \\
 F_{AREA} &= (1 - \Delta A_{ELECT} / A_{ELECT}) = \text{electrode area factor} \\
 \Delta A_{ELECT} / A_{ELECT} &= \text{cell-to-cell variation in electrode area / nominal electrode area} \\
 \Delta ASI_{FIXED} &= \text{cell-to-cell variation in ASI due to fixed ohmic resistance variations} \\
 \Delta ASI_{MEASUREMENT} &= \text{measurement-to-measurement ASI variation due to test equipment.}
 \end{aligned}$$

The three random variables are normally distributed with zero means and with input standard deviations of  $\sigma_{AREA}$ ,  $\sigma_{FIXED}$ , and  $\sigma_{MEASUREMENT}$ , respectively. Specific values of  $\Delta A_{ELECT} / A_{ELECT}$  and  $\Delta ASI_{FIXED}$  are generated for each cell using the program's built-in random number generator to obtain the cell's initial ASI at time = 0. Then, for each cell at each measurement time, the random number generator is used to obtain independent values of  $\Delta ASI_{MEASUREMENT}$  to be added to the cells' ASI. The true growth in each cell's ASI includes the effect of electrode area variation, but not  $\Delta ASI_{FIXED}$ , which remains constant over the cell's life on test.

### A-2.3 Test Data Analysis Model

Once the set of ASI measurements has been established, either by the simulation or from actual testing, the data analysis method of Appendix B is used to estimate three model parameters:  $\hat{\beta}_0$ ,  $\hat{\beta}_1$ , and  $\hat{ASI}_0$ . This is done using the following sequence.

The parameters  $\hat{\beta}_0$  and  $\hat{\beta}_1$  are calculated using a robust orthogonal regression (ROR) method developed to analyze data for which errors in the X-values are comparable to errors in the Y-values. In the ROR method, the data are given nonuniform weights to reduce the effects of outliers and data at the extremes of the range in X-values.

The parameter  $\hat{ASI}_0$  is estimated by setting the average residual error (i.e., estimated ASI minus measured ASI) to zero for the ASI data set.

The estimated life on test is calculated using the following equation:

$$\hat{L}_{TEST} = \Delta t_{RPT} \ln \left\{ \frac{\hat{\beta}_0 + [(\hat{\beta}_1 - 1) \hat{ASI}_0] / (1 - PF)}{\hat{\beta}_0 + [(\hat{\beta}_1 - 1) \times \hat{ASI}_0]} \right\} \frac{1}{\ln \hat{\beta}_1} .$$

Uncertainties in  $\hat{\beta}_0$ ,  $\hat{\beta}_1$ ,  $\hat{ASI}_0$ , and  $\hat{L}_{TEST}$  are estimated using the bootstrap method, wherein the residual errors in the parameters are resampled many times ( $\approx 100$ ) to create alternate realizations of the test data. These alternate data sets are each analyzed to get corresponding alternate values for the four parameters. The standard errors in the parameters can then be estimated from the  $\approx 100$ -sample distributions obtained. This method has become a standard approach for this kind of analysis, and it has broad applicability beyond its use in the Battery MCS program.

Finally, the estimated lives on test and their associated uncertainties are used to estimate the calendar life and life in service in an iterative procedure:

1. The calendar life is initially estimated using a weighted regression of the lives on test versus the expected acceleration factors for the several test conditions of the matrix. The calendar life corresponds to  $AF = 1$  in the regression.
2. The acceleration factors are recalculated using the estimated calendar life and the estimated lives-on-test.
3. The calendar life is re-estimated using the recalculated acceleration factors.
4. Steps 2 and 3 are repeated until the calendar life estimate converges to a final estimate.
5. The life in service is estimated from the calendar life estimate and the estimated acceleration factors for the cycle life test conditions of the matrix, adjusted for the pulse profiles specified by FreedomCAR for battery cycle life.
6. The 90% lower confidence limit for life in service is calculated approximately as:

$$LCL_{90, SERVICE} \approx L_{CAL} - t\{\alpha=0.1; v=N_{TC} - 1\} S_{CAL}$$

where

$t\{\alpha = 0.1; v = N_{TC} - 1\}$  = the  $\alpha^{\text{th}}$  percentile of the t-distribution with  $v$  degrees of freedom

$N_{TC}$  = number of test conditions in the core life test matrix

$S_{CAL}$  = standard error in the estimated calendar life, calculated using the estimated standard errors in the lives on test (see Appendix B).

## A-2.4 Alternative Equation for Life Estimation

For technologies that have self-limiting degradation mechanisms ( $\beta_I < 1$ ), the estimated life on test can become strongly dependent on the specified allowable power fade. This is because eventually, in these cases, the ASI growth rate goes to zero. The limit value of ASI as time goes to infinity is:

$$ASI_{\infty} \equiv \beta_0 / (1 - \beta_1)$$

$$\Rightarrow L_{TEST} = \frac{\Delta t_{RPT}}{\ln \beta_1} \ln \left\{ \frac{ASI_{\infty} - ASI_0 / (1 - PF)}{ASI_{\infty} - ASI_0} \right\}$$

where the condition  $ASI_{\infty} > ASI_{EOL} = ASI_0 / (1 - PF)$  is needed to obtain a finite estimate of  $L_{TEST}$ .

The effect of the allowable power fade on estimated life is illustrated in Figure A-1 for the example case of  $\dot{ASI}_{RATIO} = 0.125$ . Note that when noisy data are used to estimate the  $\beta_0$  and  $\beta_1$  parameters, it is possible that the corresponding life estimates may become infinite, even when the mean value of  $ASI_{\infty}$  satisfies the above criterion. It may then be necessary to use the statistical distribution of  $ASI_{\infty}$  to estimate the uncertainties in the estimated lives on test.

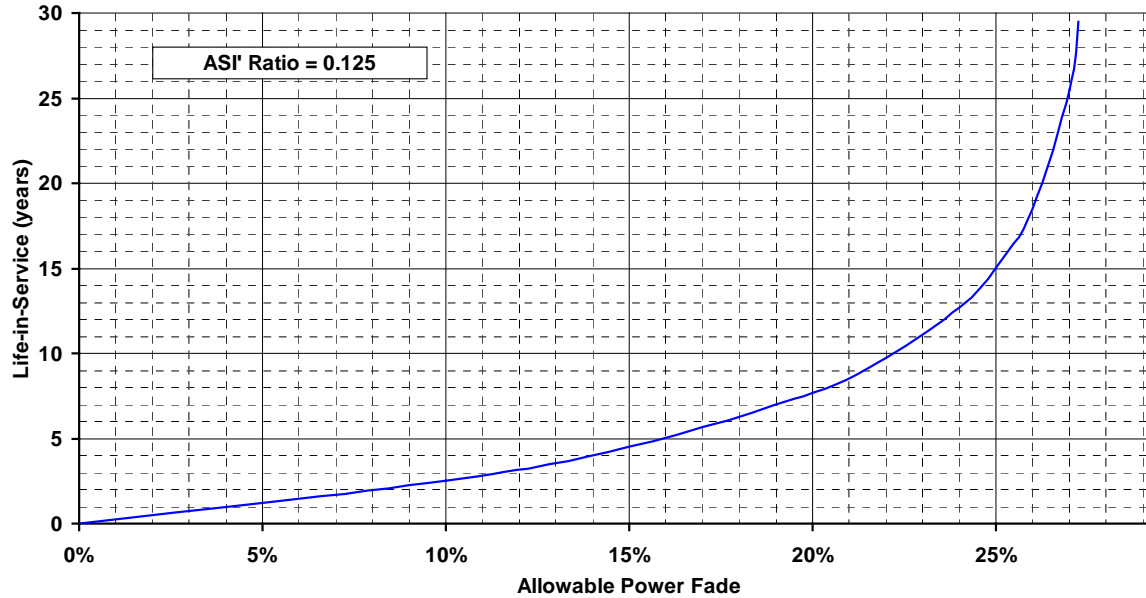


Figure A-1. Effect of allowable power fade on life in service for technologies with self-limiting degradation mechanisms.

### A-3. CELL ALLOCATOR PROGRAM

The Cell Allocator program provides an approximately optimum allocation of a given total number of test cells to the specified test conditions of the core life test matrix. The criterion used is that the standard error in the estimated calendar life be minimized, given the estimated standard errors in the lives on test. The Battery MCS program can also be used to determine this optimum allocation, but Cell Allocator is used to narrow the range of options in the preliminary experiment design stage. Then, the Battery MCS program can be used more effectively to confirm the preliminary design. The principal difference in the two programs is that Cell Allocator uses approximate analytical expressions for the propagation of noise in the ASI data into the uncertainties in the lives on test. The Battery MCS program uses the empirical data analysis procedure, including the bootstrap method, to do the same thing more realistically.

The approximate analytical expressions used in Cell Allocator are presented in the following. They are based on the total derivative of the estimated life on test with respect to the ASI data, evaluated assuming the “true” values of the parameters. It is first assumed that there is only one cell at each test condition, and the standard error in the estimated life on test will vary inversely as the square root of the number of cells allocated to any given test condition.

The estimated life on test at each test condition is expressed in terms of the estimated model parameters:

$$\hat{L}_{TEST} = \left( \frac{t_{EOT}}{N_{RPT}} \right) \ln \left\{ \frac{\hat{\beta}_o + (\hat{\beta}_1 - 1) A \hat{S} I_o / (1 - PF)}{\hat{\beta}_o + (\hat{\beta}_1 - 1) A \hat{S} I_o} \right\} \frac{1}{\ln \hat{\beta}_1} .$$

The approximate standard error in this estimate is, for only one cell on test:

$$S_{LOT,1} = \left[ \sum_{k=O, N_{RPT}} ASI_k^2 \left( \frac{d\hat{L}_{TEST}}{dASI_K} \right)^2 (S'_{ASI_k})^2 \right]^{1/2}$$

where the total variance in the ASI data is

$$(S'_{ASI_k})^2 = \left( \frac{ASI_{K,TRUE}}{ASI_o} \right)^2 (S'_{AREA})^2 + (S'_{FIXED})^2 + (S'_{MEASUREMENT})^2.$$

The total derivative of the estimated life on test with respect to each ASI measurement is calculated using the chain rule of differentiation:

$$\frac{d\hat{L}_{TEST}}{dASI_K} = \frac{\partial \hat{L}_{TEST}}{\partial \hat{\beta}_1} \cdot \frac{\partial \hat{\beta}_1}{\partial ASI_K} + \frac{\partial \hat{L}_{TEST}}{\partial \hat{\beta}_o} \cdot \frac{\partial \hat{\beta}_o}{\partial ASI_K} + \frac{\partial \hat{L}_{TEST}}{\partial \hat{A}SI_o} \cdot \frac{d\hat{A}SI_o}{dASI_K}.$$

The results for the three partial derivatives of life on test with respect to the model parameters are as follows:

$$\begin{aligned} \frac{\partial \hat{L}_{TEST}}{\partial \hat{\beta}_1} &= \left( \frac{t_{EOT}}{N_{RPT}} \right) \left( \frac{\hat{A}SI_o}{\ln \hat{\beta}_1} \right) \left[ \frac{1}{\hat{\beta}_o(1-PF) + (\hat{\beta}_1 - 1)\hat{A}SI_o} - \frac{1}{\hat{\beta}_o + (\hat{\beta}_1 - 1)\hat{A}SI_o} \right] - \left( \frac{\hat{L}_{TEST}}{\hat{\beta}_1 \ln \hat{\beta}_1} \right) \\ &\rightarrow -\frac{\hat{L}_{TEST}}{2} \left[ \frac{\hat{L}_{TEST} N_{RPT} (1-PF)}{t_{EOT} (PF)} - 1 \right] \text{ as } \hat{\beta}_1 \rightarrow 1 \end{aligned}$$

$$\begin{aligned} \frac{\partial \hat{L}_{TEST}}{\partial \hat{\beta}_o} &= \left( \frac{t_{EOT}}{N_{RPT}} \right) \left( \frac{1}{\ln \hat{\beta}_1} \right) \left[ \frac{(1-PF)}{\hat{\beta}_o(1-PF) + (\hat{\beta}_1 - 1)\hat{A}SI_o} - \frac{1}{\hat{\beta}_o + (\hat{\beta}_1 - 1)\hat{A}SI_o} \right] \\ &\rightarrow -\hat{L}_{TEST} / \hat{\beta}_o \text{ as } \hat{\beta}_1 \rightarrow 1 \end{aligned}$$

$$\begin{aligned} \frac{\partial \hat{L}_{TEST}}{\partial \hat{A}SI_o} &= \left( \frac{t_{EOT}}{N_{RPT}} \right) \left( \frac{\hat{\beta}_1 - 1}{\ln \hat{\beta}_1} \right) \left[ \frac{1}{\hat{\beta}_o(1-PF) + (\hat{\beta}_1 - 1)\hat{A}SI_o} - \frac{1}{\hat{\beta}_o + (\hat{\beta}_1 - 1)\hat{A}SI_o} \right] \\ &\rightarrow \hat{L}_{TEST} / \hat{A}SI_o \text{ as } \hat{\beta}_1 \rightarrow 1. \end{aligned}$$

The partial derivatives of the model parameters with respect to each ASI measurement are found using a variation of the ROR data analysis method in which the ASI data are uniformly weighted. The results are:

$$\frac{\partial \hat{\beta}_1}{\partial ASI_K} = \frac{\hat{\beta}_1 / (\hat{\beta}_1 - B)}{2 S_{XY}} \left[ -\frac{\partial S_{XX}}{\partial ASI_K} + \frac{\partial S_{YY}}{\partial ASI_K} - 2B \frac{\partial S_{XY}}{\partial ASI_K} \right]$$

where

$$B = (\hat{\beta}_1^2 - 1) / 2\hat{\beta}_1$$

$$S_{XY} = \sum_{k=0, N_{RPT}-1} (ASI_K)(ASI_{K+1}) - N_{RPT} \bar{X} \bar{Y}$$

$$\frac{\partial S_{XX}}{\partial ASI_K} = \begin{cases} 2(ASI_K - \bar{X}) & \text{for } K < N_{RPT} \\ 0 & \text{for } K = N_{RPT} \end{cases}$$

$$\frac{\partial S_{YY}}{\partial ASI_K} = \begin{cases} 0 & \text{for } K = 0 \\ 2(ASI_K - \bar{Y}) & \text{for } K > 0 \end{cases}$$

$$\frac{\partial S_{XY}}{\partial ASI_K} = \begin{cases} ASI_1 - \bar{Y} & \text{for } K = 0 \\ (ASI_{K-1} + ASI_{K+1}) - \bar{X} - \bar{Y} & \text{for } 0 < K < N_{RPT} \\ ASI_{N_{RPT}-1} - \bar{X} & \text{for } K = N_{RPT} \end{cases}$$

$$\bar{X} = \sum_{K=0, N_{RPT}-1} (ASI_K) / N_{RPT}$$

$$\bar{Y} = \sum_{K=1, N_{RPT}} (ASI_K) / N_{RPT}$$

and

$$\frac{\partial \hat{\beta}_o}{\partial ASI_K} = \begin{cases} -\bar{X} \frac{\partial \hat{\beta}_1}{\partial ASI_o} - \left( \frac{\hat{\beta}_1}{N_{RPT}} \right) & \text{for } K = 0 \\ -\bar{X} \frac{\partial \hat{\beta}_1}{\partial ASI_K} - \left( \frac{\hat{\beta}_1 - 1}{N_{RPT}} \right) & \text{for } 0 < K < N_{RPT} \\ -\bar{X} \frac{\partial \hat{\beta}_1}{\partial ASI_{N_{RPT}}} + \left( \frac{1}{N_{RPT}} \right) & \text{for } K = N_{RPT} \end{cases}$$

and

$$\frac{d\hat{ASI}_o}{dASI_K} = \frac{\partial \hat{ASI}_o}{\partial ASI_K} + \frac{\partial \hat{ASI}_o}{\partial \hat{\beta}_1} \left( \frac{\partial \hat{\beta}_1}{\partial ASI_K} \right) + \frac{\partial \hat{ASI}_o}{\partial \hat{\beta}_o} \left( \frac{\partial \hat{\beta}_o}{\partial ASI_K} \right)$$

where

$$\begin{aligned} \frac{\partial \hat{A}SI_O}{\partial ASI_K} &= \left( \sum_{K=0, N_{RPT}} \hat{\beta}_1^K \right)^{-1} \\ \frac{\partial \hat{A}SI_O}{\partial \hat{\beta}_1} &= - \left\{ \hat{\beta}_O \left[ \frac{\sum_{K=0, N_{RPT}} K \hat{\beta}_1^K}{\hat{\beta}_1 (\hat{\beta}_1 - 1)} - \frac{\sum_{K=0, N_{RPT}} \hat{\beta}_1^K - N_{RPT} - 1}{(\hat{\beta}_1 - 1)^2} \right] + \frac{\hat{A}SI_O}{\hat{\beta}_1} \sum_{K=0, N_{RPT}} K \hat{\beta}_1^K \right\} \frac{1}{\sum_{K=0, N_{RPT}} \hat{\beta}_1^K} \\ &\rightarrow - \frac{N_{RPT}}{2} \left[ \hat{A}SI_O + \hat{\beta}_O \frac{(N_{RPT} - 1)}{3} \right] \text{ as } \hat{\beta}_1 \rightarrow 1 \\ \frac{\partial \hat{A}SI_O}{\partial \hat{\beta}_O} &= - \left( \sum_{K=0, N_{RPT}} \hat{\beta}_1^K - N_{RPT} - 1 \right) / \left[ (\hat{\beta}_1 - 1) \sum_{K=0, N_{RPT}} \hat{\beta}_1^K \right] \\ &\rightarrow - N_{RPT} / 2 \text{ as } \hat{\beta}_1 \rightarrow 1 . \end{aligned}$$

Finally, these derivatives are evaluated by using the true values of all the parameters in the above results:

$$\begin{aligned} \hat{\beta}_1 &\rightarrow \beta_1 = (ASI_{RATIO})^{(t_{EOT} / N_{RPT} L_{TEST})} \\ &\rightarrow 1 \text{ as } ASI_{RATIO} \rightarrow 1 \\ \hat{\beta}_O &\rightarrow \beta_O = (\beta_1 - 1) ASI_O \left[ \frac{1}{(1 - PF)} - ASI_{RATIO} \right] \left( \frac{1}{ASI_{RATIO} - 1} \right) \\ &\rightarrow ASI_O t_{EOT} PF / [(1 - PF) N_{RPT} L_{TEST}] \text{ as } ASI_{RATIO} \rightarrow 1 \\ \hat{A}SI_O &\rightarrow ASI_O \\ ASI_K &\rightarrow \beta_O (\beta_1^K - 1) / (\beta_1 - 1) + ASI_O \beta_1^K \\ &\rightarrow ASI_O + \beta_O K \text{ as } ASI_{RATIO} \rightarrow 1 . \end{aligned}$$

Once the single-cell standard errors in the estimated lives on test have been calculated, the estimate for the standard error in calendar life is approximated using an unweighted regression with nonuniform standard errors for the lives on test:

$$S_{CAL} = L_{CAL} \left[ \sum_{J=1, N_{TC}} (L_{TEST, J} S_{LOT, J})^2 \right]^{1/2} / \sum_{J=1, N_{TC}} (L_{TEST, J})^2$$

where the standard errors in the estimated lives on test are reduced by the square root of the number of cells allocated to each test condition:

$$S_{LOT,J} = (S_{LOT,1})_J / \sqrt{N_{CELL,J}}$$

and where the sum of the numbers of cells allocated to each test condition is constrained to be the specified total number of cells in the core life test matrix:

$$N_{CELL,TOTAL} = \sum_{J=1,N_{TC}} N_{CELL,J} .$$

Further, it may be desirable to constrain the allocation by specifying a minimum number of cells to be allocated to any test condition:

$$N_{CELL,J} \geq N_{CELL,MIN} \text{ for all } J = 1..N_{TC}$$

where

$N_{TC}$  = number of test conditions in the core life test matrix.

The optimum allocation of cells, given these approximations, is a straightforward problem in linear programming. The Cell Allocator spreadsheet is set up to use Excel's "Solver" tool to automatically allocate cells to the test conditions. The allocation typically results in fractional cells in each of the test conditions. Note that the Solver solution will generally result in the derivatives of  $S_{CAL}$  with respect to the  $N_J$  all being equal. However, constraining the minimum number of cells per test condition may result in a slightly nonoptimum allocation, where these derivatives are not all equal. This will also be evident when the allocated numbers of cells are forced to be integer values.

## A-4. EXAMPLE OF LIFE TEST MATRIX DESIGN

The life test experiment design example presented in Section 2 of the manual is discussed in more detail in the following. Use of Cell Allocator in the preliminary design and use of Battery MCS in the final design are illustrated for this minimum core matrix.

### A-4.1 Preliminary Design Using Cell Allocator

The initial optimized results for the allocation of cells for the minimum core matrix design example are presented in Figure A-2. This allocation has not been constrained, and it can be seen that the derivatives are all equal. A chart of these results is provided in Figure A-3. The steep rise in the number of cells per test condition with expected/true life on test is evident. This is necessary to obtain balanced values of the standard deviations in the expected lives on test for the eight test conditions. Essentially, as life on test increases for a fixed test duration, the number of cells must increase to maintain an acceptable signal/noise ratio.

INPUT:		True Battery Capabilities:	Expected Noise Levels:
	Life-in-Service (years) =	15.0	Standard deviation in electrode area = 0.5%
	Calendar Life De-rating Factor =	0.986	Standard deviation in fixed ohmic resistance = 1.0%
	Implied Calendar Life (years) =	15.213	Standard deviation in ASI measurement error = 1.0%
	ASI Rate-of-Change Ratio =	0.125	
	ASI at Beginning of Life =	30	Reference Performance Test (RPT) Timing:
	Allowable Power Fade =	25%	RPT Interval (weeks) = 4
	Specified total number of cells =	148	Number of RPT Intervals = 26
	Minimum number of cells/test condition =	1	Implied Test Duration (years) = 2.00
	Life-on-test for Error Propagation =	5.985	Implied single-cell std. dev. = 7.8692
<b>RESULTS:</b>		<b>Estimated 90% Lower Confidence Limit for Life-in-Service (years) = 13.67</b>	
Actual number of cells = 148		Estimated Std. Dev. of Calendar Life (years) = 0.942	

Test Condition #	Estimated Acceleration Factors:	Expected Life-on-Test	Single-cell Std. Dev.	Number of Cells	Life-on-Test Std. Dev.	Derivatives w.r.t. N-cell	Ratios of Derivatives
	Temperature    Cycling    Total AF						
1	2.542    1.000    2.542	5.985	7.8692	79	0.886	0.3566	1.000
2	3.404    1.000    3.404	4.469	3.0069	22	0.634	0.3569	1.001
3	4.517    1.000    4.517	3.368	1.2598	7	0.473	0.3566	1.000
4	5.943    1.000    5.943	2.560	0.7082	3	0.406	0.3566	1.000
5	2.542    1.368    3.477	4.375	2.8042	21	0.619	0.3566	1.000
6	2.542    1.575    4.004	3.800	1.7905	11	0.530	0.3566	1.000
7	4.517    1.400    6.324	2.406	0.6512	3	0.402	0.3566	1.000
8	4.517    1.625    7.340	2.073	0.5565	2	0.400	0.3566	1.000

Figure A-2. Initial optimized cell allocation for the design example.

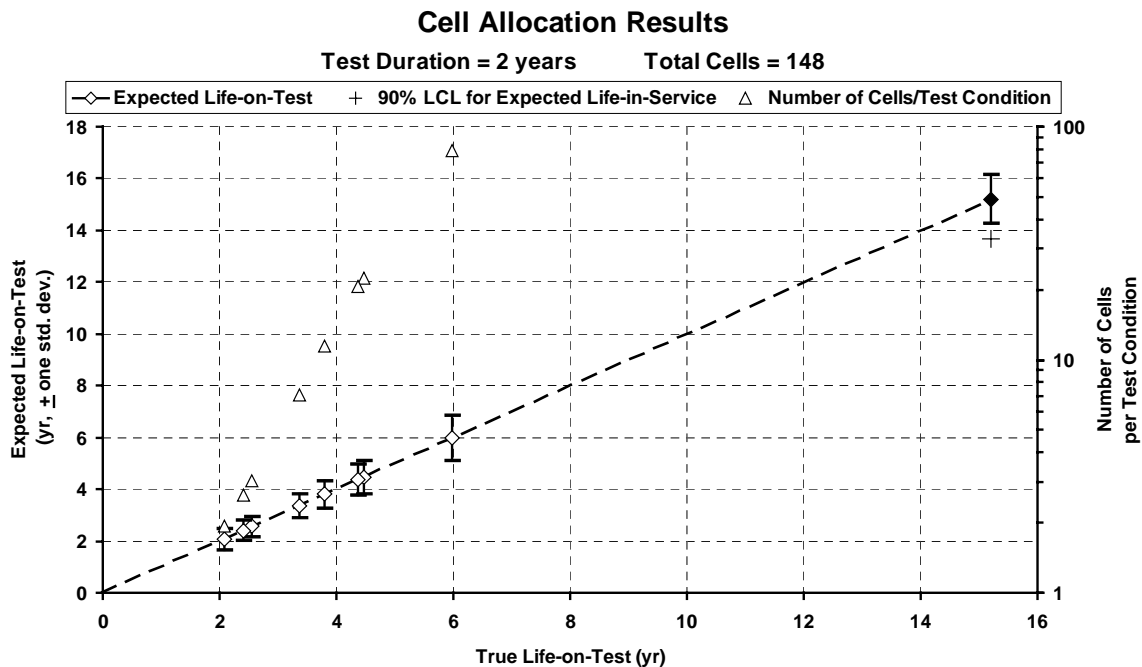


Figure A-3. Expected lives on test for the optimized design example.

The final cell allocation for the minimum core matrix design example is presented in Figures A-4 and A-5. Integer values of the cells per test condition are used, and have been adjusted to be more uniform. The effect on the 90% lower confidence limit for life in service is negligible. Note that the derivatives indicate which allocations are below optimum (derivative ratio > 1) and which are above optimum (derivative ratio < 1).

INPUT:		True Battery Capabilities:	Expected Noise Levels:						
	Life-in-Service (years) =	15.0	Standard deviation in electrode area = 0.5%						
	Calendar Life De-rating Factor =	0.986	Standard deviation in fixed ohmic resistance = 1.0%						
	Implied Calendar Life (years) =	15.213	Standard deviation in ASI measurement error = 1.0%						
	ASI Rate-of-Change Ratio =	0.125							
	ASI at Beginning of Life =	30							
	Allowable Power Fade =	25%							
	Specified total number of cells =	148							
	Minimum number of cells/test condition =	4							
	Life-on-test for Error Propagation =	2.073							
			<b>Reference Performance Test (RPT) Timing:</b>						
			RPT Interval (weeks) = 4						
			Number of RPT Intervals = 26						
			Implied Test Duration (years) = 2.00						
			Implied single-cell std. dev. = 0.5565						
<b>RESULTS:</b>		<b>Estimated 90% Lower Confidence Limit for Life-in-Service (years) = 13.65</b>							
Actual number of cells = 148		Estimated Std. Dev. of Calendar Life (years) = 0.956							
Test Condition #	Estimated Acceleration Factors:			Expected Life-on-Test	Single-cell Std. Dev.	Number of Cells	Life-on-Test Std. Dev.	Derivatives w.r.t. N-cell	Ratios of Derivatives
	Temperature	Cycling	Total AF						
1	2.542	1.000	2.542	5.985	7.8692	72	0.927	0.4278	1.398
2	3.404	1.000	3.404	4.469	3.0069	24	0.614	0.3135	1.024
3	4.517	1.000	4.517	3.368	1.2598	8	0.445	0.2813	0.919
4	5.943	1.000	5.943	2.560	0.7082	4	0.354	0.2054	0.671
5	2.542	1.368	3.477	4.375	2.8042	24	0.572	0.2613	0.853
6	2.542	1.575	4.004	3.800	1.7905	8	0.633	0.7233	2.363
7	4.517	1.400	6.324	2.406	0.6512	4	0.326	0.1534	0.501
8	4.517	1.625	7.340	2.073	0.5565	4	0.278	0.0831	0.272

Figure A-4. Final cell allocation for the design example.

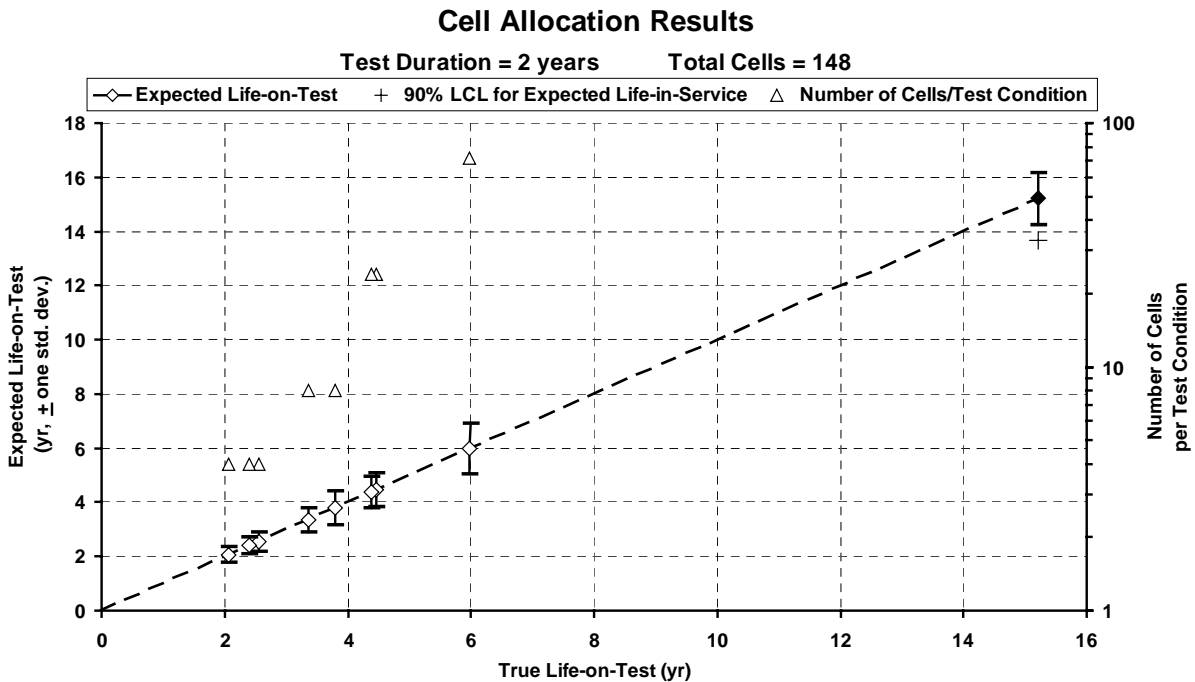


Figure A-5. Expected lives on test for the final design example.

Cell Allocator can be used to conduct initial parametric design studies before settling on a preliminary design for confirmation using Battery MCS. For example, the effect on the design of reducing the test duration from 24 months to 18 months is shown in Figure A-6. For the same number of cells, the 90% lower confidence limit in life in service is reduced by more than 14 months, to less than 12.5 years.

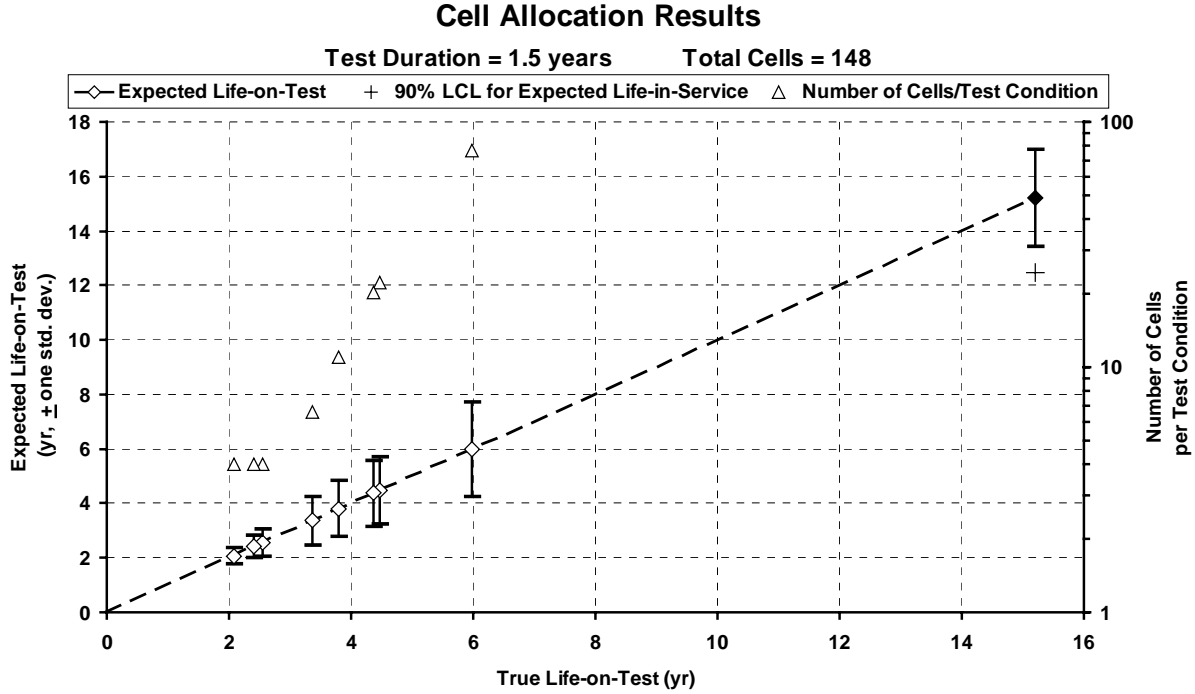


Figure A-6. Expected lives on test for reduced test duration.

The effect on the design when the test measurement noise is increased from 1 to 2% is shown in Figure A-7. If the total number of cells is not increased to compensate for the increased noise, the standard deviation in calendar life is increased by about 50%, with a corresponding decrease in the 90% lower confidence limit for life in service of 8 months.

INPUT:		<u>True Battery Capabilities:</u>		<u>Expected Noise Levels:</u>					
	Life-in-Service (years) =	15.0		Standard deviation in electrode area =	0.5%				
	Calendar Life De-rating Factor =	0.986		Standard deviation in fixed ohmic resistance =	1.0%				
	Implied Calendar Life (years) =	15.213		Standard deviation in ASI measurement error =	2.0%				
	ASI Rate-of-Change Ratio =	0.125							
	ASI at Beginning of Life =	30		<u>Reference Performance Test (RPT) Timing:</u>					
	Allowable Power Fade =	25%		RPT Interval (weeks) =	4				
	Specified total number of cells =	148		Number of RPT Intervals =	26				
	Minimum number of cells/test condition =	4		Implied Test Duration (years) =	2.00				
	Life-on-test for Error Propagation =	2.073	=====>	Implied single-cell std. dev. =	0.8417				
<b>RESULTS:</b>		<b>Estimated 90% Lower Confidence Limit for Life-in-Service (years) = <span style="border: 1px solid black; padding: 2px;">12.97</span></b>							
Actual number of cells = 148		Estimated Std. Dev. of Calendar Life (years) = 1.431							
Test Condition #	Estimated Acceleration Factors:			Expected Life-on-Test	Single-cell Std. Dev.	Number of Cells	Life-on-Test Std. Dev.	Derivatives w.r.t. N-cell	Ratios of Derivatives
	Temperature	Cycling	Total AF						
1	2.542	1.000	2.542	5.985	11.9111	77	1.361	0.8667	1.299
2	3.404	1.000	3.404	4.469	4.5318	22	0.972	0.8667	1.299
3	4.517	1.000	4.517	3.368	1.8906	7	0.723	0.8667	1.299
4	5.943	1.000	5.943	2.560	1.0657	4	0.533	0.4652	0.697
5	2.542	1.368	3.477	4.375	4.2248	20	0.948	0.8667	1.299
6	2.542	1.575	4.004	3.800	2.6909	11	0.812	0.8667	1.299
7	4.517	1.400	6.324	2.406	0.9816	4	0.491	0.3485	0.522
8	4.517	1.625	7.340	2.073	0.8417	4	0.421	0.1902	0.285

Figure A-7. Example results for increased measurement noise.

Since the standard deviation in calendar life is inversely proportional to the to square root of the total number of cells, the number of cells must be more than doubled, to about 333 cells, to compensate for the increased noise. The results in this case are shown in Figure A-8.

<b>INPUT:</b>		<u>True Battery Capabilities:</u>	<u>Expected Noise Levels:</u>						
	Life-in-Service (years) =	15.0		Standard deviation in electrode area = 0.5%					
	Calendar Life De-rating Factor =	0.986		Standard deviation in fixed ohmic resistance = 1.0%					
	Implied Calendar Life (years) =	15.213		Standard deviation in ASI measurement error = 2.0%					
	ASI Rate-of-Change Ratio =	0.125							
	ASI at Beginning of Life =	30		<u>Reference Performance Test (RPT) Timing:</u>					
	Allowable Power Fade =	25%		RPT Interval (weeks) = 4					
	Specified total number of cells =	333		Number of RPT Intervals = 26					
	Minimum number of cells/test condition =	4		Implied Test Duration (years) = 2.00					
	Life-on-test for Error Propagation =	2.073	=====>	Implied single-cell std. dev. = 0.8417					
<b>RESULTS:</b>		Estimated 90% Lower Confidence Limit for Life-in-Service (years) = <b>13.66</b>							
	Actual number of cells =	333		Estimated Std. Dev. of Calendar Life (years) = 0.948					
<u>Test Condition #</u>	<u>Estimated Acceleration Factors:</u>			<u>Expected</u>	<u>Single-cell</u>	<u>Number</u>	<u>Life-on-Test</u>	<u>Derivatives</u>	<u>Ratios of</u>
	<u>Temperature</u>	<u>Cycling</u>	<u>Total AF</u>	<u>Life-on-Test</u>	<u>Std. Dev.</u>	<u>of Cells</u>	<u>Std. Dev.</u>	<u>w.r.t. N-cell</u>	<u>Derivatives</u>
1	2.542	1.000	2.542	5.985	11.9111	178	0.893	0.1606	1.000
2	3.404	1.000	3.404	4.469	4.5318	51	0.638	0.1606	1.000
3	4.517	1.000	4.517	3.368	1.8906	16	0.474	0.1606	1.000
4	5.943	1.000	5.943	2.560	1.0657	7	0.408	0.1605	1.000
5	2.542	1.368	3.477	4.375	4.2248	46	0.622	0.1606	1.000
6	2.542	1.575	4.004	3.800	2.6909	26	0.533	0.1606	1.000
7	4.517	1.400	6.324	2.406	0.9816	6	0.404	0.1605	0.999
8	4.517	1.625	7.340	2.073	0.8417	4	0.404	0.1607	1.001

Figure A-8. Example results for increased total cells to compensate for increased measurement noise.

### A-4.2 Final Design Confirmation Using Battery MCS

The example design for the minimum core life test matrix was confirmed using Battery MCS to estimate the life on test for each test condition. The results are shown in Figure A-9, along with the estimated standard deviations of the lives on test. Comparison with Figure A-5 shows that, in this case at least, Cell Allocator provides slightly conservative estimates of the standard deviations, as well as a slightly lower value for the 90% lower confidence limit of life in service. The Battery MCS cases were all run for 100 Monte Carlo trials with the same cell allocation and noise levels as for the Cell Allocator design.

Battery MCS was also used to generate data analysis results for single-trial simulations of the example life test. The estimated lives on test and standard deviations are comparable, despite the use of just one trial for each test condition. These results are summarized in Section 4 of the manual and are discussed in more detail in Appendix B.

## RESULTS FOR LIFE TEST MATRIX EXAMPLE

Estimated ( $\pm 1$  std. dev.) vs. True Life-on-Test

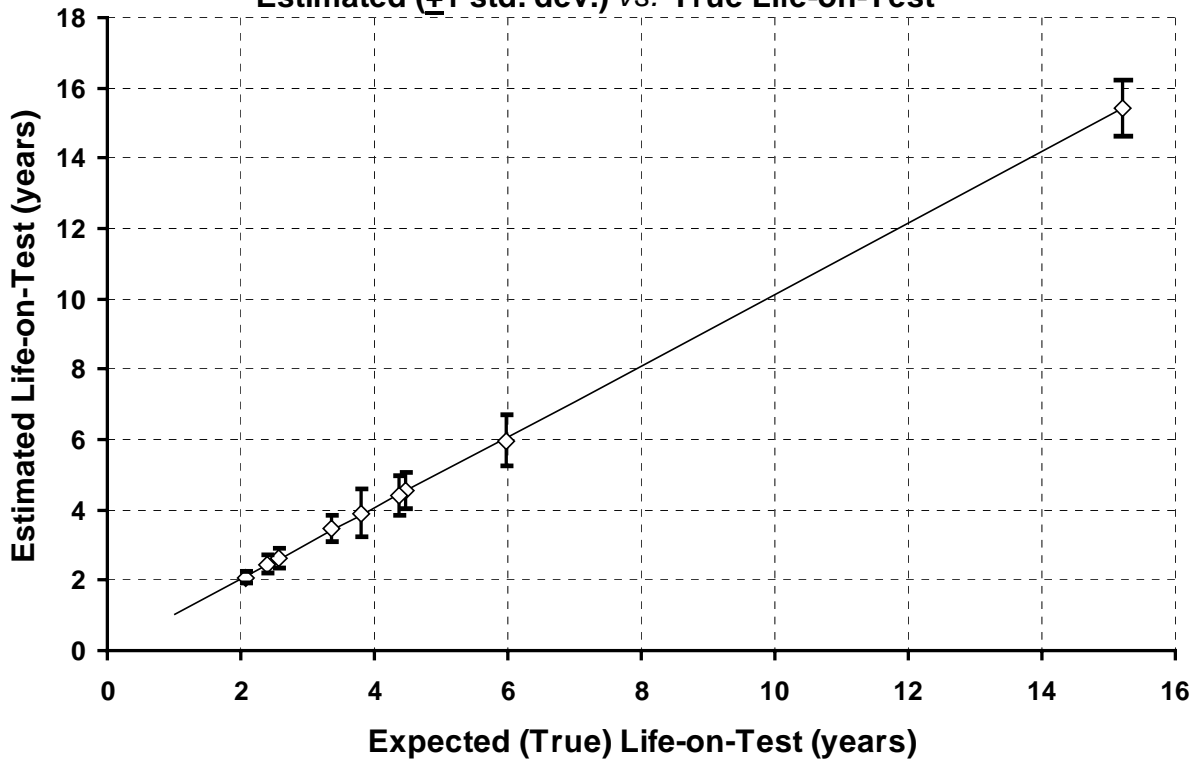


Figure A-9. Confirmation of core life test experiment design from Battery MCS results.

**Appendix B**  
**Methods for Modeling Life Test Data**



# Appendix B

## Methods for Modeling Life Test Data

### B-1. Description of Analysis Methods Used in the Manual

The nature of the experimental data should dictate an appropriate model form and influence the method of analysis. However, it is impossible to describe all models and methods of analysis that might be useful for modeling accelerated degradation data. A useful discussion of modeling and analysis issues is contained in Reference 20.

In terms of the model and analysis some important issues are:

- Minimization of model parameterization (minimize complexity)
- Maximization of model fidelity (accuracy)
- Quantification of model uncertainty.

Here, we present a relatively simple model that describes the way in which area-specific impedance (ASI) changes over time. Sections B-1.1, B-1.2, B-1.3, and B-1.4 present the model, describe a method for estimating the model parameters (and cell life), and describe a method for assessing estimation uncertainties. Section B-2 illustrates the use of this model with Advanced Technology Development ATD Gen 2 experimental data.

#### B-1.1 Assumed ASI Model

The underlying ASI model is of the form  $ASI(t + \Delta t_{RPT}) = \beta_0 + \beta_1 \cdot ASI(t)$ , where  $\beta_0$  and  $\beta_1$  are parameters to be estimated. In addition, another model parameter,  $ASI_0$ , is used to represent the value of ASI at time 0.

Using this model, the life on test is given by

$$L_{TEST} = \frac{\Delta t_{RPT}}{\log(\beta_1)} \cdot \left\{ \log \left[ \beta_0 + (\beta_1 - 1) \cdot \left( \frac{ASI_0}{(1 - PF)} \right) \right] - \log [\beta_0 + (\beta_1 - 1) \cdot ASI_0] \right\} .$$

#### B-1.2 Robust Orthogonal Regression for Estimating ASI Model Parameters

Standard regression seeks to minimize the vertical distances ( $Y$  coordinate) from the regression line to the data points. Use of standard regression assumes that the  $X_i$  have no (or negligible) error. In this case, it is clear that the errors in  $X$  are of comparable size to the errors in  $Y$ . In cases where the errors in  $X$  are nontrivial compared with the range of  $x$ , the use of standard regression will result in biased estimates of the slope ( $\beta_j$ ). (This may be the case if ASI is changing very little over time.) Orthogonal regression mitigates this defect of standard regression.

The method for performing robust orthogonal regression (ROR) is based the work of Amman and Van Ness (Reference 4). ROR involves two adaptations of standard least-squares regression of  $Y$  on  $X$ . Standard least-squares regression is described in many texts (see, e.g., Reference 6). The first adaptation

(robustness) makes the estimation of the model parameters less likely to be adversely affected by unusually large measurement errors in  $X$  and  $Y$ . The second adaptation (orthogonality) treats the  $X$  and  $Y$  variables symmetrically. That is, orthogonal regression finds the solution for  $\beta_0$  and  $\beta_1$  that minimizes the orthogonal distances from the regression line to the data points given by  $\{(X_1, Y_1), (X_2, Y_2), \dots, (X_n, Y_n)\}$ .

Analysis of the ASI data (simulated or real) is as follows. The data from the current Monte Carlo trial (or a real data set) are transposed from the basic array of test measurements into  $Y = \text{ASI}(t + \Delta t_{RPT})$  and  $X = \text{ASI}(t)$ . Robust orthogonal linear regression is used to estimate the parameters ( $\beta_0$  and  $\beta_1$ ) in the assumed model:  $y = \beta_0 + \beta_1 \cdot x$ , where  $X = x + \delta$  and  $Y = y + \varepsilon$ . The values of  $x$  and  $y$  are unobservable due to the random errors  $\delta$  and  $\varepsilon$ , which reflect cell-to-cell variation as well as measurement error. The ROR estimates of  $\beta_0$  and  $\beta_1$  are then used with the data to estimate  $ASI_0$ .

Robust orthogonal regression is implemented as follows.

1. Compute the average values of  $X$  and  $Y$

- a.  $\bar{X} = \frac{1}{n} \cdot \sum_{i=1}^n X_i$

- b.  $\bar{Y} = \frac{1}{n} \cdot \sum_{i=1}^n Y_i$

2. Center the values of  $X$  and  $Y$

- a.  $X_i = X_i - \bar{X}$

- b.  $Y_i = Y_i - \bar{Y}$

3. Initialize result matrix

- a.  $D = \begin{bmatrix} 1 & 0 \\ 0 & 1 \end{bmatrix}$

4. Obtain initial estimate of slope ( $b$ ) using iteratively re-weighted least-squares regression (IRWLS):

$$b = \text{IRWLS}\{(X_1, Y_1), (X_2, Y_2), \dots, (X_n, Y_n)\}$$

5. Loop: While  $b > 0.0001$

- a. Compute angle of regression line (line with slope  $b$  through origin):

$$\theta = \arctan(b)$$

- b. Compute rotation matrix:  $R = \begin{bmatrix} \cos(\theta) & -\sin(\theta) \\ \sin(\theta) & \cos(\theta) \end{bmatrix}$

- c. Rotate  $X_i$  and  $Y_i$ :

$$X_i^{rot} = X_i \cdot \cos(\theta) + Y_i \cdot \sin(\theta)$$

$$Y_i^{rot} = -X_i \cdot \sin(\theta) + Y_i \cdot \cos(\theta)$$

$$X_i = X_i^{rot}$$

$$Y_i = Y_i^{rot}$$

d. Adjust result matrix:  $D = D * R$

e. Estimate slope using rotated data:  $b = \text{IRWLS}\{(X_1, Y_1), (X_2, Y_2), \dots, (X_n, Y_n)\}$

$$\hat{\beta}_1 = -\frac{D_{12}}{D_{22}}$$

6.  $\hat{\beta}_0 = \bar{Y} - \hat{\beta}_1 \cdot \bar{X}$

The orthogonal regression adaptation is accomplished by a series of iterations, where each iteration involves a robust regression of the current X on the current Y followed by a data rotation. At each iteration, the data are rotated such that the current regression line is horizontal. The robust regression is accomplished by using iteratively reweighted least squares regression (IRWLS) (see, e.g., Reference 15.)

IRWLS is implemented as follows.

1. Set initial error weights:  $W_i^S = 1$  for  $i = 1 : n$

2. Set leverage weights:

a. 
$$T_i = \frac{X_i \cdot X_i}{\sum_{i=1}^n X_i \cdot X_i}$$
 for  $i = 1 : n$

b.  $W_i^T = \text{BIWEIGHT}\{T_1, T_2, \dots, T_n\}$  for  $i = 1 : n$

3. Loop 3 times

a.  $W_i = W_i^S \cdot W_i^T$  for  $i = 1 : n$

b. Estimate  $b$  using weighted regression

$$b = \frac{\sum_{i=1}^n X_i \cdot W_i \cdot Y_i}{\sum_{i=1}^n X_i \cdot W_i \cdot X_i}$$

a.  $S_i = Y_i - b \cdot X_i$  for  $i = 1 : n$

b.  $W_i^S = \text{BIWEIGHT}\{S_1, S_2, \dots, S_n\}$  for  $i = 1 : n$

4. Return  $b$ .

Two sets of weights, multiplied together, are used to form an aggregate weight for each observation. The idea is to downweight observations that have high residual (fall far from the fitted line in the current y-dimension) and/or high leverage (are located away from the origin in the current x-dimension). The first set of weights relates to the residual value. At the first IRWLS iteration, the

residual weights are uniformly set to one. In the two IRWLS iterations that follow, the residual weights depend on how far off the predicted y-dimension is from the observed y-dimension in the previous fit. The leverage weights for an observation depend on how far in the current x-dimension the observation is from zero. The leverage weights remain constant over the three IRWLS iterations.

Both the residual and leverage weights are obtained using Tukey's biweight function (e.g., see Reference 16), with  $c = 6$ . Let  $\text{BIWEIGHT}\{Z_1, Z_2, \dots, Z_n\}$  represent the biweight function and its generic arguments.

1. Compute median absolute value of  $Z_i$ 's:  $MAV$
2. Compute standardized values of  $Z_i$ 's:  $U_i = \frac{Z_i}{(c \cdot MAV)}$
3.  $WEIGHT_i = 0$  if  $Z_i \geq 1$  for  $i = 1 : n$
4.  $WEIGHT_i = (1 - U_i^2)^2$  if  $Z_i < 1$  for  $i = 1 : n$
5. Return WEIGHTs.

The estimation of  $ASI_0$  is as follows. For each RPT (value of  $t$ ), the average ASI value across all test cells is computed. Denote these average values by  $\{A\bar{S}I_0, A\bar{S}I_1, \dots, A\bar{S}I_N\}$ . The estimate of  $ASI_0$  is given by:

$$A\hat{S}I_0 = \left\{ \sum_{i=0}^N A\bar{S}I_i - \hat{\beta}_0 \cdot \left[ \sum_{i=0}^N \hat{\beta}_1^k - (N+1) \right] \cdot \left( \frac{1}{\hat{\beta}_1 - 1} \right) \right\} \cdot \left( \frac{1}{\sum_{i=0}^N \hat{\beta}_1^k} \right).$$

### B-1.3 Estimation of Life on Test

The life on test estimate is obtained via the estimated ROR model parameters,  $\Delta t_{RPT}$ , and  $PF$  (which is the maximum allowable fraction of degradation). The life on test estimate is

$$\hat{L}_{TEST} = \frac{\Delta t_{RPT}}{\log(\hat{\beta}_1)} \cdot \left\{ \log \left[ \hat{\beta}_0 + (\hat{\beta}_1 - 1) \cdot \left( \frac{A\hat{S}I_0}{(1 - PF)} \right) \right] - \log \left[ \hat{\beta}_0 + (\hat{\beta}_1 - 1) \cdot A\hat{S}I_0 \right] \right\}.$$

### B-1.4 Use of the Bootstrap Method for Estimating Uncertainties of Model Parameters and Life on Test

The uncertainty of the various estimated model parameters and life on test can be assessed by using the bootstrap, which is a procedure for estimating the uncertainty associated with complex estimation procedures. The motivation for using the bootstrap here is the complex nature of the estimation procedure ROR, for which it is difficult to analytically derive a useful estimate of the standard errors for the model parameters:  $ASI_0$ ,  $\beta_0$ , and  $\beta_1$ .

While the bootstrap is applied here for ROR with the given model, it is intended to be a general methodology for obtaining useful confidence limits for a quantity produced by any model and data analysis method used by a developer. Thus, it should be useful even in the absence of specific information on what developers might use in the future.

A simple way to think of the bootstrap is that it is a procedure for creating multiple realizations of experimental data from the single realization of actual data. In fact, one can view the bootstrap as a simulation using the experimental data. The bootstrap creates the multiple data realizations by sampling “with replacement.” The data analysis is then performed separately on each data realization resulting in a quantity of interest (e.g., “life on test”) for each realization.

Given the estimates of the three model parameters, we estimate  $\{ASI_1, ASI_2, ASI_3, \dots, ASI_m\}$  recursively using the relationship  $A\hat{S}I_k = \hat{\beta}_0 + \hat{\beta}_1 \cdot A\hat{S}I_{k-1}$ . Next, we compute the differences between the elements of  $\{A\hat{S}I_0, A\hat{S}I_1, A\hat{S}I_2, \dots, A\hat{S}I_m\}$  and  $\{ASI_{i0}, ASI_{i1}, ASI_{i2}, \dots, ASI_{im}\}$  for all values of  $i$ . Denote these differences as  $\mathbf{e} = \{e_{10}, e_{11}, \dots, e_{1m}, \dots, e_{20}, e_{21}, \dots, e_{2m}, \dots, e_{n0}, e_{n1}, \dots, e_{nm}\}$  and the average error for the  $i^{\text{th}}$  cell as  $\bar{e}_i$  (i.e.,  $\bar{e}_i = \text{avg}\{e_{i0}, e_{i1}, \dots, e_{im}\}$ ). Define measurement error as

$$\mathbf{f} = \{e_{10} - \bar{e}_1, \dots, e_{1m} - \bar{e}_1, \dots, e_{n0} - \bar{e}_n, \dots, e_{nm} - \bar{e}_n\}.$$

The  $\bar{e}_i$ ’s represent cell-specific effects (cell-specific ohmic and electrode area effects (see Section 2 of the manual). The values of  $A\hat{S}I_k$  ( $k=0, 1, 2, \dots, m$ ), the  $\bar{e}_i$ ’s, and the elements of  $\mathbf{f}$  are the essential ingredients of the bootstrap.

The bootstrap procedure suggested here assumes that  $\{A\hat{S}I_0, A\hat{S}I_1, A\hat{S}I_2, \dots, A\hat{S}I_m\}$  represents “truth.” The set of “measurement errors” to draw from is given by  $\mathbf{e}$ . The bootstrap procedure constructs a number of artificial data sets (say  $N$ ), from which the model parameters and other statistics (e.g., life on test) are estimated. Each data set is constructed as follows:

1. Draw  $n$  samples from  $\{\bar{e}_1, \bar{e}_2, \dots, \bar{e}_n\}$  with replacement:  $\{E_1, E_2, \dots, E_n\}$ . These values become simulated cell-specific effects.
2. Draw  $n$  samples of size  $m+1$  from  $\mathbf{f}$  with replacement:  $F_i = \{F_{i0}, F_{i1}, \dots, F_{im}\}$  for  $i = 1:n$ . This is the simulated measurement error.
3. Form a simulated ASI data set. Simulate the observed ASI measurements of the  $i$ th cell by adding  $E_i$  and  $F_i$  to  $\{A\hat{S}I_0, A\hat{S}I_1, A\hat{S}I_2, \dots, A\hat{S}I_m\}$ .
4. Using ROR on simulated data set, get estimates of the parameters:  
 $A\hat{S}I(\text{boot}), \hat{\beta}_0(\text{boot})$  and  $\hat{\beta}_1(\text{boot})$ .
5. Estimate the life on test (LOT( $\text{boot}$ )) given:  $A\hat{S}I_0(\text{boot}), \hat{\beta}_0(\text{boot})$ , and  $\hat{\beta}_1(\text{boot})$ .

This 5-step process is repeated  $N_{\text{boot}}$  times to give  $N_{\text{boot}}$  values for  $A\hat{S}I_0(\text{boot})$ ,  $\hat{\beta}_0(\text{boot})$ , and  $\hat{\beta}_1(\text{boot})$  as well as  $\hat{L}_{\text{TEST}}(\text{boot})$ . A suggested value for  $N_{\text{boot}}$  is 100.

The bootstrap standard error for any of these quantities is simply the standard deviation of the quantities taken over the  $N_{boot}$  bootstrap simulations (e.g.,  $S_{L\hat{O}T(boot)}$ ). Confidence intervals for any of these quantities can be derived directly from percentiles of the empirical distributions of the bootstrap estimates.

## **B-2. Example Use of the Data Analysis Methods Applied to Advanced Technology Development Life Test Data**

Testing of the second generation of ATD cells (i.e., Gen 2 cells) is nearing completion. These 18650-size cells, consisting of both a baseline and variant chemistry, have been distributed over a matrix consisting of several SOCs, temperatures, and life tests (Reference 2). Life testing is performed in accordance with the *PNGV Battery Test Manual* (Reference 19), with interruptions every 4 weeks for reference performance tests (RPTs). The L-HPPC test is regularly included as part of the Gen 2 RPT, and is used to calculate changes in ASI as a function of test time (the Gen 2 discharge ASI data are based on the 18-s pulse at a 5C rate, as defined in Reference 19).

### **B-2.1 Background**

The data analysis methods for modeling battery life test data presented above are the results of intensive efforts to analyze such data from the Advanced Technology Development program. The data set first used was from cycle-life testing of Gen 2 Baseline cells at 45°C. One approach involved a form of auto-correlation to quantify the sources of variation in the measured ASI for this group of cells (Reference 12). The values of pulse power measured at four weeks (Y-coordinate) were plotted against the corresponding values measured in the initial cell characterization (X-coordinate). This form of scatter plot revealed a linear relationship between the two variables, with a high positive correlation coefficient (+0.96). Extension of the method to Variant C cells in cycle-life testing at 45°C, and to cells in calendar-life testing at 45°C, gave similar results.

The implications of this linear relationship were not immediately clear. Analysis of the linear regression using an iterated solution from a Taylor-series expansion led finally to the general solution presented previously:

$$ASI\{t+\Delta t_{RPT}\} = \beta_0 + \beta_1 ASI\{t\}$$

$$ASI\{t\} = \{[\beta_0 + (\beta_1 - 1) ASI\{t=0\}] \exp[\ln(\beta_1) t/\Delta t_{RPT}] - \beta_0\} / (\beta_1 - 1).$$

This basic approach to the modeling of ASI test data was subsequently refined into its present state of development, as illustrated in the following.

### **B-2.2 Application to the Gen 2 Cycle-Life Data**

Figure B-1 shows the ASI as a function of test time for all of the Baseline cells cycle-life tested at 25°C, and the observed linear relationship for these cells between the values at time  $t+\Delta t$  and  $t$  weeks is shown in Figure B-2. Figure B-3 shows the ASI as a function of test time for the 45°C cycle-life Baseline cells. Both the 25 and 45°C cells were cycled using the 25-Wh power assist profile with RPTs every 33,600 cycles. Each temperature group began with 14 cells, but pairs of cells were removed at regular power fade increments for diagnostic analysis (Reference 2). Consequently, only four 25°C Baseline cells have been testing beyond 72 weeks. These cells have completed 112 weeks of cycling, and will

continue until 50% power fade. Only two 45°C Baseline cells were tested beyond 44 weeks, and they reached end of test after 68 weeks of cycling.

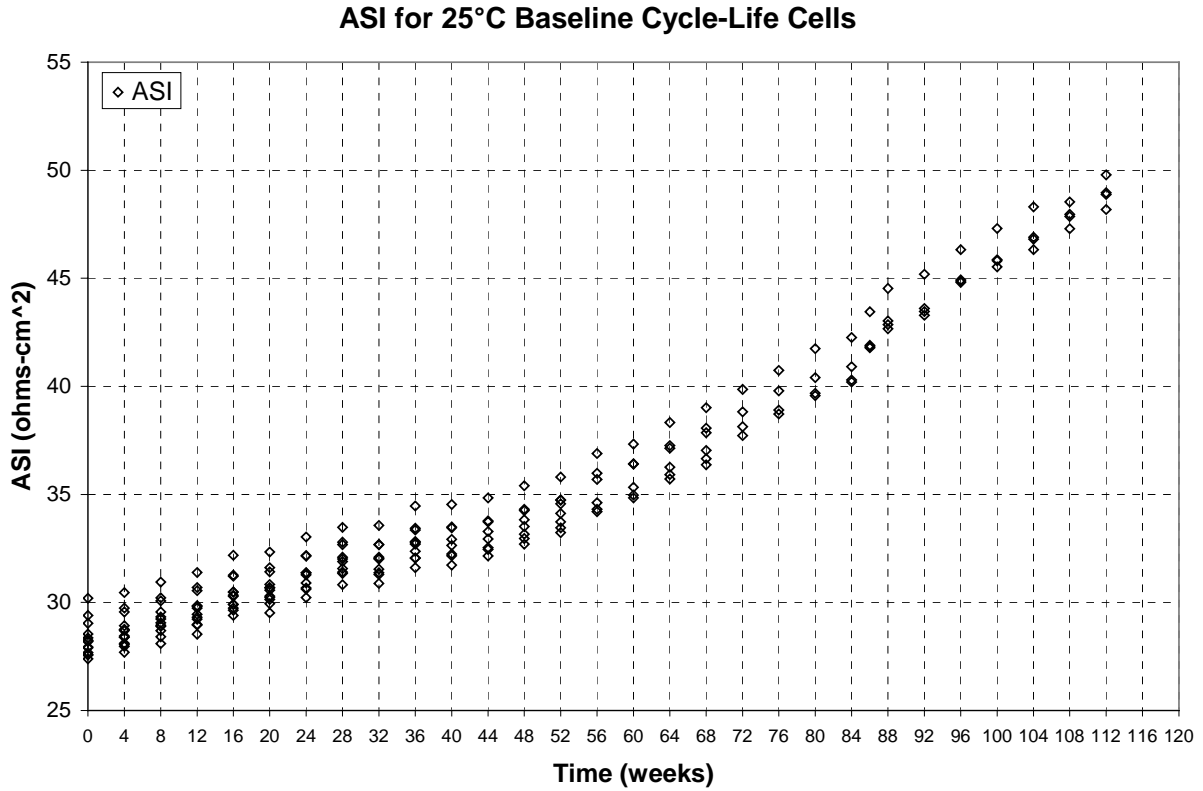


Figure B-1. ASI data for the 25°C Baseline cycle-life cells as a function of test time.

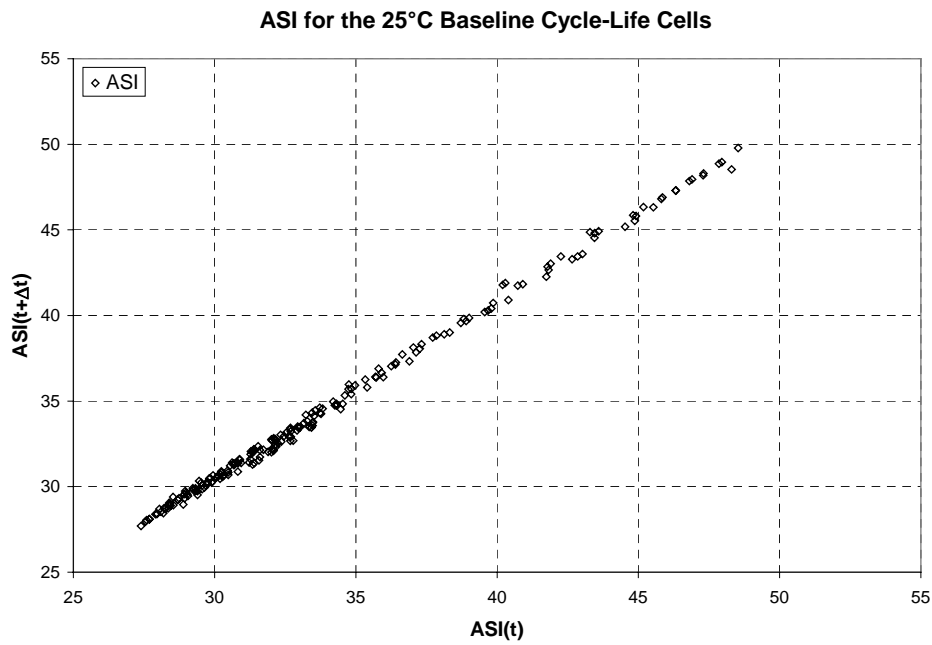


Figure B-2. ASI data at time  $t+\Delta t$  versus time  $t$  for the 25°C Baseline cycle-life cells.

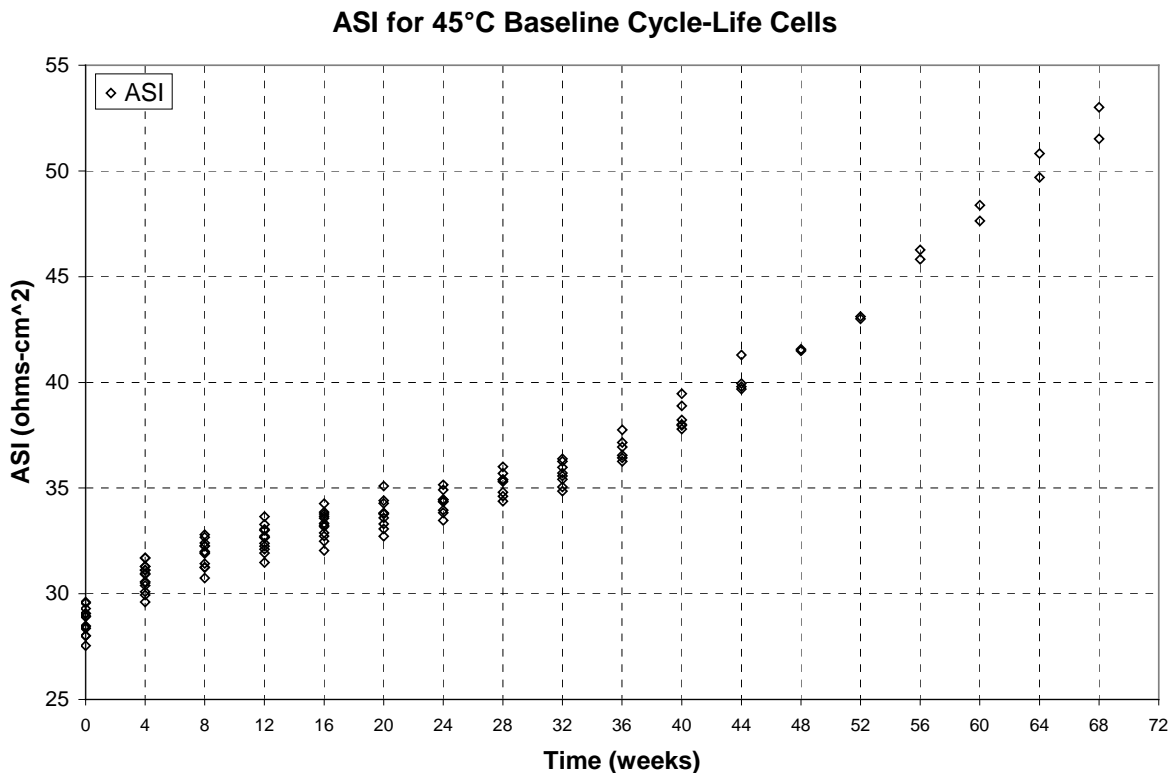


Figure B-3. ASI data for the 45°C Baseline cycle-life cells as a function of test time.

Figure B-4 shows the 25°C Baseline cell ASI at time  $t+\Delta t$  as a function of the ASI at time  $t$ . As mentioned above, the data are very linear, and, consequently, the ROR fit to the data is in excellent agreement. Also shown are the aggregate weights (the product of the residual and leveraging weights) for each observation. As discussed above, the early and late data are high leverage points, and so are down-weighted to avoid possible detrimental influences to the slope ( $\beta_1$ ).

Figure B-5 shows the ROR fit for the 45°C Baseline cycle-life cells. Unlike the 25°C cells, these data do not show a simple linear relationship. The initial characterization data [with an ASI(t) less than 30 ohm-cm<sup>2</sup>] are offset compared to the remaining ASIs. This may be primarily due to improper formation cycling, as discussed in Reference 1 and Appendix C. Therefore, these data need to be ignored in the ROR analysis for more accurate life on test projections. The 45°C data also showed a mechanistic change, with a higher rate of degradation, after 32 weeks of aging (Reference 2). Consequently, the ROR analysis also had to be split into two components at 32 weeks. As shown in Figure B-5, the two ROR fits match their respective data sets more accurately than a single ROR fit would be able to accomplish.

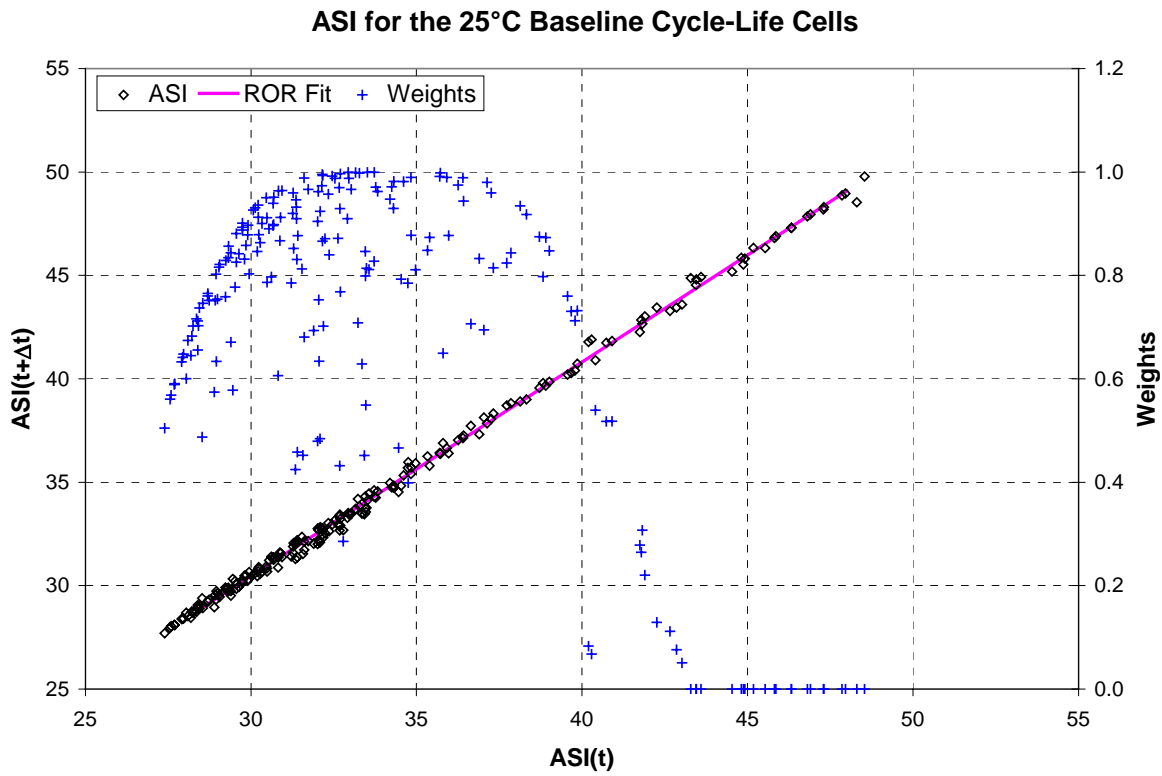


Figure B-4. ASI data for the 25°C Baseline cycle-life cells.

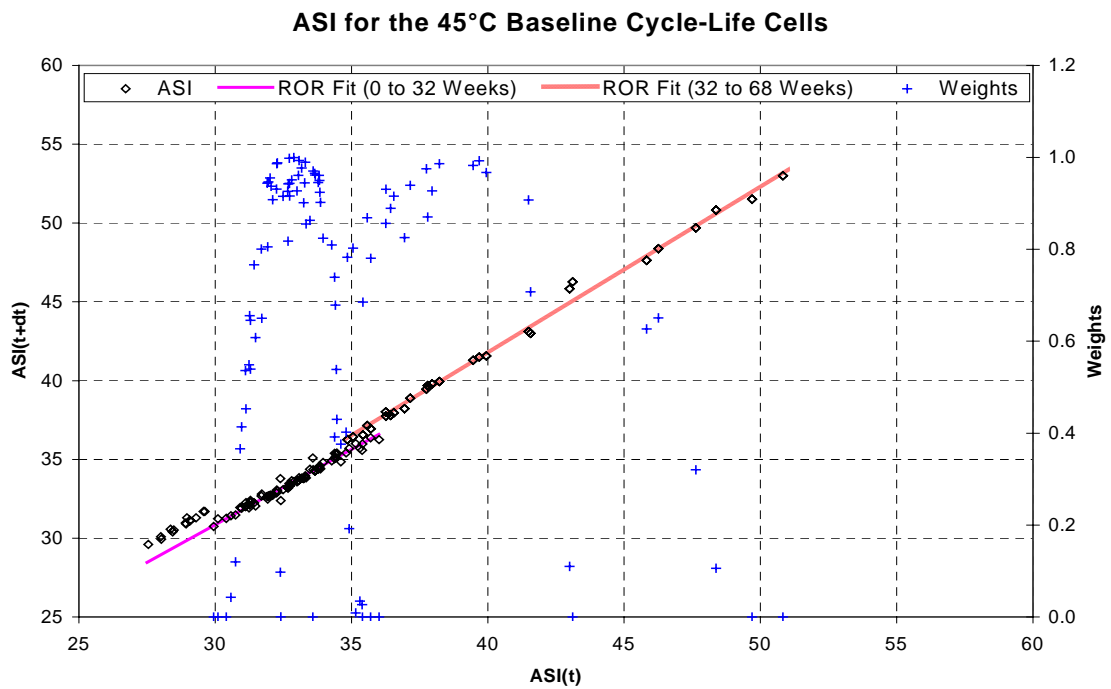


Figure B-5. ASI data for the 45°C Baseline cycle-life cells.

Based on the ROR-estimated values for the slope ( $\beta_1$ ) and intercept ( $\beta_0$ ), and the corresponding value for the initial ASI ( $ASI_0$ ), the ASI as a function of test time can be estimated and compared to the actual data. Figure B-6 shows that the ROR method accurately portrays the ASI for both the 25 and 45°C Baseline cycle-life cells. Since the initial 45°C cell data were ignored in the ROR analysis,  $ASI_0$  is higher than the measured data, but this resulted in a good fit at the end of testing.

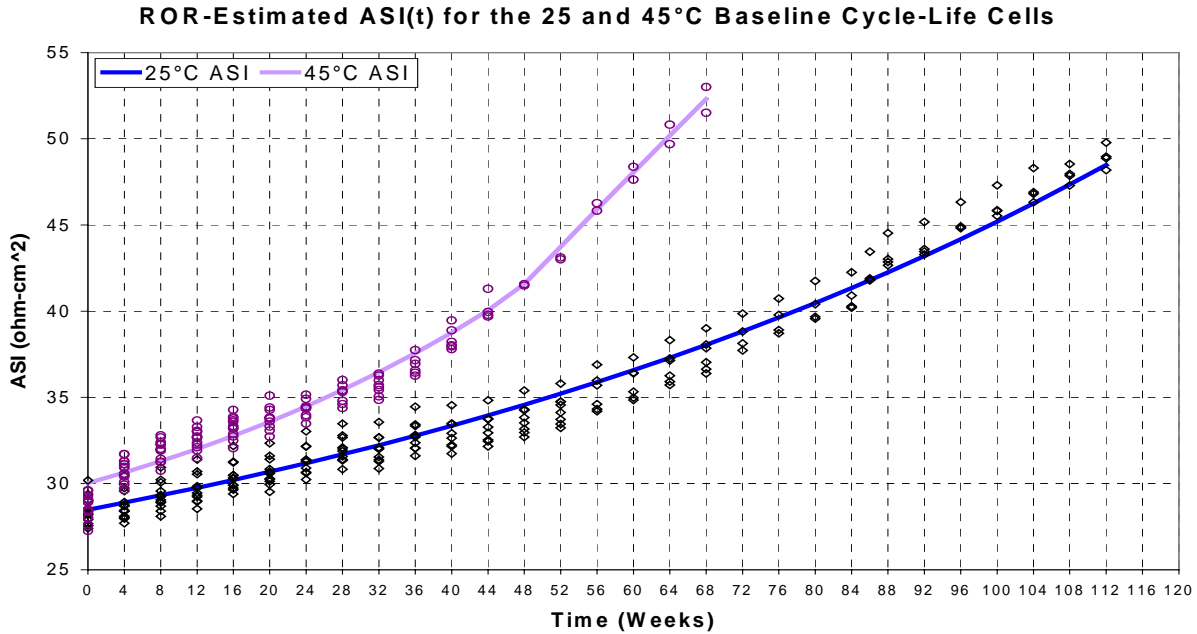


Figure B-6. ROR-estimated ASI compared to the test data.

Table B-1 shows the parameter estimates from the ROR analysis ( $\beta_1$  and  $\beta_0$ ),  $ASI_0$ , and the LOT projections. The estimate of life on test  $\hat{L}_{TEST}$  is based on the equation shown in Section B-1.3 of this appendix. The  $LOT_{90}$  is the estimated life on test with a 90% confidence after 100 iterations of the bootstrap method. The maximum allowable fraction of degradation ( $f$ ) was set to 50% for the 25°C cells, and the second set of ROR estimates for the 45°C cells. For the first set of 45°C cell ROR estimates, the allowable fraction of degradation was set to 22.5%, based on the actual average power fade at 32 weeks. As shown,  $\hat{L}_{TEST}$  consistently overestimates compared to the bootstrap approach, but the bootstrap estimation changes with each set of 100 trials, since the errors are randomly distributed.

Table B-1. Parameter estimates from the ROR and bootstrap analysis.

	Test Interval	Test		$ASI_0$ (ohm-cm <sup>2</sup> )	$\hat{L}_{TEST}$ (years)	$LOT_{90}$ (years)
		$\beta_0$	$\beta_1$			
25°C Baseline Cells	0-42 wk	-0.551	1.034	28.46	2.760	2.643
45°C Baseline Cells	0-32 wk	2.193	0.955	30.83	1.127	0.910
	32-66 wk	-0.759	1.063	35.35	1.161	1.075

### B-2.3 Effects of Temperature Sensitivity

Temperature sensitivity is an important issue in estimating life on test, and the MPPC has been designed to allow for temperature compensations at each RPT interval (Section 3.1.2.2). Although the Gen 2 RPT was not designed for continuous temperature adjustments, a methodology has been developed to compensate for temperature fluctuations on the cycle-life Baseline cell data to determine the effects of temperature on life on test estimations. The Gen 2 data were adjusted using the equations defined in Section 4.1.3, with a linearly increasing  $T_{ASI}$ . The  $T_{ASI}$  coefficient was determined from the Arrhenius slope of the cycle-life pulse resistances based on similar average ASIs, but at different RPT intervals.

Figure B-7 shows the ROR-estimated ASI as a function of test time for the temperature compensated data compared to the original estimations (also shown in Figure B-6). Table B-2 shows the parameter estimates and bootstrap analysis from the adjusted data. For the first set of the 45°C cells, the allowable fraction of degradation was set to 21.0%, based on the average adjusted power fade at 32 weeks. As shown, the impact of temperature results in small changes to the life on test estimations.

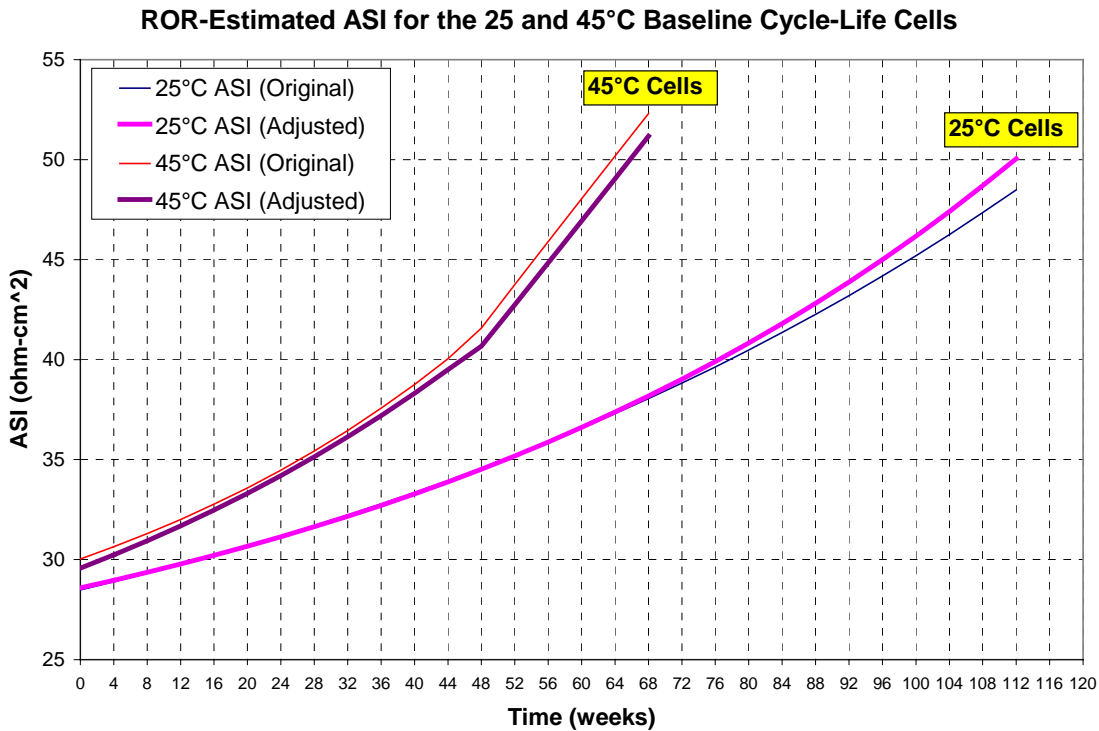


Figure B-7. ROR-estimated ASI for the measured and adjusted ASI data.

Table B-2. Parameter estimates from the ROR and bootstrap analysis of the adjusted data.

	Test		ASIO		$\hat{L}_{TEST}$ (years)	LOT90 (years)
	Interval	$\beta_0$	$\beta_1$	(ohm-cm <sup>2</sup> )		
25°C Baseline Cells	0-42 wk	-0.717	1.039	28.49	2.642	2.500
45°C Baseline Cells	0-32 wk	2.464	0.946	30.57	1.089	0.818
	32-66 wk	1.320	1.012	34.27	1.359	1.201

## B-2.4 Noise Levels

Figure B-8 shows the cell-to-cell residual ASI error for the four longest lasting 25°C Baseline cycle-life cells. The residual error was determined based on the difference between the actual cell ASI and the estimated ASI from the ROR analysis for each individual cell. The noise is somewhat correlated, which reduces the effectiveness of adding cells to reduce the noise. (Noise would be reduced by a factor of  $1/\sqrt{N}$  for uncorrelated noise using  $N$  cells.)

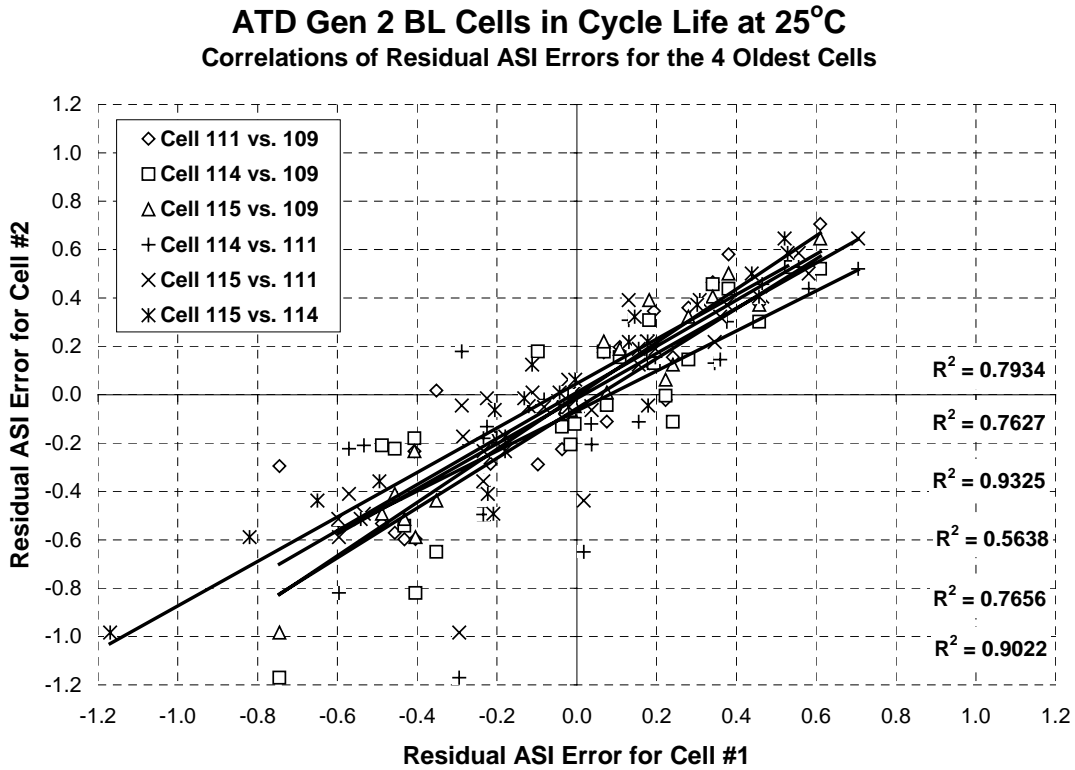


Figure B-8. Correlations of residual errors.

**Appendix C**  
**Study of Life-Limiting Mechanisms in High-Power  
Lithium-Ion Cells**



# Appendix C

## Study of Life-Limiting Mechanisms in High-Power Li-Ion Cells

### C-1. INTRODUCTION

DOE's Advanced Technology Development (ATD) program has studied the aging mechanisms of high-power lithium-ion cell chemistries since it was initiated in 1999. Several cell chemistries were developed on the ATD program and then studied in high-power 18650 spiral-wound cells. They were subjected to accelerated aging tests and then extensively investigated using a wide range of diagnostic tools. All groups of cells studied to date reach end-of-life due to increasing impedance and corresponding power loss. For the latest high-power cell chemistry (denoted the Gen 2 cell chemistry), a phenomenological cell model was developed and used to study and identify possible phenomena that could be limiting specie transport within the cell chemistry and causing the observed impedance rise during cell aging. The model was used to link the diagnostic findings to the aging characteristics of the cells. This appendix provides a brief summary of the latest cell chemistry and the studies performed on these cells in an attempt to identify the main factors responsible for impedance rise and power fade in these cells. Since this is a cell chemistry that was studied extensively, it is being used as an example of a technology-specific approach for developing life prediction methodologies, as recommended in this manual.

### C-2. GEN 2 CELL DESCRIPTION

The Gen 2 cells are of the standard 18650 size, however they were custom designed for high power and for better hermeticity. They employ 10 tabs along the length of both the positive and negative electrodes. This significantly reduces the resistance associated with the current collection system during high-current charge and discharge pulses. Also, the cells employ an aluminum case, which is connected to the positive electrode, and the cells are sealed via a laser weld. All cells were leak checked to ensure a high degree of hermeticity, prior to being shipped.

Table C-1 lists the cell chemistry that was employed in the ATD Gen 2 baseline cells. The electrode materials were selected on the basis of material screening tests of advanced low-cost materials available from international suppliers in 2000. The electrolyte formulation was developed jointly by Argonne National Laboratory (ANL) and the U.S. Army Research Laboratory (ARL) and made for the ATD program by Quallion, LLC, the same company that designed and built the Gen 2 high-power 18650 cells (to ANL specifications).

Table C-1. Gen 2 Baseline Cell Chemistry

<p><b><u>Positive Electrode:</u></b>            84 wt% LiNi<sub>0.8</sub>Co<sub>0.15</sub>Al<sub>0.05</sub>O<sub>2</sub> (Fuji CA1505)            8 wt% PVdF binder (Kureha KF-1100)            4 wt% SFG-6 graphite (Timical)            4 wt% carbon black (Chevron)            8 mg/cm<sup>2</sup> loading density            35 μm thick coating /side            30 μm thick Al current collector</p>	<p><b><u>Negative Electrode:</u></b>            92 wt% MAG-10 graphite (Hitachi)            8 wt% PVdF binder (Kureha #C)            4.9 mg/cm<sup>2</sup> loading density            35 μm thick coating/side            18 μm thick Cu current collector</p>
<p><b><u>Electrolyte:</u></b>            1.2M LiPF<sub>6</sub> in EC:EMC (3:7)</p>	<p><b><u>Separator:</u></b>            25 μm thick polyethylene (Celgard)</p>

A second group of cells were built using a very similar cell chemistry. The only difference in the chemistry was the level of aluminum dopant in the positive electrode active material—the level of aluminum was increased from 5% to 10%. This material was also produced by Fuji Chemical, using the same spray drying process that was used for making the positive electrode material for the Gen 2 baseline cells and both materials were subjected to the same calcination process. This second group of cells is denoted the Gen 2 Variant C cells.

### C-3. ACCELERATED AGING TESTS

A total of 165 cells were built using the Gen 2 baseline cell chemistry described above. Most of the cells were used in accelerated tests and in studying acceleration parameters, while others were used in abuse tolerance testing. Forty-seven cells went to cycle and calendar life testing at the Idaho National Engineering and Environmental Laboratory (INEEL) and ANL, respectively. Fourteen cells were cycle life tested at 25°C, fourteen cells were cycle life tested at 45°C, and 14 cells were calendar life tested at 55°C. Two additional cells were put on calendar life test at 45°C. Three cells were simply characterized before being sent to the diagnostics labs (ANL, Brookhaven National Laboratory, and Lawrence Berkeley National Laboratory) for benchmark evaluation. Another 30 cells were made with Variant C chemistry. Several of these cells arrived at ANL with soft shorts and were set aside. Of those that passed the initial characterization tests, 14 were put on cycle life test at 45°C and 10 were put on calendar life test at 45°C. The test regime and the laboratory responsible for the testing are given in Table C-2.

Table C-2. Gen 2 Cell Test Conditions

Testing Laboratory	Baseline Cells		Variant C Cells	
	Calendar	Cycle	Calendar	Cycle
ANL	14 cells - 55°C 2 cells - 45°C		10 cells - 45°C	
INEEL		14 cells - 25°C 14 cells - 45°C		14 cells - 45°C

(Calendar- and cycle-life testing were performed at 60% SOC, which, based on the initial  $C_{1/25}$  tests, corresponded to 3.723 and 3.741 V for baseline and Variant C cells, respectively.)

The calendar-life cells were subjected to a daily 3C current pulse at temperature for 28 consecutive days to monitor cell impedance changes, as defined in the test manual.<sup>16</sup> The cycle-life cells were aged using the BSF-scaled, 25-Wh profile of Reference 19. Before cycle-life testing, the operating set point stability (OSPS) test was performed to verify cycling stability. The OSPS test consists of 100 consecutive cycle-life profiles. The requirement is that at its completion, the actual SOC should be within  $\pm 2\%$  of 60% SOC, based on the OCV following a 1-h rest at the beginning and end of the 100 pulses. If the SOC is charge positive or charge negative (i.e., unstable), then the control voltage at the end of the discharge pulse is changed and the OSPS test is repeated until stable cycling occurs.

As shown in Table C-2, the cycle-life cells were tested at 25 and 45°C. After four weeks at temperature (33,600 profiles), RPTs were performed, as described below. End-of-life for these cells was defined as 30% power fade. Throughout the testing, selected cells were removed at predetermined intervals and forwarded to the diagnostic team for tear down and evaluation. At first, two cells were removed after 4 weeks of testing. The removal scheme was then changed to depend on power fade increments. For the baseline cells, the increments were approximately 5.2% and 3.6% for the cycle life cells at 25 and 45°C, respectively. For the baseline calendar life

cells at 55°C, the increment was approximately 3.6%. For the Variant C cycle life cells, the power fade increment was approximately 3%; and for the calendar life cells, it was approximately 3.6%. Thus, by 30% power fade, 12 cells were removed from test. The final two cells were left on test until 50% power fade. The two calendar life tested cells at 45°C were left on test for the full 50% power fade. The power values used in these removal schemes were defined by the intersection of the curve for a given cell and the 300-Wh line on the Available Energy vs. Power graph, as defined in the test manual.<sup>16</sup>

For all cells, RPTs were performed at 4-week intervals, but, at first, not all cells received the full RPT given in Table C-3. In the time interval of 4 to 12 weeks, only two selected cells, plus any that were scheduled for removal, received the full RPT. The more-limited RPT omitted the EIS and C/25 experiments. At 16 weeks and thereafter, all cells received the full RPT. The RPT for these test cells was more extensive than the RPTs found in the FreedomCAR test manuals. The reason for this was to extract as much electrochemical information as reasonably possible during aging. A description of the low-current hybrid pulse power characterization (L-HPPC) test is provided in Reference 19.

Table C-3. ATD Reference Performance Test Sequence

Temperature (°C)	ANL (Calendar Life)	INEEL (Cycle Life)
25	C <sub>1</sub> /1 discharge	C <sub>1</sub> /1 discharge
25	C <sub>1</sub> /25 discharge	L-HPPC
25	C <sub>1</sub> /25 charge	C <sub>1</sub> /25 discharge
25	EIS at 60% SOC	C <sub>1</sub> /25 charge
25	L-HPPC	EIS at 60% SOC

As the cells age, the C/25 capacity fades. A plot of the average C/25 capacity versus time for the cells along with the least squares fit to  $at^{1/2} + d$  is given in Figure C-1. From the values of  $r^2$ , 0.96 to 1.00, the fits are excellent. The order of C/25 capacity fade is 55°C calendar life > baseline cycle life at 45°C  $\approx$  baseline calendar life at 45°C > Variant C calendar life at 45°C  $\geq$  Variant C cycle life at 45°C  $\approx$  25°C cycle life. The fact that all the curves can be fit to a  $t^{1/2}$ -dependent equation (parabolic kinetics) indicates that there is a common, diffusion-controlled, lithium-consuming reaction occurring in both chemistries, such as a lithium corrosion reaction at the anode.

The time-dependent behavior of the C/1 capacity is more complex (see Figure C-2). Instead of a smooth curve, the curves have breaks in them which change, primarily, with temperature. As will be shown below, the breaks in the curves from the baseline cells can be attributed to the changes in the ASI.

As the cells age, the area-specific impedance (ASI) increases. Plotting the ASI values at 60% SOC vs. time shows that there are cathode-dependent (i.e., Al content) differences in the way ASI increases. This is shown in Figure C-3. The baseline chemistry follows a two-step mechanism that depends on  $t^{1/2}$  at first then on  $t$  at later times. In this experiment, temperature controls only where the change from  $t^{1/2}$  to  $t$  occurs. The data from the Variant C cells shows that ASI also depends on  $t^{1/2}$  and on  $t$ . The change in time dependency appears in the long-term aging data; it occurs later in cell life (35 vs. 55 weeks, respectively, for baseline and Variant C chemistries).

Since the only known difference between the two cell chemistries is the composition of the cathode, the cathode could play a significant role in the cell impedance rise. The fact that the

Variant C cells show the second-stage  $t$  dependence at a later time in the experiment suggests that the additional AI retards the second-stage aging process.

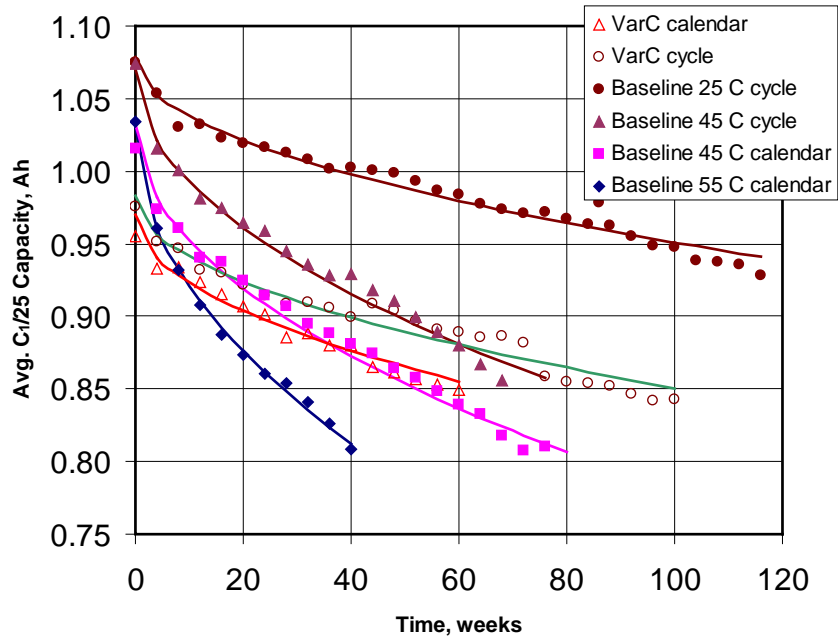


Figure C-1. Average C/25 capacity vs. time.

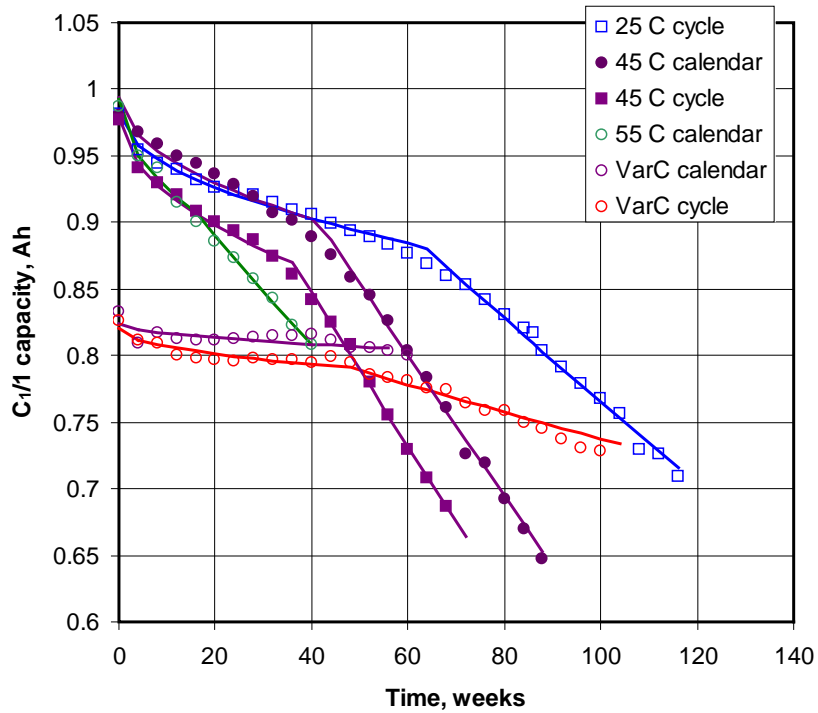


Figure C-2. C/1 capacity as a function of time for both cell chemistries.

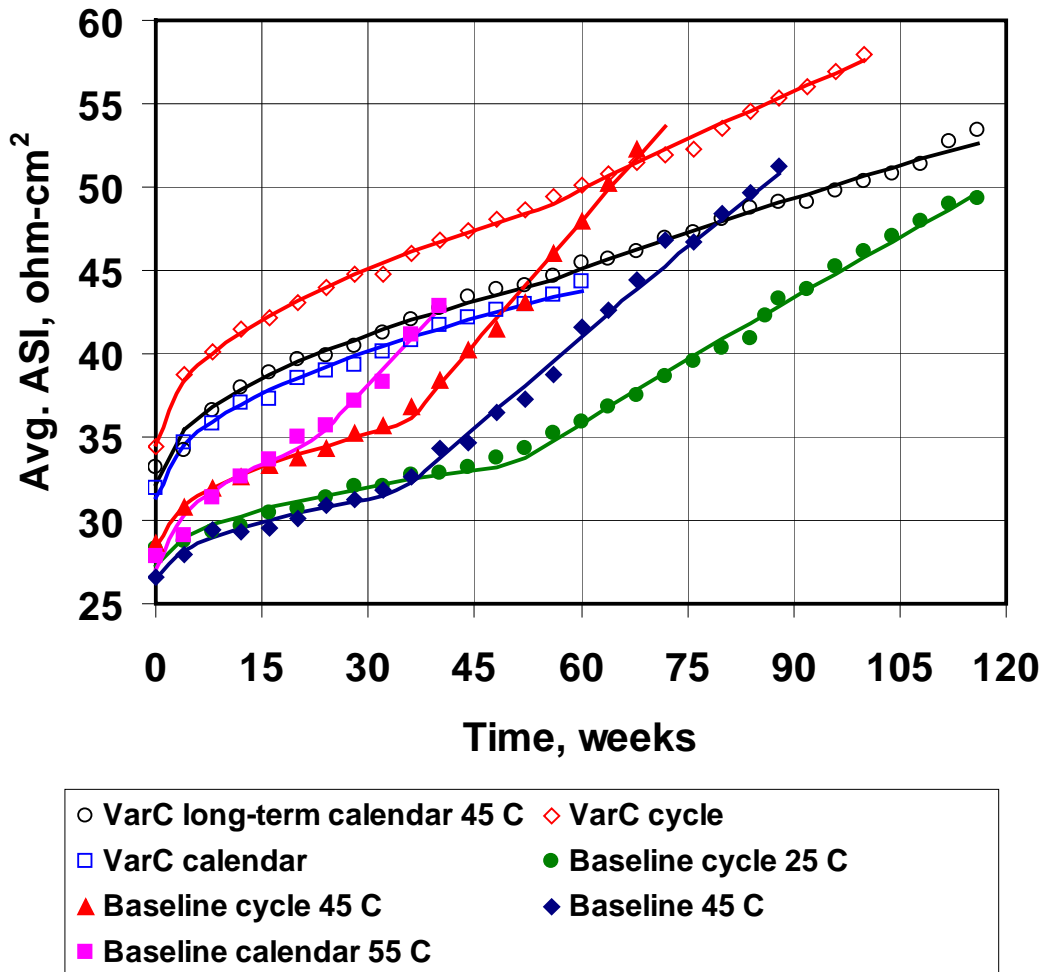


Figure C-3. Average ASI vs. time for both cell chemistries.

Fitting the ASI vs. time data to a nonlinear equation, such as  $at^{1/2} + c(t-t_0)$ ,  $c=0$  when  $t < t_0$ , shows that there is a statistically significant difference in the  $a$  coefficient for both groups of cells calendar- and cycle-life tested at 45°C. This difference can be attributed to the additional stress that cycling puts on the cells.

Another method for data analysis is outlined in this manual, Robust Orthogonal Regression (ROR, see Appendix B). As an example, the ROR results from the baseline calendar life data at 55°C will be used. Since the ASI data from the above aging tests does not follow a simple curve, the data was split into two parts: 0 to 20 weeks and 20 to 40 weeks. The ROR analysis was performed on each section separately. A plot from the ROR analysis is shown in Figure C-3a. The values of the ROR parameters are given in Table C-4. A plot of the data shown in Figure C-3a against time and compared to the data in Figure C-3 is given in Figure C-3b.

Table C-4. Results of ROR analysis of the baseline calendar life data at 55°C

	ASI <sub>0</sub>	β <sub>0</sub>	β <sub>1</sub>
0 to 20 weeks	28.063	2.74	0.96
20 to 40 weeks	35.05	-8.65	1.27

The data in Figure C-3 shows that, sometimes, the transition from one mechanism to another is obvious and, at other times, it is subtle. Good examples of obvious transitions are the ASI data from the baseline cells. An example of a subtle change is illustrated by the ASI data from the Variant C cycle life cells. Replotting the data on log-log axes helps elucidate the change in mechanism. Examples are shown in Figure C-4, using the data mentioned. If the data had followed one mechanism, the plot on the log-log axes will be a straight line, with the slope dependent on the exponent of time. From Figure C-4, the curves are not linear, indicating that the exponent of time has changed. Hence, there is a change in mechanism.

Additional information was obtained from EIS experiments. A typical EIS spectrum is given in Figure C-5. From this figure, the high-frequency minimum does not change appreciably with time. Proceeding to lower frequencies, the real part of the impedance of the next local minimum increases with time. Finally, the length of the low-frequency tail seems to be increasing with time. The mid-frequency arc is typically associated with interfacial impedance, while the low-frequency tail is typically associated with diffusional impedance.

The mid-frequency-range data in Figure C-5 (through interfacial arc) were modeled using the equivalent circuit shown in Figure C-6. The results show that R1 (materials resistance) does not increase significantly. This is also apparent in Figure C-5. The other two resistances, R2 and R3, representing interface impedance, change with time. A plot of these values is shown in Figure C-7. From the plot, R2 increases linearly with time while R3 increases non-linearly, similar to that seen in Figure C-3. The shape of the ASI data is, in part, due to the behavior of R2+R3.

A separate study was conducted to examine the importance of various acceleration factors on the aging characteristics of the Gen 2 baseline cells. Since, these tests were conducted using different protocols and different RPTs, data from those tests are not directly comparable and are not included here to avoid confusion. However, these tests clearly showed that cell state-of-charge (SOC) was another parameter that had a significant impact on the rate of impedance rise and capacity fade in the Gen 2 cells (Reference 21).

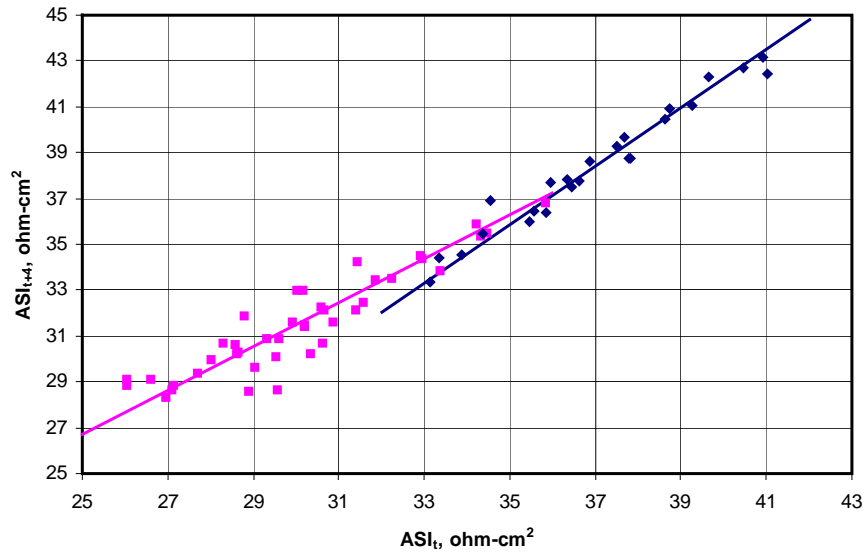


Figure C-3a. Plot of the initial ROR analysis results using the baseline calendar at 55°C data.

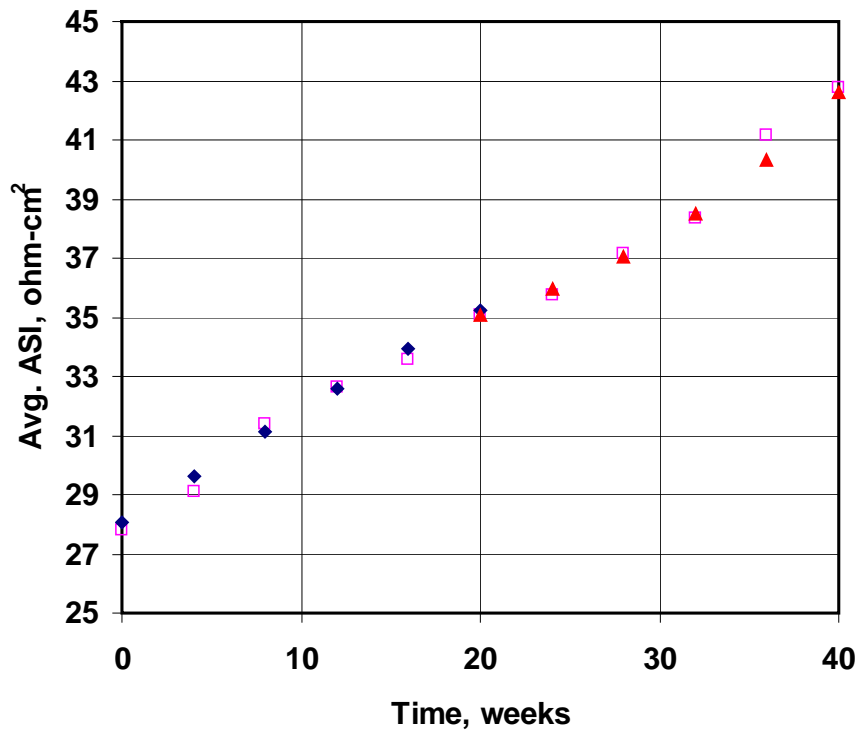


Figure C-3b. Replot of data from Figure C-3a against time. The open markers are the experimental points; the filled diamonds are from the 0-to-20-week fit; and the filled triangles are from the 20-to-40-week fit.

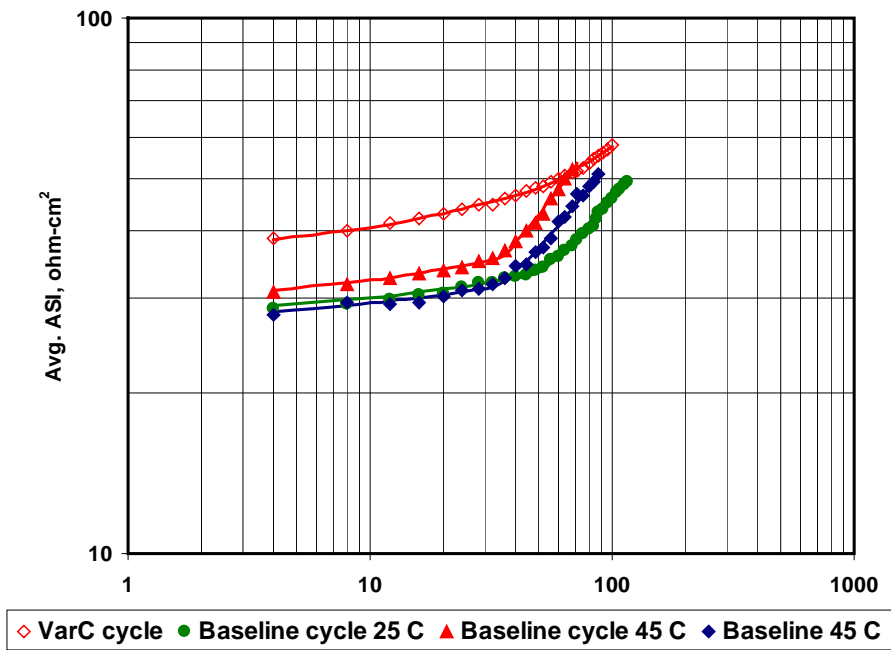


Figure C-4. Log-log plot of the some of the data shown in Figure C-3.

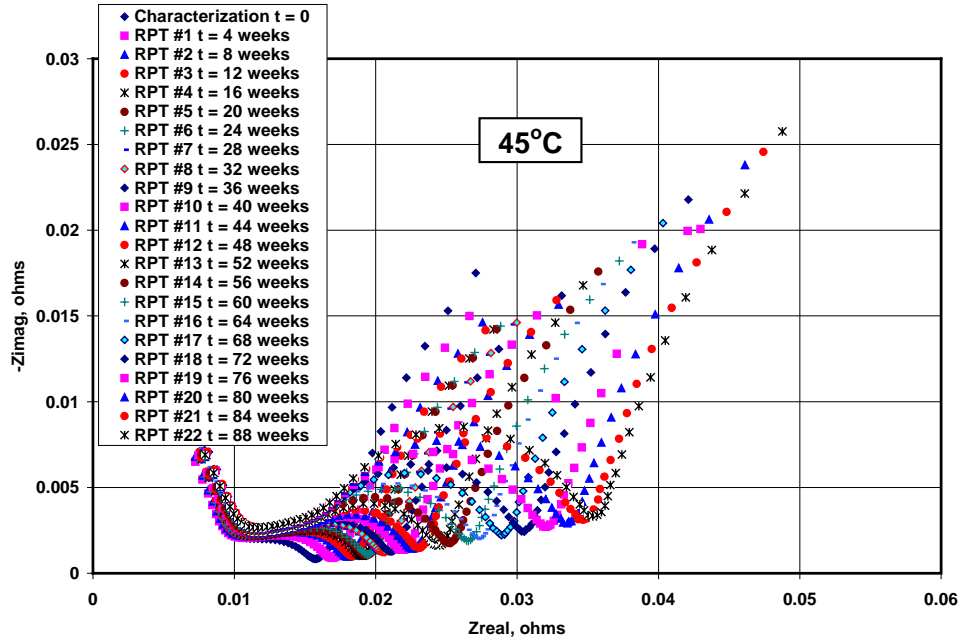


Figure C-5. Typical Nyquist plot from a baseline calendar life cell tested at 45°C. The plots from the cycle life and Variant C cells are similar in appearance.

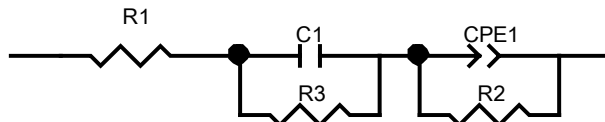


Figure C-6. Equivalent circuit used for modeling the data in Figure C-4.

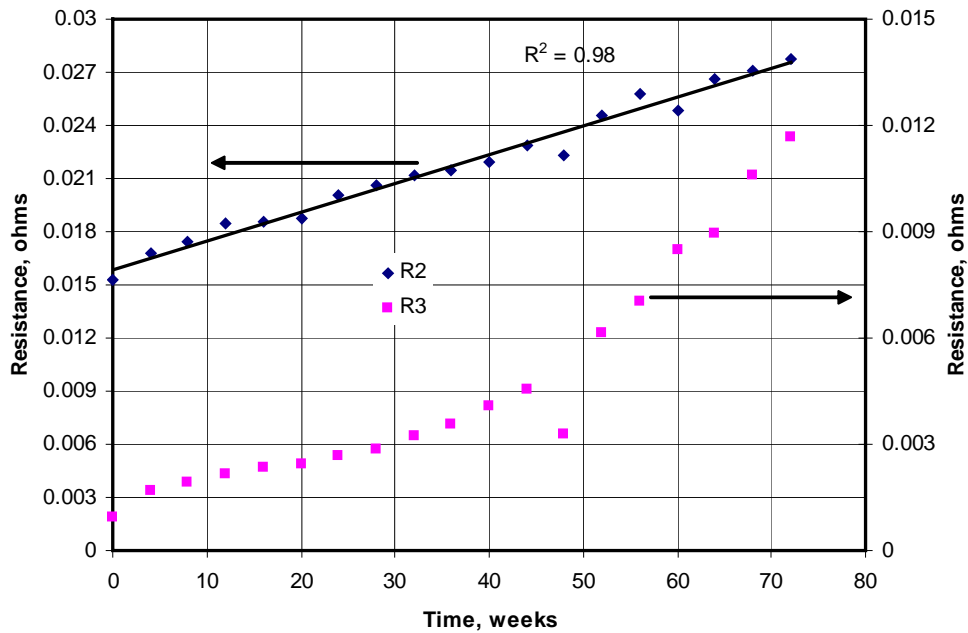


Figure C-7. Values of two of the equivalent circuit model parameters, R2 and R3, vs. time.

## C-4. ELECTROCHEMICAL DIAGNOSTICS

In an effort to identify the sources of capacity fade and impedance rise, electrochemical tests were conducted on electrodes harvested from 18650-cells that showed varying levels of performance degradation. Coin cells (2032-type) were assembled with 1.6-cm<sup>2</sup> area samples punched from the harvested electrodes, lithium-metal counter electrode, fresh Celgard 2325 separator, and fresh 1.2M LiPF<sub>6</sub> + EC:EMC (3:7) electrolyte to determine the effect of aging on electrode capacity. The cells containing the positive electrode (cathode) were cycled thrice from 3 to 4.3 V, and the cells containing the negative electrode (anode) were cycled thrice from 0 to 1.5 V. The cycling was conducted at various current densities ( $\sim C/5$  to  $C/200$ ) to determine the effect of cycling rate on cell capacity.

Figure C-8 shows representative discharge data measured with a 0.064 mA current ( $< C/25$  rate) obtained from cells prepared with cathodes harvested from the 18650-cells. It is evident that the cell capacity is a function of electrode age. For example, the cells prepared with cathodes from 18650-cells that showed 0%, 18% and 30% capacity fade (CF) had capacities of 2.5, 2.0, and 1.8 mAh, respectively. Cycling at slower rates increased capacity, especially for cells containing highly aged electrodes. However, the capacities were always smaller than those observed for the control cells (0% capacity and power fade). Because these cells contain a lithium-metal counter electrode, the capacity decline suggests the following scenarios:

- Oxide particle isolation, which may result from (a) partially insulating films on the oxide surface that impede lithium motion into the particles, (b) breakup of secondary particles into fragments that are not in contact with the carbon (electronic conduction) media, and (c) retreat of carbon away from the particles.
- Oxide particle damage, which may include (a) changes in the layering structure of the particle bulk, and (b) changes in the ionic conductivity of the Li<sub>x</sub>Ni<sub>1-x</sub>O-type layer that has been observed on the oxide surface.

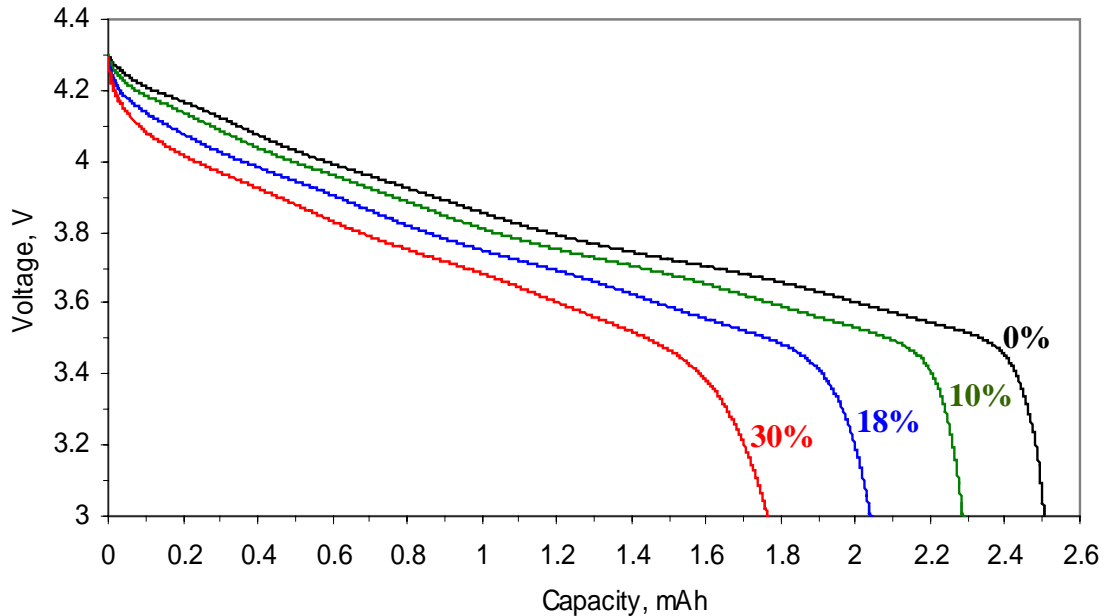


Figure C-8. Capacity data from cathodes (vs. Li) harvested from 18650-cells; the numbers indicate capacity fade of the 18650-cells.

Figure C-9 shows representative discharge data measured with a 0.064 mA current ( $<C/25$  rate) obtained from cells prepared with the graphite anodes harvested from the 18650-cells. In general, the cells containing anodes from the higher CF cells showed lower capacities. For example, the capacity of the 0% CF anode cell was  $\sim 3.0$  mAh, whereas the cell containing the 30% CF showed a capacity of only 2.4 mAh. The insert in Figure C-9 shows the discharge data after normalizing for the capacity variations of the different cells. The curves from the various cells lie atop each other, which suggests that the bulk of the graphite anode is unaffected by cell aging.

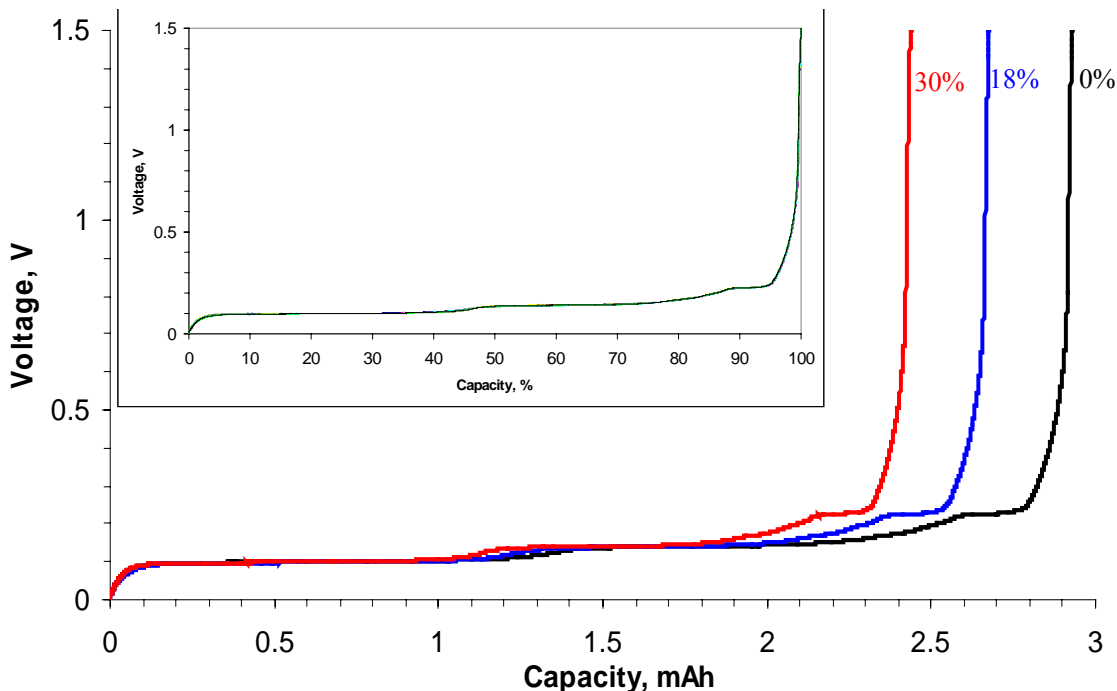


Figure C-9. Capacity data from anodes (vs. Li) harvested from 18650-cells; the numbers indicate capacity fade of the 18650-cells. Inset shows same data after normalizing for cell capacity variations.

Planar type cells, incorporating micro-reference electrodes, were used to isolate the individual positive and negative electrode contributions to cell impedance. These reference electrode cells were assembled with  $15.5\text{-cm}^2$  electrodes, two Celgard 2325 separators enveloping a Li-Sn micro-reference electrode, and fresh electrolyte. The individual electrode contributions to the fairly rapid early-life impedance rise were studied in cells employing fresh one-side coated Gen 2 electrodes. HPPC and AC impedance studies on these cells showed that the early-life impedance rise is primarily associated with interfacial phenomena that occur at the positive electrode. Mid-life studies were conducted in reference electrode cells using positive and negative electrode laminates that were harvested from the 18650-cells. Figure C-10 shows representative AC-impedance and 18-s pulse discharge HPPC data from these reference electrode cells. The HPPC data clearly indicate that a significant portion of the cell impedance rise occurs at the positive electrode. The AC impedance data also indicate that the positive electrode is the main contributor to cell impedance rise. Furthermore, the main increase of the positive electrode impedance is observed at the mid-frequency semicircular arc, which is usually associated with charge-transfer and mass-transfer processes at the electrode-electrolyte interface. These early- and mid-life reference-electrode data provide fairly strong evidence that the same phenomena are controlling the cell impedance rise throughout much of the useful life of these cells. In addition, reference

electrode cells, prepared with electrodes from highly-aged (late-life) 18650 cells, showed significant Warburg impedances in the AC impedance spectra, which were again primarily attributable to the positive electrode. These data indicate that late in the life of these 18650-cells it becomes increasingly difficult to transport lithium into and/or through the oxide particles.

The electrochemical diagnostic studies show fairly conclusively that phenomena occurring at the positive electrode are controlling the impedance rise and limiting the life of the Gen 2 cells. Therefore, most of the physicochemical diagnostic studies were focused on the positive electrode, in an effort to identify phenomena than can cause the observed impedance rise. Similarly, early efforts to develop and employ a phenomenological model, to help establish a more fundamental understanding of the factors that control life in the Gen 2 cells and to help quantify their potential contributions, were focused on the positive electrode. These studies are summarized in the next two subsections.

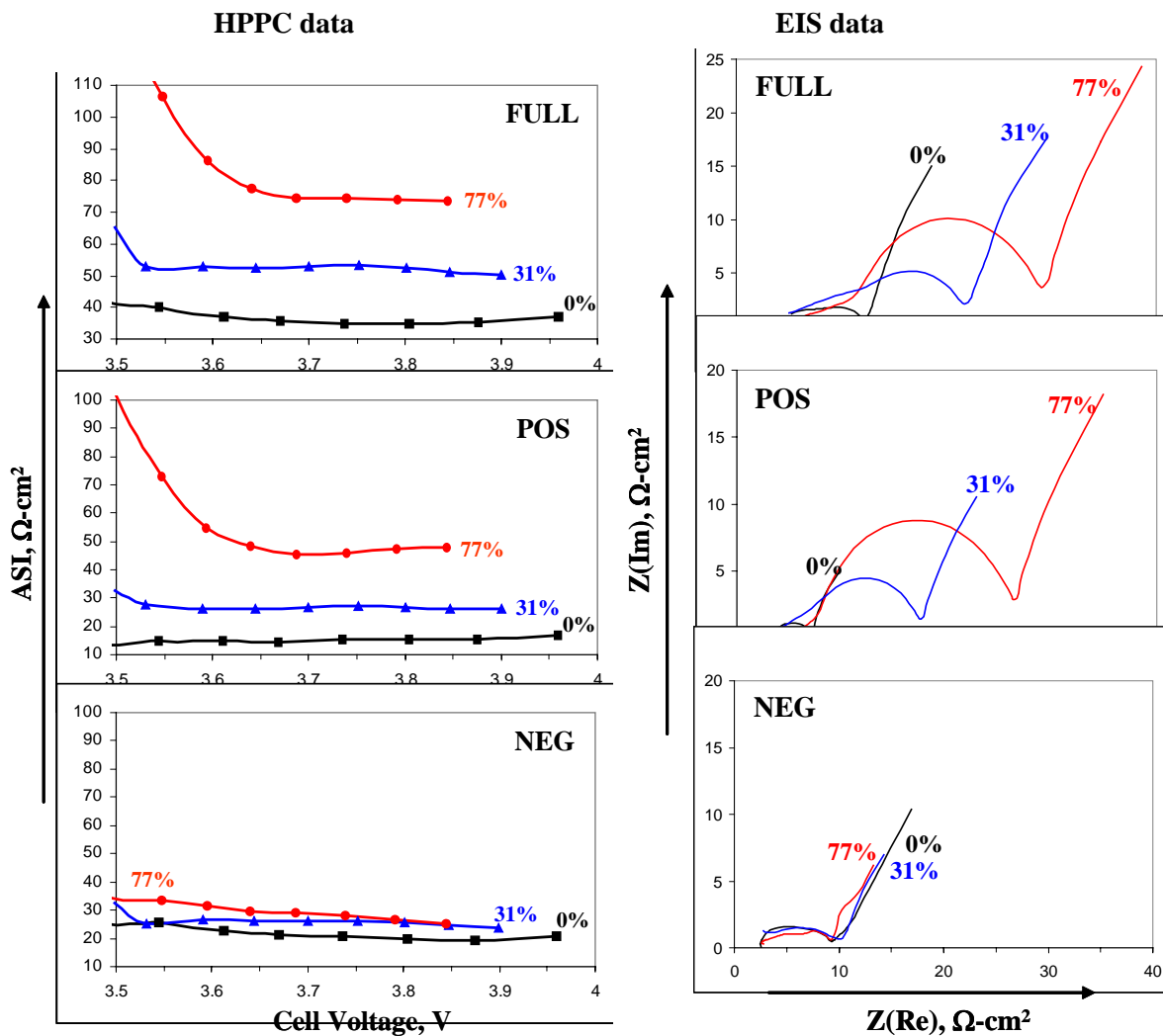


Figure C-10. Area specific impedance (ASI) measured from the HPPC test and AC impedance data from reference electrode cells containing electrodes harvested from 18650-cells; the numbers in the plots indicate the impedance rise of the 18650-cells.

## C-5. PHYSICOCHEMICAL DIAGNOSTICS

A large variety of physicochemical diagnostic techniques were employed to study degradation of the Gen 2 cell components, most of which are described in detail elsewhere (see reference 3). This subsection will focus on the techniques used to study phenomena that can directly or indirectly affect the interfacial impedance of the Gen 2 positive electrode. Representative SEM images (see Figure C-11) show spherical secondary particles  $\sim 5 \mu\text{m}$  in diameter that are composed of  $\sim 0.2\text{--}0.5 \mu\text{m}$  wide faceted primary particles,  $\sim 5 \mu\text{m}$  size plate-like graphite, and irregularly-shaped acetylene black agglomerates.

Microscopic examination and adhesion tests indicated that the PVDF binder was relatively unaffected by cell aging. Examination of Al current collectors from cells with various fade levels indicated that they too were improbable contributors to the positive electrode impedance rise.

Measurement of the overall carbon content of cathode samples from various aged cells indicated that there was no significant loss of the bulk cathode carbons as a result of cell aging. X-ray diffraction data of cathodes from various cells also showed that the shape and position of the carbon peaks were unchanged on aging. However, Raman microscopy images have indicated significant changes in the  $\text{LiNi}_{0.8}\text{Co}_{0.015}\text{Al}_{0.05}\text{O}_2$ /elemental-carbon surface concentration ratio at the surface and in the bulk of the composite cathode that accompany cell storage and cycling at elevated temperatures. The  $\text{LiNi}_{0.8}\text{Co}_{0.015}\text{Al}_{0.05}\text{O}_2$ /elemental-carbon surface concentration ratios appear to increase monotonically with increasing cell power loss, up to an apparent break point at about 20% cell power loss. Acetylene black was observed to “retreat” at a faster rate than graphite. This carbon retreat occurred faster in cells that were stored at elevated temperatures (45 and 55°C) than in cells stored at 25°C. Also cycle-life test cells showed faster carbon retreat than the calendar-life cells. This carbon retreat may be responsible for a loss of electronic conductivity within the composite cathode. The loss of a direct electronic path through the receding carbon matrix could lead to an increased resistance within the cathode composite agglomerate and, eventually, to a total isolation of some oxide particles.

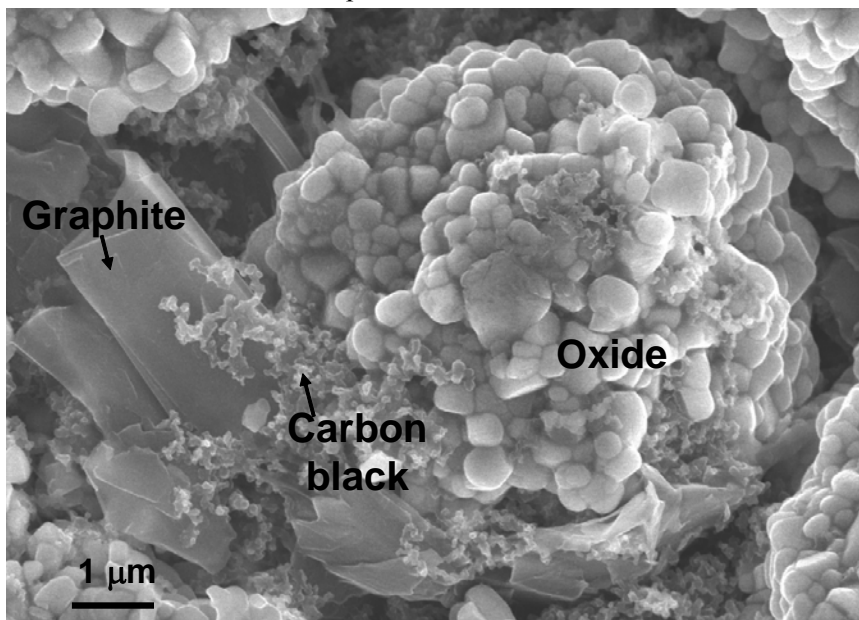


Figure C-11. SEM micrograph showing the oxide particles, graphite, and acetylene black on the cathode laminate.

The electrochemical data on the harvested electrodes suggest that the positive electrode impedance rise results from changes in the bulk and on the surface of the  $\text{LiNi}_{0.8}\text{Co}_{0.15}\text{Al}_{0.05}\text{O}_2$  particles. These oxide particles are known to have a thin surface  $\text{Li}_x\text{Ni}_{1-x}\text{O}$  layer, which has electronic and ionic properties that are different from the oxide bulk. The  $\text{Li}_x\text{Ni}_{1-x}\text{O}$  layer may contribute to impedance rise when  $x < 0.3$  because the random distribution of Li and Ni ions lowers the lithium ionic conductivity through the NaCl-type crystal structure. However, TEM observation showed that the thickness of this  $\text{Li}_x\text{Ni}_{1-x}\text{O}$  layer was similar for oxide samples from 0 to 54% PF cells.

On the other hand, current-sensing AFM (CSAFM) measurements of composite cathodes have shown substantial loss of surface electronic conductance in aged cathodes that increased with cell test temperature and test duration. Furthermore, CSAFM conductance images of individual  $\text{LiNi}_{0.8}\text{Co}_{0.15}\text{Al}_{0.05}\text{O}_2$  particles embedded in gold substrates revealed that the  $\text{LiNi}_{0.8}\text{Co}_{0.15}\text{Al}_{0.05}\text{O}_2$  agglomerates were not uniformly conductive due to poor inter-granular electronic contact. Also, Raman microscopy spectra showed that the state of charge (SOC) of harvested cathodes was non-uniform, which indicated that the various oxide particles were delithiated to various levels. This non-uniform SOC indicates electronic isolation of particles from the rest of the electrode. Taken together, the CSAFM and Raman microscopy suggest that the electronic isolation of oxide particles from the rest of the electrode contributes to cathode impedance rise.

TEM studies have shown that oxide particle physical damage is not commonly observed for most cells. Although point and line defects are occasionally observed in the microstructure, planar defects such as stacking faults and cracks, which could impede the motion of lithium ions, are not common. However, some cracking was observed in oxide particles from cells that were aged well beyond their useful life (142% impedance rise). Particle separation could cause particle isolation and explain the lower cathode capacities of the cells that exhibit extremely high impedance. Partial or total separation could lead to impedance rise in several ways: (a) it can reduce the electrochemically active surface area, (b) it can retard the direct  $\text{Li}^+$  diffusion between primary oxide particles, and/or (c) it can increase the  $\text{Li}^+$  diffusion path length within the secondary oxide particles by altering the path for particle-to-particle diffusion.

Surface films observed on the oxide particles by microscopy techniques (SEM and TEM) could also contribute to electrode capacity loss (by isolating oxide particles) and impedance rise (by increasing resistance to lithium-ion transport). These surface films have been identified by various techniques including nuclear magnetic resonance (NMR), soft X-ray absorption spectroscopy (XAS), X-ray photoelectron spectroscopy (XPS) and time-of-flight secondary ion mass spectrometry (TOF-SIMS). XPS data have indicated that these surface films contain a mixture of organic and inorganic constituents that include lithium alkyl carbonate,  $\text{LiF}$ ,  $\text{Li}_x\text{PO}_y$  and  $\text{Li}_x\text{PO}_y\text{F}_z$  species, which probably result from electrolyte decomposition processes. Phosphorous K-edge XAS data have also shown the presence of insoluble phosphates in the electrode that cannot be removed by repeated washing.  $^{31}\text{P}$  NMR data obtained from the cathodes also show the presence of fluorophosphates ( $\text{OPF}_2\text{OR}$ ,  $\text{OPF}(\text{OR})_2$  ..) which may transform to organophosphate compounds during cell cycling and aging.

The XPS data have shown a clear correlation between electrode impedance rise and composition changes in the oxide surface films. The increasing oxygen content of the films with electrode age suggests that these films are products of electrolyte oxidation, possibly produced by reaction with lattice oxygen. However, XPS and SIMS data have indicated that the thickness of these surface films does not increase with electrode age. Increased blocking of the oxide edges (from which the lithium-ions enter and leave the oxide particles) combined with increased clogging of the

oxide particle pores could degrade the oxide-electrolyte interface and contribute to the observed impedance rise.

## **C-6. PHENOMENOLOGICAL MODEL**

The phenomenological modeling effort is also aimed at examining the impedance rise in Gen 2 technology cells. The overall goal of this work is to associate changes that are seen in the post-test diagnostic studies with the loss of electrochemical performance, as measured by the HPPC tests on 18650 cells. The approach taken in this effort is to develop a model based on the analytical diagnostic studies, establish the model parameters, and conduct parametric studies with the model. The parametric studies are conducted to gain confidence with the model, examine degradation mechanisms, and analyze cell limitations. To accomplish these tasks two versions of the model have been developed. One version simulates the cell response from AC impedance studies, and another model version is utilized for examining HPPC tests. Both of these experimental techniques are extensively used in the program to quantify the cell's electrochemical performance and those of its components. The underlying basis for both models is the same, as well as their parameter set. The modeling effort has concentrated on the positive electrode because of its importance in the cell's overall impedance rise

The general methodology for the phenomenological model follows the work of Professor Newman at Berkeley. Concentrated solution theory is used to describe the transport of salt in the electrolyte. Volume-averaged transport equations account for the composite electrode geometry. Electrode kinetics, thermodynamics, and diffusion of lithium in the oxide active particles are also included. The detailed theoretical description of the oxide active material/electrolyte interface, commonly referred to as the solid electrolyte interface or SEI, is based on post-test analytical diagnostic studies. The SEI region is assumed to be a film on the oxide and an oxide layer at the surface of the oxide. The film on the oxide is taken to be an ill-defined mixture of organic and inorganic material through which lithium ions from the electrolyte must diffuse and/or migrate across to react electrochemically at the surface of the oxide. The lithium is then assumed to diffuse through the oxide surface layer and into the bulk oxide material in the particle. A double layer capacity is added in parallel with the Butler-Volmer kinetic expression. A localized electronic resistance between the current carrying carbon and the oxide interface can be added, and a secondary film capacitance can also be included.

In the AC impedance version of the model, the pertinent electrochemical reaction, thermodynamic, and transport equations were linearized for a small sinusoidal perturbation. The resulting system of differential equations was solved numerically using a partial differential equation solver over the frequency range of interest. The level of complexity of the model made determining all of its approximately 35 parameters independently a challenge. More than half of the parameters were set by cell construction, obtained from the literature, or estimated. Electrode open circuit voltage curves were determined from the slow cycling of half-cells. Diffusion, Hittorf, and concentration cell studies were performed on the electrolyte to obtain a set of transport and thermodynamic parameters for the electrolyte. The remaining 10 parameters, most of which were associated with SEI phenomena, were determined from the reference electrode cell measurements. A comparison of the model simulation with the positive electrode experimental AC impedance is given in Figure C-12. Even for fresh cells, a bimodal particle size distribution for the positive active material was needed to achieve a reasonable fit to the low-frequency Warburg tail and the best fit was achieved with particles that differ by only a factor of 2.6 in their characteristic diffusion lengths.

The HPPC version of the model was utilized primarily to gain confidence in the model and for cell optimization studies. The parameter set developed for the positive electrode using the AC impedance version of the model was employed in the HPPC version. HPPC simulations of the positive electrode compared favorably with experimental tests on reference electrode cells. Further, parametric studies with the HPPC version of the model suggest that increasing electrode thickness would improve the initial electrochemical performance, as well as the cell's aging characteristics.

EIS studies on the aging of Gen 2 technology cells, described above, indicate that the interfacial impedance (i.e. the mid-frequency arcs on the Nyquist plot) of the cells grow all through their life. Furthermore, the low frequency Warburg diffusional impedance tail also begins to increase late in life. The initiation of the increase in the cell's diffusional impedance roughly corresponds to the change in impedance growth rate (i.e. from square-root of time to proportional in time) of the Gen 2 technology cells as measured by the HPPC tests.

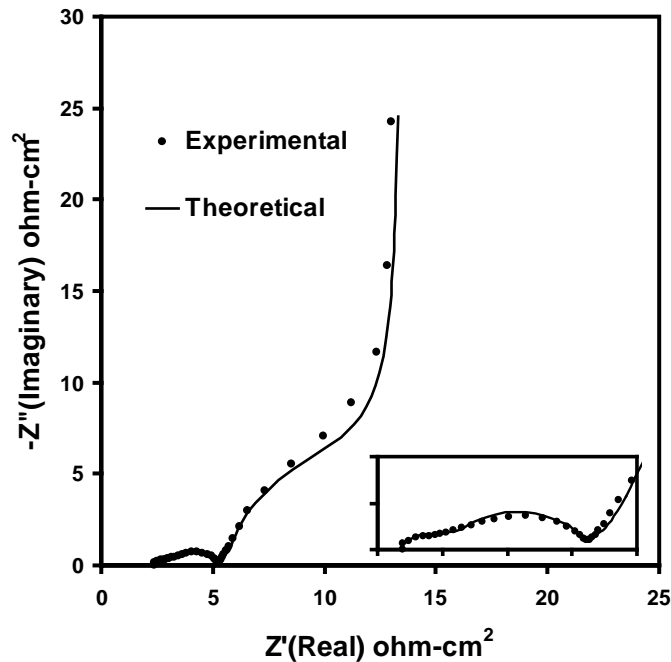


Figure C-12. Comparison between phenomenological model and experiment for the positive electrode AC impedance (100 kHz-1 mHz) at 60% state-of-charge.

The phenomenological AC impedance model was utilized to examine aging effects associated with the positive electrode when only its interfacial impedance increases. Three possible sources for the interfacial impedance increase were identified, which are consistent with experimental observations. First, an interfacial impedance increase would result from a degradation of the ionic pathway for lithium ions between the electrolyte in the electrode pores and the bulk oxide active material. This could result from changes in the electrolyte/oxide interfacial structure, composition, and/or properties and would have a direct impact on the positive electrode's interfacial impedance. In addition, the size of the model parameter changes needed to account for the impedance increase suggests that there is a general degradation of the ionic pathway significantly affecting many of the model's interfacial parameters. Second, a loss of positive electrode capacity, particularly isolation of the finer oxide particles would also cause the interfacial impedance to increase. Simulations based on the measured cell capacity loss suggest

that this effect can at best only be a minor contributor to the positive electrode's interfacial impedance increase. Finally, an interfacial impedance increase would result from a degradation of the electronic pathway between the carbon matrix and the oxide active material, provided that the carbon matrix has a sufficiently large double layer capacitance associated with it. Degradation of the electronic pathway is simulated in the model by a large increase in the electronic resistance between the electronically conducting carbon matrix and oxide active material.

The increase in interfacial impedance of the positive electrode from some combination of the three mechanisms listed above likely continues throughout the life of the cell. While the model is able to estimate an upper bounds for the impact of the capacity loss resulting from the isolation of the oxide active material, the model by itself cannot establish the relative importance of the changes in the interfacial ionic pathway vs. changes in the interfacial electronic pathway to the oxide active material. The interfacial ionic pathway tends to be more sensitive to changes in the interface than the electronic pathway for a wide variety of electrochemical systems, including many lithium-ion technologies, which suggests that it is most likely to be the primary source of the impedance increase. Also, it is possible that all three mechanisms are related. As an example, chemical or physical changes in the SEI could cause degradation of the ionic pathway, as well as the electronic pathway, at the oxide interface, which could eventually lead to oxide particle isolation and capacity loss. This type of degradation phenomenon would be consistent with the square-root of time impedance growth observed in test cells.

Late in the cell's life, as the diffusional impedance starts to grow, model simulations indicate that other positive electrode aging phenomena can contribute to the cell's impedance rise. These include a slowing of lithium diffusion within the oxide particles, a loss of electrochemically active area, degradation of electrolyte properties, and a change in electrode microstructure. Degradation of lithium diffusion through the oxide could be caused from changes in the oxide structure (e.g. micro-cracks), but also could result from changes in the intra-granular region between primary particles. A degradation of the intra-granular region and the loss of electrochemically active area are both consistent with an extensive general degradation of the oxide primary particles' interfaces. The degradation of electrolyte transport properties and/or a change in electrode microstructure that increases the electrode's tortuosity by approximately a factor of 100 can produce an electrode impedance similar to those observed experimentally, but these degradation mechanisms are not commonly supported by the post-test diagnostic results.

## **C-7. STATUS SUMMARY**

Extensive accelerated aging data were collected on the Gen 2 cells. This appendix reports on the average values obtained on multiple cells at each test condition and illustrates the differences in aging characteristics for the Gen 2 baseline and Variant C cells. The only known difference in these two groups of cells was the level of Al doping in the positive electrode and this apparently provided some enhanced stability. Although end-of-life for these cells is determined on the basis of power fade, capacity fade data are included to illustrate the relative ratio of power/capacity fade for both groups of cells. For a given state of power fade, the Variant C cells exhibited lower capacity fade than the baseline cells.

In the area of accelerated aging, the following insights were gleaned:

- Periodic RPTs were found useful in monitoring changes in the performance characteristics of the cells as they age:
  - EIS was found useful in helping to identify the type of impedance that dominates

- The possibility exists that one or more elements of the RPTs used in this study contributed in a significant manner to accelerating the aging process(es) and studies are currently underway to determine the role of some of these elements.
- Aging cells at elevated temperature accelerates the aging process(es) and two or more different levels of elevated temperature are recommended.
- Aging cells at higher SOC accelerates the aging process(es) and two or more different levels of SOC are recommended. [Information on this topic is not specifically discussed in this appendix. However, the sensitivity to SOC was obtained in a separate study conducted by SNL. See reference 21.]
- To a somewhat lesser extent, cycling the cells around a given SOC (vs. non-cycling at the same SOC) accelerates the aging process(es)
- Several different methods of analyzing the cell aging data were studied and the merits of each are reported herein.

A considerable amount of diagnostic work, coupled with the phenomenological modeling work, was performed on cells that incorporate the Gen 2 cell chemistries. The electrochemical diagnostic studies showed that the major source of impedance rise in these cells was interfacial impedance at the cathode. Extensive physicochemical diagnostic studies were conducted on all components of the cells, but for brevity sake this appendix focuses only on the information gained about phenomena that could impact on the interfacial impedance of the cathode, via both the diagnostic studies and the phenomenological modeling work. *It should be noted that much care is needed during the post-test diagnostic studies in order to avoid introducing artifacts associated with the electrode harvesting and/or sample preparation processes.*

In the area of diagnostic studies and phenomenological modeling, the following insights were gleaned:

- Removing cells from test at various stages of aging (various levels of power fade) was useful in that it permitted the periodic characterization and study of individual cell components at different stages of the aging process.
- The electrochemical diagnostic studies—using reference electrodes and Li<sup>0</sup> counter electrodes—were extremely beneficial in isolating the major source of cell impedance rise (interfacial impedance at the cathode), as well as in characterizing the individual performance capabilities and limitations of anodes and cathodes harvested from new cells and cells at various stages of aging.
- A large variety of bulk and surface analysis techniques were employed in studying the physicochemical changes that occur in and on the surfaces of the Gen 2 cathodes during aging. Since the cathodes are non-homogenous composite electrodes that have ~35% porosity, it is extremely challenging to obtain quantitative information regarding the observed changes. The techniques discussed in this appendix are the ones that were found to be the most useful in providing qualitative information about physicochemical changes associated with the cathodes during aging.
- The phenomenological model was found to be quite useful in conducting parametric studies of phenomena that could impact on the interfacial impedance of the cathode and to investigate the magnitude of the individual phenomenon needed to cause the observed impedance.
  - Results suggest that multiple mechanisms—operating simultaneously—are most probably needed to account for the magnitude of the impedance rise and power fade observed experimentally.
  - The model was able to quantify the possible contribution to impedance rise (and power fade) associated with particle isolation. The model indicates that this

phenomenon can only be a minor contributor to power fade, based on the ratio of power/capacity fade observed experimentally for these cells.

The goal of this work was to develop a thorough mechanistic understanding of the factors that contribute to impedance rise and power fade in these Gen 2 cells. Most, if not all, of the contributing mechanisms associated with the cathode were identified, however quantifying the individual contributions of each contributing factor has not yet been achieved. This is extremely challenging and separate model experiments are currently being used to help develop more quantitative information on some of the individual contributions. It should be noted that an essential element of validating any mechanistic model is its ability to correlate degradation rates to known stress factors, e.g. temperature, SOC, and cycling conditions.

**Appendix D**  
**Use of the Monte Carlo Simulation Tool**



## Appendix D

### Use of the Monte Carlo Simulation Tool

#### D-1. INTRODUCTION

The purpose of the battery life test simulation tool is to aid and support technology life verification test (TLVT) planning. The life test simulation tool was implemented using Microsoft Excel and its integrated Visual Basic for Applications (VBA) programming language.<sup>a</sup> The tool as provided implements the life model found in Section 2.3.1 of the manual, which represents the “true” ASI function of time as:

$$ASI_K = \frac{\beta_0(\beta_1^K - 1)}{(\beta_1 - 1)} + ASI_0 \beta_1^K$$

where  $K = (\text{test time})/(\text{RPT interval})$ ,  $\beta_0$  and  $\beta_1$  are constant coefficients, and  $ASI_0$  is the true area-specific impedance at time 0. Provisions are included for the user to modify this model if required.

The tool uses the Monte Carlo approach to add small, random amounts of “noise” to the above equation to generate simulated cell ASI data. The “noise” comes from variations in the cell-to-cell ohmic resistance, active area, and measurement errors. The simulated ASI data from one or more cells are then statistically analyzed using a robust orthogonal regression (ROR) method to approximate the values of  $\beta_0$ ,  $\beta_1$  and  $ASI_0$ . (Reference 4)

The same statistical analysis can be used on data from actual cell tests. Values of  $ASI_0$  and life on test are calculated from the data. The analysis of experimental data also includes bootstrap analysis, used to estimate the lower 90% confidence interval in the life on test (see Reference 7).

#### D-2. START-UP

When started, the workbook has four worksheets containing the input data, intermediate results, and final results. These sheets are called Test Data, Life Projection, Experimental Data, and Seeds respectively. They should not be altered or removed by the user.<sup>b</sup>

Select the “Test Data” sheet by clicking on its tab. A display similar to that shown in Figure D-1 will be seen. Here, values of various parameters can be seen along with some values of the calculated ASI. *Execution of the tool is started by left-clicking on the square labeled “MCS.”*

---

a. The tool is contained in Excel spreadsheet file “*Battery MCS.ver.4b.XLS*.” Computer system requirements to use the tool are one of the following: (PC) Office97 or later installed, Office2000 or later preferred; WP Drawing Characters font installed within Excel. (Mac) OS9 with Office2001.

b. If the tool finds a sheet missing, a fatal error will be generated, telling the user which sheet is missing. The user may add a new sheet and rename it appropriately, although some of the text in the cells may be missing if this is done. It is preferable to revert to a saved copy of the tool to avoid user-introduced errors.

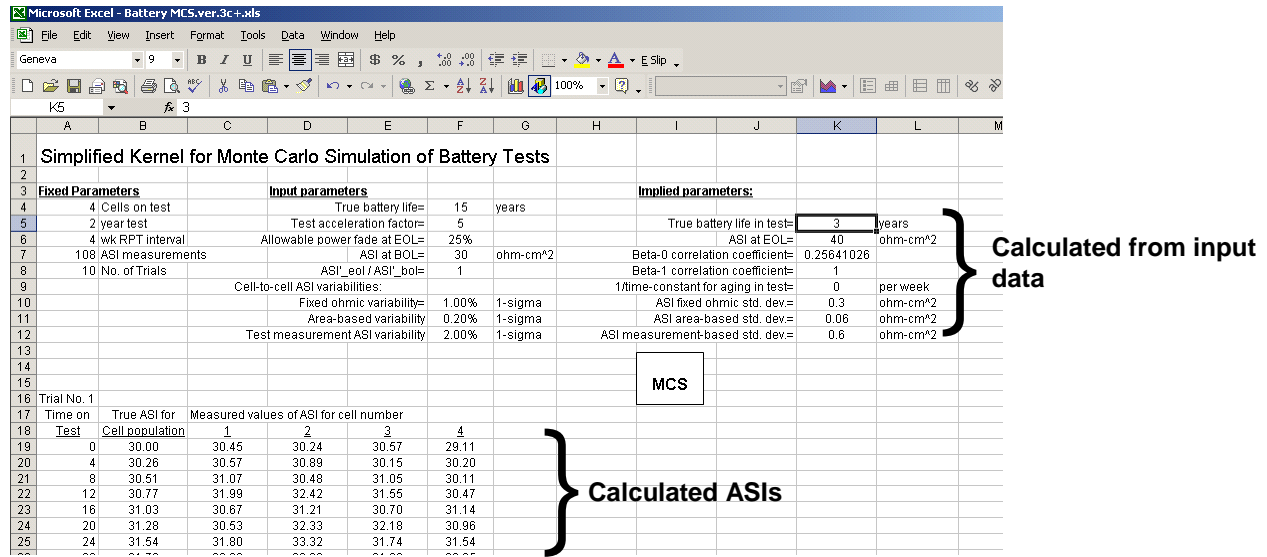


Figure D-1. Typical display seen when starting the simulation tool.

The main menu will appear, as shown in Figure D-2. The choices on the menu are Monte Carlo Simulation, ROR Analysis of Experimental Data, and Exit. Exit will stop program execution. The other choices are described in the following sections.

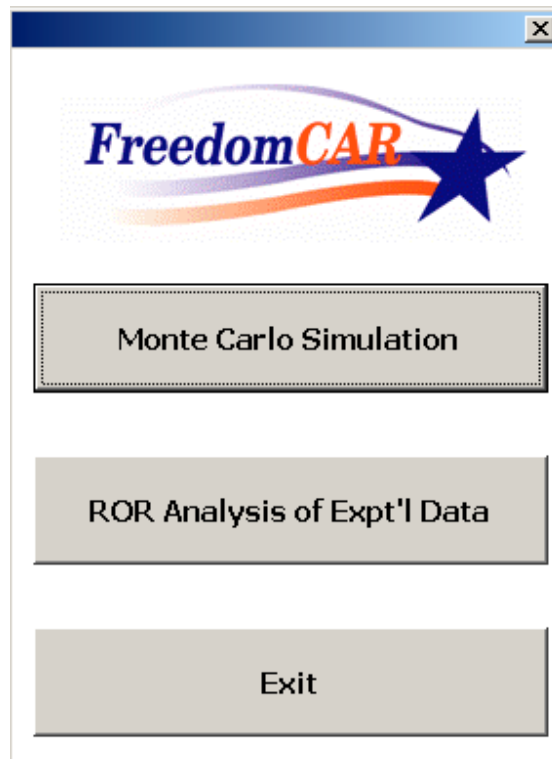


Figure D-2. Main menu of simulation tool.

## D-3. MONTE CARLO SIMULATION

### D-3.1 Description of Menu Choices

Clicking on the Monte Carlo Simulation button will bring up a second menu with four options, as shown in Figure D-3 and described below.

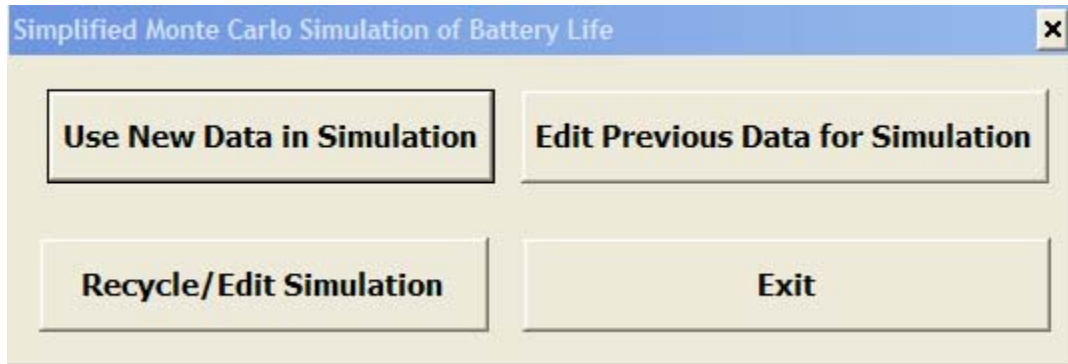


Figure D-3. Monte Carlo menu.

*Use New Data In Simulation.* This choice is used for starting a completely new simulation. The display shown is very similar to that shown in Figure D-4, except that all input values are initially set to zero and must be entered by the user. See "Edit Previous Data" for more details.

The screenshot shows a window titled "Simplified Monte Carlo Simulation for Battery Life Projection" with a close button (X) in the top right corner. The window is divided into two columns of input fields:

Fixed Parameters		Cell-to-Cell Variabilities	
Number of Cells	4	Fixed ohmic, % (1- $\sigma$ )	1
RPT frequency, weeks	4	Area-based, % (1- $\sigma$ )	.2
Length of Test, years	2	Measurement-based, % (1- $\sigma$ )	2
<b>Input Parameters</b>		Number of Trials	10
True Battery Life, years	15	Error Messages On? (checked=yes)	<input checked="" type="checkbox"/>
Test Acceleration Factor	7.5		
Allowable Power Fade, %	25		
ASI at BOL, ohm-cm <sup>2</sup>	30		
ASI' at EOL / ASI' at BOL	1		
Tuning const. for leverage wts.	6		
Tuning const. for outlier wts.	3		

At the bottom right of the form are two buttons: "GO" and "Cancel".

Figure D-4. Edit data display.

*Edit Previous Data for Simulation.* This choice is used for starting a new simulation while retaining some or all of the inputs for the previous run. A display similar to Figure D-4 is shown, allowing the user to change any of the values in the white boxes, which are the parameters that control the

simulation behavior. The user can also turn on or off some error messages by clicking on the “Error Messages On?” box. A complete list of these error messages is given under “*Error Messages On?*” (See Section D-3.3 for more information.)

The ratio (ASI’ at EOL / ASI’ at BOL) has a profound effect on the shape of the ASI<sub>true</sub> versus time curve. See Section 2.1 of the manual for information on this parameter.

The values marked “Tuning constants” are used by the ROR analysis. The recommended initial value is 6 for both, although values between 2 and 9 are allowable. See Appendix B of the manual for a description of leveraging and outlier weighting.

Maximum allowable values for other parameters are given in Table D-1. Additionally, the length of the test (in weeks, where a year equals 52 weeks) must be evenly divisible by the RPT interval (in weeks).

Table D-1. Maxima for some of the values used in the simulation calculation.

Parameter	Maximum Value
Number of cells	250
Length of test, number of trials, RPT Interval	$(\text{No. of trials} \times \text{test length} \times 52) / (\text{RPT interval}) + (\text{No. of trials}) \times 3 + 18 \leq 65000$
Allowable power fade	25%
Tuning constants	>2 and <9

All inputs are checked for validity. Negative number inputs are not valid. Invalid inputs will generate an error message, such as “RPT interval: RPT interval=0!” if the RPT interval were mistakenly set to zero. Click “GO” to start the calculation or “Cancel” to go back to the previous menu.

*Recycle/Edit Simulation.* This choice is used for making repeated runs with a fixed cell population. It reuses the data from the most recent simulation run, which is stored in the Seeds spreadsheet. A display similar to Figure D-4 is shown, except that the values that affect cell population size, test length, etc., cannot be changed. The parameters that can be changed are shown in white boxes and consist of allowable power fade, ASI at BOL, ASI’ at EOL / ASI’ at BOL, and the percent cell-to-cell variabilities (ohmic, area, and measurement).

Error messages can be turned on or off, and inputs are checked for validity, as described in the “Edit Previous Data” case. Click “GO” to start the calculation or “Cancel” to go back to the previous menu.

*Exit.* This choice returns to the previous menu.

## D-3.2 Normal Operation

The calculation will start after clicking “GO.” If Excel97 or Excel for Office2001 is running, Excel will disappear until the calculation is complete or an error is encountered (depending on the status of “Error Messages On?”). With more recent versions of Excel, a progress bar will appear, as shown in

Figure D-5, displaying the actual number of trials as well as the percentage of completion based on the input number of trials.<sup>c</sup>

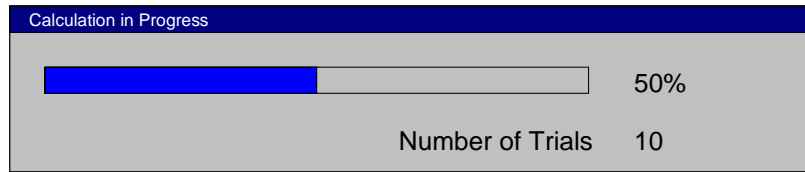


Figure D-5. Progress bar showing status of calculation in Excel XP.

Assuming that the run was successful, a display similar to that given in Figure D-6 will be shown to the user. The display summarizes all the input data and shows the results of the life projections. *T*-statistics are used to estimate the upper and lower limits for the 90% confidence interval. Of interest is the estimated minimum life with 90% confidence, shown in the boxed area.

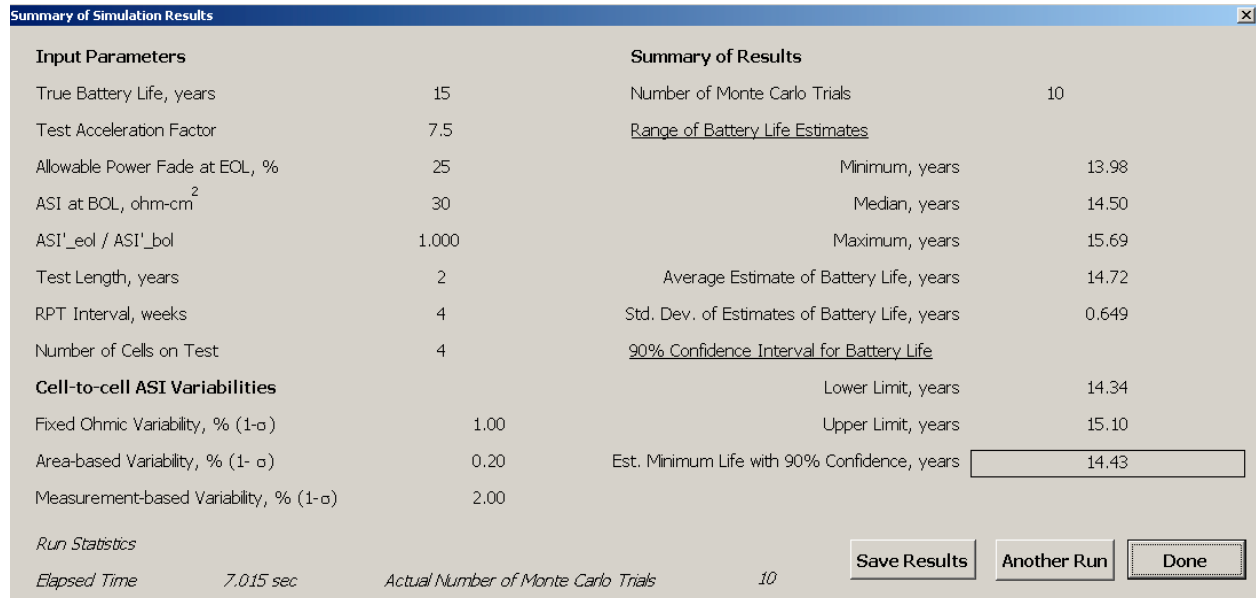


Figure D-6. Results of a simulation calculation.

Clicking on “Save Results” will allow the user to save the current life projection results for later use. Clicking here produces the dialog box shown in Figure D-7. The user is asked to enter a valid sheet name (length of name < 32 characters). If the sheet name already exists, the user will be prompted to try another name. Clicking “OK” copies the contents of the Life Projection sheet to a new sheet and renames that new sheet to whatever the user entered.<sup>d</sup> The user is taken to the menu shown in Figure D-3 when the desired operation is complete. Clicking on “Cancel” aborts the operation and returns the user to the display shown in Figure D-6.

c. This display will only be seen if the “WP Box Drawing” font set is installed in Excel. Otherwise a dollar sign, ‘\$’, will appear.

d. The user is cautioned not to add too many worksheets. The maximum number of worksheets is limited by available computer resources (not checked by the tool). Adding many worksheets slows loading and saving of the tool and results.

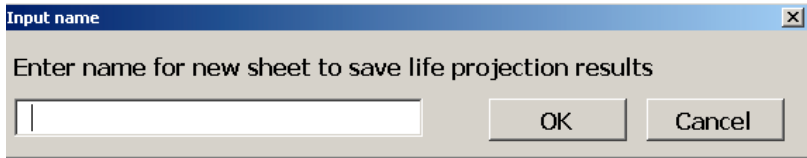


Figure D-7. Dialog box for saving life projection results.

Clicking on “Another Run” in Figure D-6 will take the user back to the Edit Data screen (Figure D-4). The results of the most-recent calculation are stored in the Life Projection sheet. Starting another run will replace these values.

Clicking on “Done” in Figure D-6 will end the program and return the user to Excel. The user will see the Life Projection sheet, which contains more detailed results from the calculation. (See Figure D-8 for an example of typical results.) Averages and standard deviations are given for the median residual  $Y$ , RMS residual  $Y$ ,  $\beta_0$ ,  $\beta_1$ , some of the cell-to-cell variabilities, the ASI at BOL and at EOL and  $ASI_0$ . The user can also restart execution of the tool from the Life Projection sheet by left-clicking on the MCS icon.

Summary of Results from multiple Monte Carlo trials of the Life Test Simulation														
Input parameters:					Summary of Results:									
True battery life =	15	years			Number of Monte Carlo trials =	10								
Test acceleration factor =	5				Range of battery life estimates:									
Allowable power fade at EOL =	25%				Minimum =	12.64	years							
ASI at BOL =	30	ohm-cm <sup>2</sup>			Median =	15.16	years							
ASI-eol / ASI-bol =	1.000				Maximum =	21.34	years							
Test duration =	2.0000	years			Average estimate of battery life =	16.06	years							
RPT interval =	4	weeks			Standard deviation of estimates of battery life =	2.684	years							
Number of cells on test =	4				90% Confidence interval for battery life:									
Cell-to-cell ASI variabilities:					Lower limit =	14.50	years							
Fixed ohmic variability =	1.0%	1-sigma			Upper limit =	17.61	years							
Area-based variability =	0.2%	1-sigma			Estimated minimum life with 90% confidence =	14.88	years							
Test measurement ASI variability =	2.00%	1-sigma												
Detailed results:														
Trial No.	ASI smoothing parameters:				Linear fit of smoothed ASI:		As-built average true ASI:		Measured average ASI values:		Trial No.	Estimated ASI at EOL	ASI rates of change per RPT int.:	
	Signal/Noise	Med. res. Y	RMS res. Y	Beta-0	Beta-1	Fixed Incr.	Area Factor	at BOL	at EOT			BOL	EOT	Avg.
1	9.66871727	0.39165699	0.68356777	1.23279825	0.9706355	0.12253039	0.99959063	29.77208634	36.3813099	1	38.1503436	0.36392695	0.11381657	0.16
2	6.94607213	0.64198925	0.91999892	0.11570719	1.0039143	-0.0177768	1.00156037	30.14032461	36.5307028	2	40.0474263	0.23322958	0.27161286	0.16
3	9.65978095	0.51027232	0.75364272	-0.44945924	1.0220224	-0.12248477	1.0010711	29.71416415	36.9942077	3	42.7308491	0.20268478	0.47402337	0.16
4	7.61951893	0.81833939	0.93301067	0.58703831	0.9905394	-0.05678768	1.00017101	29.92981736	37.0379768	4	39.6547316	0.30533106	0.21075095	0.1
5	6.83798314	0.70985455	0.98744564	0.76268276	0.984893	0.15019715	1.00023593	29.94907159	36.7012356	5	39.0786934	0.31260925	0.17265323	0.17
6	7.7764286	0.48623713	0.82315559	-0.0239928	1.0080937	0.17238616	1.00050656	30.47879132	36.880002	6	40.5613857	0.22179789	0.30373372	0.16
7	8.16823321	0.53398603	0.89284684	0.22133889	1.0017835	-0.0784568	0.99950824	29.66727187	36.9602531	7	40.7603671	0.27400556	0.29372446	0.16
8	7.9508055	0.61601101	0.99079645	0.56920703	0.9911049	0.10922084	1.00043551	29.37299133	36.4555407	8	39.9641615	0.30930787	0.21830093	0.16
9	7.99714595	0.54005497	0.78884217	0.88660603	0.9805276	-0.14367581	1.00108522	29.73225024	36.0407362	9	38.2106609	0.31068218	0.14429432	0.16
10	7.76358944	0.60006326	0.8750178	1.01481345	0.977004	-0.375448	0.99799051	29.2115418	36.0048207	10	38.0898492	0.34707027	0.14007943	0.17
Averages and Standard Deviations of Results:														
	Smoothed ASI and Linear Fit of smoothed data:				As-built average true ASI:		Measured average ASI values:		Estimated ASI at EOL	ASI rates of change per RPT int.:				
	Med. Resid. Y	RMS Resid. Y	Beta0	Beta1	Fixed Incr.	Area Factor	at BOL	at EOT		BOL	EOT	Avg.		
Averages of results:	0.66504729	0.85483285	0.49167399	0.9930518	-0.02403053	1.00021551	29.79683306	36.5986785	39.7157469	0.28806543	0.23429888	0.17		
Std deviations of results:	0.09074241	0.09190626	0.51999348	0.0158231	0.16998546	0.0010151	0.361251354	0.38095615	1.44731334	0.05373193	0.10714322	0.06		

Figure D-8. Typical results displayed in the Life Projection sheet.

### D-3.3 Error Handling

*Error Messages On?* Certain error messages can be turned off and on by clicking on the “Error Messages On?” box, as shown in Figure D-4. This option is available from the New Simulation, Edit Simulation and Recycle/Edit Simulation dialog boxes. A complete list of the error messages that can be turned off is given in Table D-2. When these errors appear, the user has the choice of stopping the calculation (End Run) or repeating the trial that caused the error (Continue). When the messages in Table D-2 are disabled, it is assumed that the user wants to repeat the trial that produced the error. If the

error is repeatedly produced due to the random numbers being used in the simulation, the user has to wait until either better-behaved results are obtained or a runaway calculation is detected, as described below.

Table D-2. List of error messages.

---

Bad values in estimation of ASIo!
Poorly-behaved FittedBeta1 found! Trial #x will repeat.
FittedBeta0 + (FittedBeta1 - 1) * ASIo <= 0! Trial #x will repeat.
FittedBeta0 + {1 / (1-AllowablePFade)} * (FittedBeta1-1) * ASIo <= 0! Trial #x will repeat.
[FittedBeta0+(1/{1-AllowablePFade})*(FittedBeta1-1) * ASIo]/[FittedBeta0+(FittedBeta1-1)*ASIo] <= 0! Trial #x will repeat.

---

If the “Error Messages On?” box is checked, error messages will be shown when certain criteria are met, such as  $\beta_I=1$ . In the case of  $\beta_I=1$ , the second message in Table D-2 will be shown. The user is then given the chance to stop the entire calculation or repeat the trial.

If a runaway calculation is found, an error message stating “Bad input data!” will be generated, and the run will end. A runaway calculation is defined as the actual number of trials exceeding the requested number by 20.

## D-4. ROR ANALYSIS OF EXPERIMENTAL DATA

In addition to simulating cell performance data, the tool can import and analyze actual cell data. Clicking on the ROR Analysis of Experimental Data button on the main menu (Figure D-2) produces the dialog box shown in Figure D-9. It is assumed that the data to be imported are in an Excel workbook and form a contiguous block. Data import will stop where empty cells are encountered.

The information needed to read the data is specified in the dialog box, which is illustrated with typical values in Figure D-9. This information includes the complete path to the workbook and its file name (drive:\directory\filename.ext), the worksheet name that contains the cell data, the number of actual cells tested, the maximum number of RPTs per cell in the file, the starting location of the cell data, the RPT interval, the allowable power fade for life on test estimation (maximum of 25%), tuning constants for leverage and outlier weights (see the “Edit Previous Data” section for more details), and the data orientation on the worksheet.

The worksheet name is case sensitive; other inputs are not. They are retained while the program is running. If ROR Analysis is used more than once while the program is running, they will appear again. This is used when multiple analyses of data are done from the same source or when the path and/or sheet names for different workbooks differ only slightly.

For the “maximum number of RPTs,” the RPT count starts at 0 weeks and ends with the last RPT from the longest-lived cell in the dataset. For example, if all cells last 104 weeks and the RPT interval is 4 weeks, the maximum number of RPTs per cell in file is 27. This is true even if some cells do not continue for the full 104-week duration.

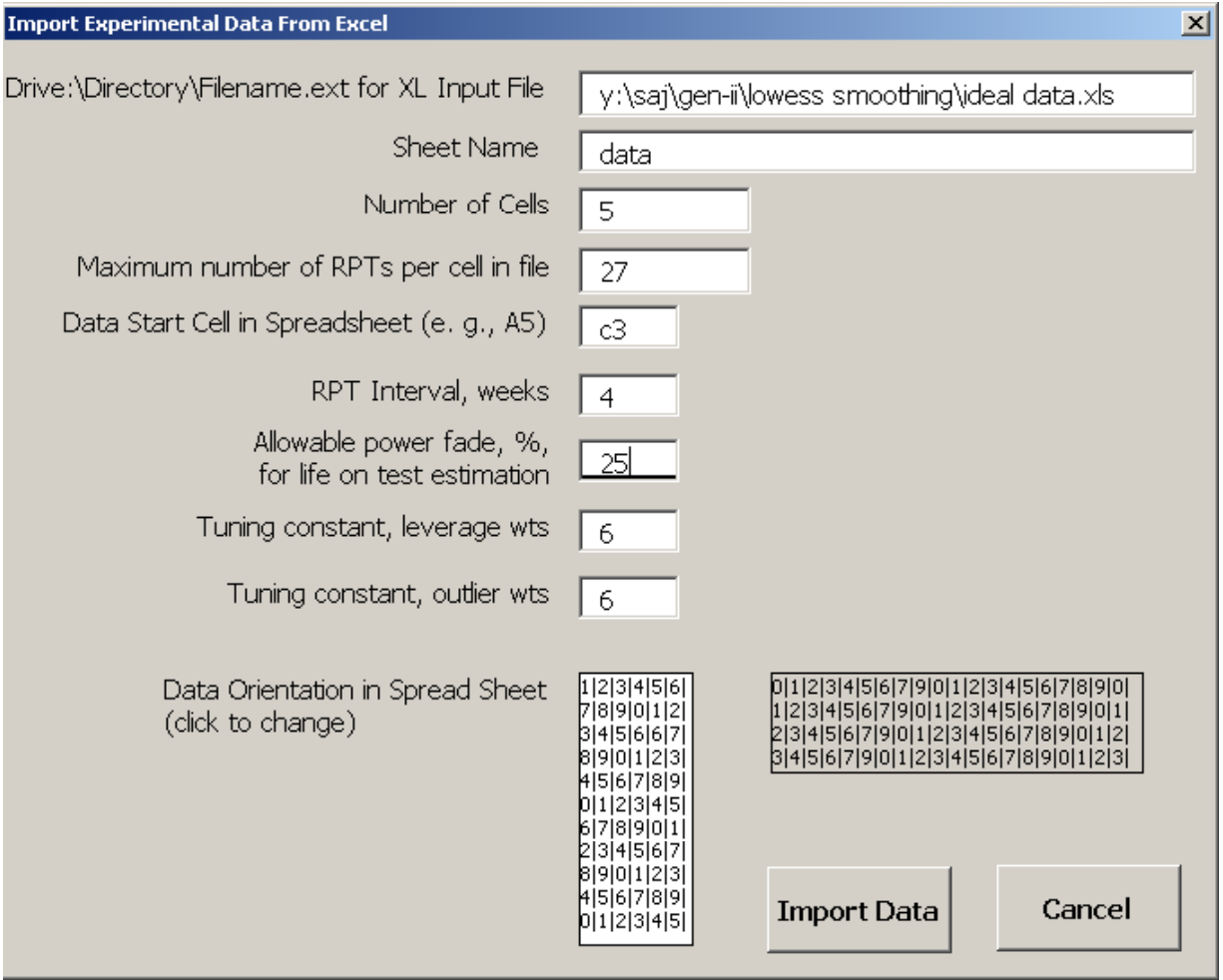


Figure D-9. Dialog box for importing experimental data from Excel for analysis.

Data orientation refers to the direction of increasing time in the worksheet. An example of vertical orientation is given in Figure D-10, and horizontal in Figure D-11. In Figure D-10, time increases down a column, e.g., 0 weeks in cell A2, 4 weeks in A3, 8 weeks in A5, etc. In Figure D-11, time increases across a row, e.g., 0 weeks in B1, 4 weeks in C1, 8 weeks in D1, etc. For these examples, both blocks of ASI data begin at cell B2. The user indicates the orientation of the data by clicking on the icons next to the “Data Orientation in Spread Sheet” label. The program will indicate the user’s selection by changing the selected icon to white and the icon not selected to gray. In Figure D-9, the vertical data orientation is selected.

	A	B	C	D	E	F	G	H	I	J	K	L	M	N	O	P
1		201	208	202	203	204	205	206	207	213	212	209	215	210	211	214
2	0	26.61357	28.25002	26.04976	26.04309	26.01763	27.10036	27.72041	24.91578	27.16469	30.21782	26.96704	28.90818	29.55309	30.36787	29.56313
3	4			28.80808	29.09325	29.94017	28.64929	29.34408	26.61367	28.79454	31.45409	28.30418	28.58019	30.03966	30.17061	28.61363
4	8					31.59533	30.2712	30.88767	29.06377	31.85787	34.21941	30.63103	30.6127	32.95375	32.93168	30.20883
5	12							31.60462	29.61161	33.38822	35.83615	30.67233	32.25577	34.32237	34.46043	31.41414
6	16							32.44766	30.82248	33.78656	36.76216	32.10728	33.47454	35.30757	35.45331	32.10005
7	20									34.83173	36.61908	33.13377	35.4696	35.58373	35.84492	33.88757
8	24										37.79206	33.33137	35.95663	36.45355	36.34991	34.53409
9	28										38.77425	34.37715	37.67203	37.49129	37.8053	36.87634
10	32											35.43045	39.64459	39.28113	38.72126	38.61814
11	36												42.30223	41.02306	40.92103	40.46147
12	40													42.46677	43.17808	42.72622

Figure D-10. An example of vertical data orientation.

	A	B	C	D	E	F	G	H	I	J	K	L	M	N	O	P	Q
1		0	4	8	12	16	20	24	28	32	36	40	44	48	52	56	60
2	VC003	32.40867	34.03017	35.9253	37.04164	37.73512											
3	VC004	31.31498	33.86942	35.0227	35.91715	37.06866	37.88909	38.24152	38.44692	39.19288	39.64785	41.00011	41.42919	41.78342	42.19863	42.6873	43.56298
4	VC005	32.21618	34.64515	35.71604	36.88936	37.78713	38.29711	38.79479	39.08149	39.93757	40.73222	41.43037					
5	VC007	32.3882	34.78258	36.02871	37.17296	34.11739	37.96731	38.80751	39.1276	39.71226	40.37148	41.26979	41.7917	42.21742	42.72281	43.14598	44.00971
6	VC010	30.57849	35.88068	35.10814	36.33513	36.84534											
7	VC012	38.00054	44.59951														
8	VC014	32.48128	34.84324	36.38412	37.64324	38.13024	38.83677	39.2484	39.76079	40.61351	41.26866	42.22861					
9	VC015	33.16448	34.25444	36.63578	37.97979	38.87839	39.65094	39.84896	40.40241	41.29162	41.98903	42.70858	43.35489	43.88818	44.10299	44.60647	45.41062
10	VC022	31.36042															
11	VC024	32.23163	42.34673														

Figure D-11. An example of horizontal data orientation.

All imported data are used to calculate the average initial value of the ASI. This is generally a good approximation of the  $ASI_0$  parameter discussed in the Monte Carlo Simulation section. Cells with only one observation of ASI, such the cells labeled “201” and “208” in Figure D-10 or “VC022” in Figure D-11, will not be included in the ROR regression analysis.

Once the required inputs have been provided, clicking on “Import Data” will start the reading and analysis process. Clicking on “Cancel” will return to the previous menu. After the bootstrap analysis begins, users of Excel2000 and later will see a progress bar. When the process is complete, results similar to those in Figure D-12 will be shown. Data in the “Experimental Data” sheet include the values of average ASI at BOL and at EOL, the values of  $\beta_0$ ,  $\beta_1$ ,  $ASI_0$ , and the values of  $ASI_k$  (“X”) and  $ASI_{k+1}$  (“Y”) used in the analysis. Additionally, the results of the bootstrap analysis are given in columns P through S of the worksheet. The standard deviations for these values from the bootstrap analysis are given in cells P105 through S105. The estimate of the 90% lower confidence level value for life on test ( $L_{TEST}$ ) is given in cell H25. The calculation results are summarized in a display such as that shown in Figure D-13.

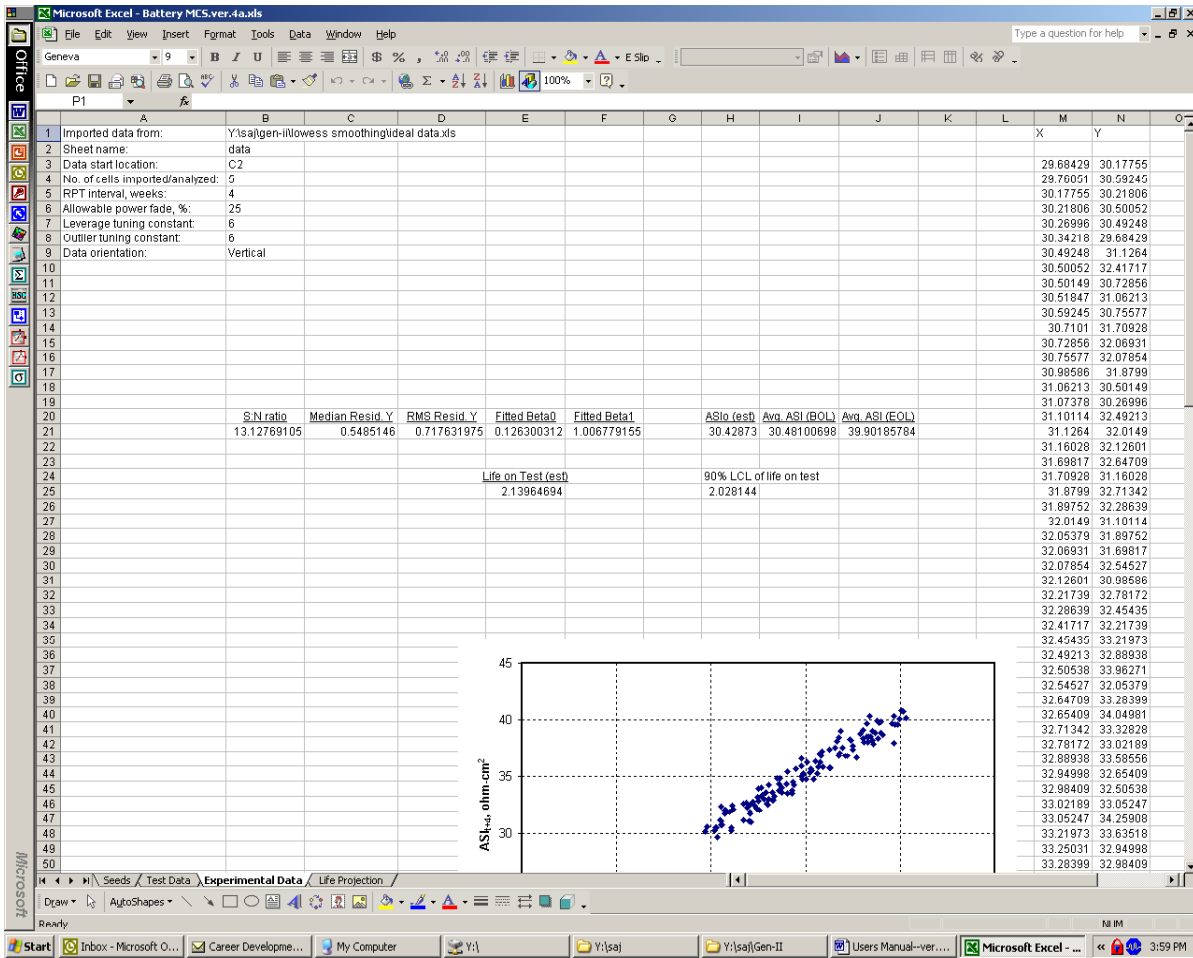


Figure D-12. Example results from the Import Data function.

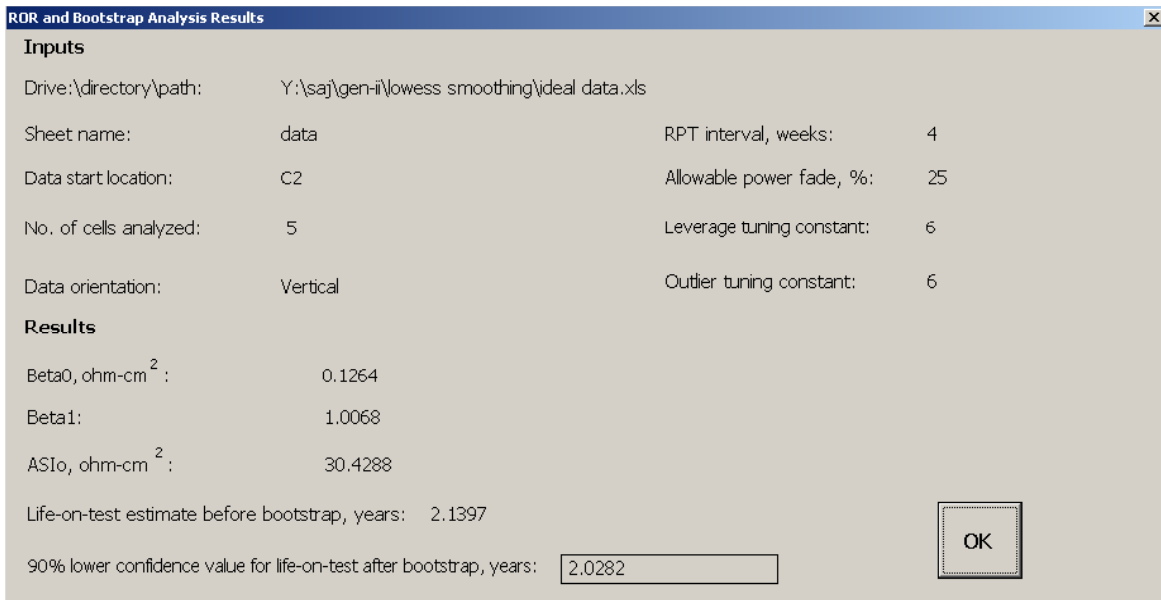


Figure D-13. Display showing results from ROR and bootstrap analysis on experimental data.

## D-5. USER LIFE EQUATIONS

The tool has provisions for use with technology-dependent life equations, which can be substituted for the default ones described in this manual. These technology-dependent computer routines are stored in a single VBA module.<sup>e</sup> The following discussion assumes some familiarity with VBA.

Double-clicking on the Modules icon in the window labeled "Project-VBAProject" will display two user-modifiable modules, called *MakeVisible* and *UserEquations*. The *MakeVisible* module (accessed by double-clicking on its icon) contains a single subroutine, to be used only when needed due to premature termination of the program, as might occur with a poorly handled error condition.

The *UserEquations* module contains three functions: *LifeEquation*, *EstimateASI\_at\_EOT*, and *EstimateLife*. The function names and variables in the function headers cannot be changed without impairing the operation of the tool. The three functions contain some internal documentation that describes their internal variables. This information may provide some guidance in constructing replacement functions. *The user is warned that error detection and trapping is necessary when these modules are modified. Aberrant behavior is likely to occur without it.* The nature and extent of error detection and trapping to be provided is left to the user.

*LifeEquation*. Test time in weeks is passed to the function. Based on the true values of *beta0* and *beta1*, the function will return the true value of ASI. If the user changes this function, error trapping akin to that shown below is needed. The case where *beta1=1* for the default life function is illustrated here.

```
' VARIABLES:
' beta0                value of beta0 based on initial "true" conditions (passed globally)
' beta1                value of beta1 based on initial "true" conditions (passed globally)
' ASI_at_BOL           true value of ASI at time=0 (passed globally)
' T                   time on test, in weeks
' RecipTimeConstant    ln(beta1) / RPTInterval
'
    If beta1 = 1 Then
        a = ASI_at_BOL + beta0 * T / RPTInterval
    Else
        a = ((beta0 + (beta1 - 1) * ASI_at_BOL) * Exp(T *
            RecipTimeConstant) - beta0) / (beta1 - 1)
    End If
```

The condition *beta1=1* would produce a divide by zero error if it were not trapped by the **If** statement.

*EstimateASI\_at\_EOT*. This boolean function contains the life equation and is passed three variables: *WhichCase*, *fbeta0*, and *fbeta1*. It returns the estimated ASI at end of test, *ASIfest*, as well as status (see below for more information). The function header is given below. If the user modifies this function, function status must be returned or the rest of the analysis may not work. If *EstimateASI\_at\_EOT* equals true, it means a successful calculation with no errors.

---

<sup>e</sup> Windows users can access the VBA development environment using Ctrl+F11 keystrokes. (Option+F11 for Mac users.) The description here is based on the Windows version of Excel, although the Macintosh environment is similar.

' VARIABLES

' *Whichcase* = used for program run control. Do not change  
' *fbeta0* = fitted beta0; passed to function by value. Do not change in header  
' *fbeta1* = fitted beta1; passed to function by value. Do not change in header  
' *ASlest* = returned value of estimated ASI  
' *RealBatteryLife* = true battery life; passed globally  
' *AcceleratingFactor* = stress level or acceleration factor; passed globally  
' *RPTInterval* = time between RPTs; passed globally  
' *EMsgsOn* = boolean set by the user on new, edit or recycle simulation  
' *MCSMsgBox* = simple control to either terminate or continue program based on user selection

*Function EstimateASI\_at\_EOT(ByRef WhichCase As Integer, ByVal fbeta0 As Double, ByVal fbeta1 As Double, ByRef ASlest As Double) As Boolean*

The user is responsible for providing error trapping. (See the VBA code in the *UserEquations* module for examples.)

*EstimateLife*. This boolean function is the life equation solved for time in terms of beta0, beta1, and ASI. It is passed three values, *WhichCase*, *fbeta0*, and *fbeta1*, and it returns the estimate of life on test, *Life\_est*, as well as status (see below for more information). The function header is given below. If the user modifies this function, function status must be returned or the rest of the analysis may not work. If *EstimateLife* equals true, it means a successful calculation with no errors.k

' VARIABLES

' *Whichcase* = used for program run control. Do not change  
' *fbeta0* = fitted beta0; passed to function by value. Do not change in header  
' *fbeta1* = fitted beta1; passed to function by value. Do not change in header  
' *Life\_est* = returned value of estimated life in test  
' *AllowablePfade* = allowable power fade; passed globally  
' *ASlo* = estimate of ASI; passed globally  
' *RPTInterval* = time between RPTs; passed globally

*Function EstimateLife(ByRef WhichCase As Integer, ByVal fbeta0 As Double, ByVal fbeta1 As Double, ByRef Life\_est As Double) As Boolean*

The user is responsible for providing error trapping. (See the VBA code in the *UserEquations* module for examples.)

**Appendix E**  
**Test Measurement Requirements**



# Appendix E

## Test Measurement Requirements

The important measurement parameters for life testing are current, voltage, and temperature (and, implicitly time). All other reported parameters are derived (e.g., charge and energy) or calculated (e.g., resistance, pulse power capability, etc.) from voltage and current measurements, and the test temperature also affects many of the parameters when measurements are taken.

### E-1. ELECTRICAL PARAMETERS

For life testing and life prediction purposes, the critical aspects of current and voltage measurements are (a) linearity and (b) test-to-test repeatability (i.e., stability). Absolute accuracy of electrical measurements is important for some calculated parameters, but the simplest parameter used for life prediction [resistance, or equivalently ASI (area-specific impedance)] is computed using a  $\Delta V/\Delta I$  formula whose results for a single test are affected only by random errors or calibration linearity errors in voltage or current.

The relationship between current and voltage errors and the resulting uncertainty in calculated pulse resistance is detailed in Reference 22, Volume 1, Section 3.2.4. Voltage and current calibration errors are directly additive (in an RMS sense), while random measurement errors are “amplified” according to the fraction of the measurement range used to measure  $\Delta V$  or  $\Delta I$ . Thus, the uncertainty in resistance is data-dependent; but a high-quality measurement system using 16-bit data acquisition and precision current shunts (if properly calibrated) should yield data adequate to calculate resistance with an uncertainty of 0.5% or less for a single measurement. For example, Reference 22, Volume 2, shows the calculated resistance uncertainty (one standard deviation) for a Maccor battery tester (claimed voltage and current repeatability of 0.02% of full scale) to be less than 0.4% of reading, even when  $\Delta V$  and  $\Delta I$  were only 5 and 8% of full scale, respectively. (A majority of this uncertainty was due to the 0.25% current shunts used for calibration at the time this report was written.)

Note that computing pulse resistance and other dynamic battery characteristics in this fashion requires paired current and voltage measurements that are essentially simultaneous in time (i.e., acquired within <0.01s of each other). A significant time skew between current and voltage measurements will create device-dependent errors in the calculated results that cannot be compensated for and are not accounted for in the uncertainty values described above.

Test-to-test repeatability may involve additional errors that affect this result. Only a limited study of the effect of voltage or current calibration drift in actual testing has been made. However, as long as drift effects are contained within the calibration uncertainty specifications, they should not affect this result substantially.

To ensure that resistance can be determined with an uncertainty of 0.5% or less, the following specifications can be used as a guideline:<sup>a</sup>

- Voltage calibration uncertainty <0.1% of full scale

---

a. There are two important caveats on these specifications. (1) These values are based on a one-standard-deviation uncertainty for resistance. Raising the confidence level substantially (e.g., to two standard deviations) while maintaining a 0.5% limit is possible but probably near the limit of present measurement capabilities in any known battery-testing laboratory. (2) The higher allowable errors for current measurements are due to the likelihood that  $\Delta V$  measurements will use a smaller fraction of the measurement range than the corresponding current measurements.

- Current calibration uncertainty <0.25% of full scale
- (Standard deviation of) voltage measurement random error <0.01% of full scale
- (Standard deviation of) current measurement random error <0.02% of full scale.

## **E-2. TEMPERATURES**

Accurate control of test temperatures during life testing is important so that the resulting life behavior can be accurately correlated to temperature. However, this is primarily a matter of average behavior over time (as long as variations are small), and standard laboratory temperature chambers are capable of adequate performance for this purpose.

Temperature behavior during the periodic reference performance tests is substantially more important, because small, perhaps short-duration, variations in device temperature can result in unacceptable *jitter* in the subsequent calculated values of cell resistance and other parameters from test to test.

Studies for this manual suggest that resistance or ASI errors due to temperature should be limited to 1% (of reading) or less. Depending on temperature sensitivity, this can imply that the corresponding temperature errors should be no more than 0.2°C. This is beyond the performance expected from standard test chambers, so the approach adopted for this manual is to measure the actual device temperature at the time of the RPT and then compensate the calculated resistance/ASI using a temperature sensitivity determined from other test results. Consequently, the requirement for measurement of temperature during RPTs is a measurement channel repeatability of 0.2°C or less (one standard deviation) over the duration of life testing. Because the life prediction process in this manual accounts to a large extent for cell-to-cell variability, the absolute accuracy of temperature measurement needs not be this high, but it should probably not exceed 1°C.

## **E-3. PARAMETER SAMPLING FREQUENCIES**

Battery test equipment varies widely in its data acquisition capabilities and characteristics, so only the minimum data requirements important to life prediction are given in Table E-1. (The FreedomCAR application-specific testing manuals generally include more detailed requirements for test monitoring and data archiving needs.)

Table E-1. Data sampling rate requirements.

Test Procedure	Data Requirement	Conditions and Notes
Static capacity ( $C_1/1$ ) $C_1/1$ segments of HPPC and MPPC tests, other constant discharge segments	Adequate voltage and current sampling rate to compute (integrate) capacity and energy to <1% Temperature measurement at start of all discharges	Required if integration of recorded data is done externally. (May be an internal test station function not subject to alteration.)
HPPC and MPPC tests, special PPC profiles during life test intervals	One voltage, current, and temperature sample (a) just before each pulse and (b) at the designated time during each discharge and regen pulse Voltage and current samples at 1s intervals during pulse profiles (for lumped parameter model pulse power verification).	In some cases, random errors can be reduced if multiple samples are averaged (but within <0.1s during pulses)
OCV versus SOC at selected temperatures	Minimum 20 SOC values, one measured OCV value per step Temperature measurement at end of each OCV period	Averaging multiple voltage measurements for each step value is recommended
Self-discharge test at selected temperatures	Same sampling requirement as static capacity Temperature measurement at start of all discharges	Same as static capacity
Cold-cranking power test	Voltage and current just before test profile start, at ~0.1-s intervals during all three pulses, and at ~1-s intervals during interpulse rests Temperature measurement at start of pulse profile	(Only the last point in each pulse is used for calculations. Others are needed, mostly to verify that voltage limiting does not occur during the test.)
AC impedance spectrum testing	Not specified	See general guidance in Reference 11, Appendix C
Stand (calendar) life test intervals at temperature (other than pulse profiles)	Voltage and temperature measurement at intervals as needed for SOC monitoring	
Cycle life test intervals	Voltage and temperature measurements at intervals as needed to monitor stable SOC and temperature during cycling	
General pretest (for all discharges and pulse profiles)	Additional measurements at ~1-min intervals for 30 min before discharge or test profile start are <i>recommended</i>	Shows stable voltage and temperature conditions